UNIVERSITY OF CALIFORNIA SAN DIEGO

Towards a Comprehensive Analysis of the Impact Biomass Burning Aerosols have on the West African Monsoon

A dissertation in partial satisfaction of the requirements for the degree Doctor of Philosophy

in

Oceanography

by

Osinachi F. Ajoku

Committee in charge:

Arthur J. Miller, Co-chair
Joel R. Norris, Co-chair
Dr. Ivan Evans
Myrl Hendershott
BT Werner

2020

The dissertation of Osinachi Ajoku is approved, and it is acceptable in quality and form for publication on microfilm and electronically:

_____

_____

_____

_____
Co-chair

_____
Co-chair

University of California San Diego

2020

DEDICATION

The term “It takes a village to raise a child” could not be any truer as it pertains to my life. For as long as I can remember, my life has been influenced and positively steered towards my current destination. Without my mother’s sacrifices, blood, sweat, tears and a successful bout with breast cancer, I would not know how to tackle adversity head on. The greatest advice she gave me is that it does not matter how many times life knocks you down, it is about whether you have the will to rise back up. She is the main reason that I have made it this far on my journey, and so, I would like to thank her. I love you more than words can justify. To my siblings, thank you for always being in my corner and believing in me.

I would like to thank my advisor, Arturo. Without your generous check-up after open house, I am not sure I would have decided to come to Scripps. He not only embraced me as his student, he and his lovely wife Jenny created a family and a community full of love and appreciation. You taught me how to truly be a researcher and I will be forever indebted to you. To the entire Miller group, each of our gatherings were considered like therapy for me. It seems that every time we gathered, there were nothing but smiles shared.

I would also like to thank my co-advisor for teaching me how to think about research critically, Joel Norris. He spent invaluable time with me to make sure that I thoroughly understood scientific concepts and equations. I will never forget spending endless days in your office on the whiteboard deriving equations. Your hands-on approach made sure that my research ideas did not cut any corners, and this is a valuable skill I will hold onto. I would like to extend a special thanks to the entire Norris group, all of our meetings allowed us to share current research findings. It put me at ease hearing research from others, especially since I felt a little

lonesome on my research journey at times. Being able to bounce my research presentations and directions amongst you all proved critical as I submitted articles for peer-review and presented at research conferences.

A significant portion of my time in graduate school was spent in diversity-related programs. As a black male, my experiences have been different relative to my peers and these programs allowed an outlet to voice the needs of underrepresented students. I have received invaluable guidance from our Director of Diversity Initiatives, Keiara Auzenne, who gave me a chance to join her team as a community Equity Diversity and Inclusion (EDI) fellow. Honestly, these experiences have given me the utmost confidence to engage communities about increasing diversity efforts and bias awareness.

Being in graduate school can be very taxing on one's spirit and so I'm grateful for my close friends and spiritual advisors, Keisha and B. Righteous. The hour-long conversations and east coast getaways kept my spirit in balance, especially when I felt down and out.

To my numerous friends in South central Los Angeles, you all are my motivation and the bonds we share through memories and friendships are the reason I have made it this far. This is definitely for you.

EPIGRAPH

I know where I'm going and I know the truth, and I don't have to be what you want me to be. I'm

free to be what I want.

-Muhammad Ali

Even though you’re fed up, gotta keep your head up.

-Tupac Shakur

I think what motivates people is not great hate but great love for other people.

-Huey P. Newton

They don’t know about them sleepless nights,

Them looking for a reason nights,

They say it’s six degrees in life,

Opportunity, preparation, they meet, it’s nice

-Ermias Joseph Asghedom

TABLE OF CONTENTS

LIST OF FIGURES

LIST OF TABLES

ACKNOWLEDGEMENTS

I would like to acknowledge Dr. Arthur Miller and Dr. Joel Norris for their guidance and long hours spent helping to refine my thesis.

Chapter 2, in full, is a reprint of the material as it appears in Climate Dynamics 2020. Ajoku, O., Norris, J. R., & Miller, A. J. (2020). Observed monsoon precipitation suppression caused by anomalous interhemispheric aerosol transport. *Climate Dynamics*, *54*(1-2), 1077-1091. The dissertation author was the primary investigator and author of this paper.

Chapter 3, in part is currently being prepared for submission for publication of the material. Ajoku, Osinachi; Miller, Arthur; Norris, Joel; Buchholz, Rebecca. The dissertation author was the primary investigator and author of this material.

Chapter 4, in part is currently being prepared for submission for publication of the material. Ajoku, Osinachi; Miller, Arthur; Norris, Joel. The dissertation author was the primary investigator and author of this material.

VITA

2011 Bachelor of Science in Geology, California State University, Dominguez Hills

2012-2014 Research Assistant, University of California Riverside

2013-2014 Teaching Assistant, University of California Riverside

2014 Master of Science in Geosciences, University of California Riverside

2014-2020 Research Assistant, University of California San Diego

2020 Doctor of Philosophy in Oceanography, University of California San Diego

PUBLICATIONS

Ajoku, O., Norris, J., Miller, A.J**.,** (2019). Observed Monsoon Precipitation Suppression Caused by Anomalous Interhemispheric Aerosol. *Climate Dynamics,* DOI: 10.1007/s00382-019-05046-y.

Allen, R. J., & Ajoku, O. (2016). Future Aerosol Reductions and Widening of the Northern Topical Belt. *Journal of Geophysical Research: Atmospheres*, *121*(12), 6765-6786.

FELLOWSHIPS

National Science Foundation GRFP

San Diego Fellowship

UC Dissertation Year Fellowship

GPS Science Policy Fellowship

FIELDS OF STUDY

Major Field: Oceanography/Climate Science

Co-Advisors: Dr. Arthur J. Miller and Dr. Joel R. Norris

ABSTRACT OF THE DISSERTATION

Towards a Comprehensive Analysis of the Impact Biomass Burning Aerosols Have on the West African Monsoon

by

Osinachi F. Ajoku

Doctor of Philosophy in Oceanography

University of California San Diego, 2020

Dr. Arthur J. Miller, Co-Chair

Dr. Joel R. Norris, Co-Chair

This dissertation is motivated by the lack of research depth on the influence biomass burning produced aerosols impose on West African monsoon dynamics during daily time scales. The impacts of such aerosols on atmospheric thermodynamics and cloud microphysics are investigated using a combination of satellite observations and global climate model simulations.

Using observations, we find (1) suppression of precipitation rates over the Guinea coastline with elevated aerosol transport and (2) an increase in rates with decreased aerosol amounts. Decreases in the amount of shortwave radiation reaching the surface over land and

ocean attributed to increases in low-level cloud coverage and the absorptive nature of biomass aerosols observed in nature on dirty conditions are matched with reductions in convective available potential energy (CAPE), vertical air mixing essential for deep-convection cloud cover. Increased aerosol content is also associated with decreases in cloud droplet effective radius, a defining feature of aerosol indirect effects.

Guided by available observations, model experiments are designed for NCAR's CESM2 with meteorology being nudged to observations using MERRA2 reanalysis to visualize data not available through such observations. Simulations successfully reproduce aerosol transport and corresponding precipitation changes found in observations. However, this model is not in agreement with changes in low-level cloud fraction which leads to increases (decreases) in shortwave radiation reaching the surface (top of atmosphere) during dirty conditions. Our model simulations show that aerosol semidirect and indirect effects interact together to alter cloud formation processes and ultimately control the precipitation response.

Throughout the equatorial Atlantic, smoke aerosols impact the structure of stratocumulus to cumulus transition (SCT) through an alteration of atmospheric stability and moisture availability. Boundary layer deepening and increasing sea surface temperatures put the location of this transition within the Gulf of Guinea. Increased low-level clouds occur over the Atlantic cold tongue where aerosol layers reside above low cloud tops, reflecting a negative aerosol semidirect effect. Coupled with significant changes in cloud top height and tropospheric stability further South, these aerosol effects combine to extend in space during increased aerosol loading episodes.

Chapter 1: An Introduction to Biomass Burning Aerosols and the West African Monsoon

1.1 Introduction

Biomass burning is defined as the combustion of organic matter, which can occur by either anthropogenic or natural means. During this process, particulate matter suspended aloft, known as aerosols, are injected into the atmosphere and transported around through meteorology. Africa is the single largest continental source of biomass burning emission and has a vast, complex terrain with stark contrast in geography, most notably the elevation and land cover transitions from southern to central Africa that aid the process of natural fires. African biomass burning peaks during local dry seasons, occurring near savannah-dominated land, and is thus geographically constrained by seasonal variations. Smoke emissions from biomass burning account for 20% of the global sum of all aerosol emissions, but smoke emissions in tropical regions account for 12% of the global aerosol burden alone (Dentener et al., 2006; Marlon et al., 2008). In the Northern Hemisphere burning is confined between the Sahara Desert to the north and the Congo Rainforest to the south, and in the Southern Hemisphere, burning is confined between the Kalahari Desert to the south and the rainforest towards the north.

1.2 West African Monsoon Description

The West African Monsoon (WAM), like any other monsoon, is a seasonal phenomenon caused by a reversal of low-level winds driven by meridional temperature contrasts between seawater and adjacent land peaking during boreal summer months (June-September). Such a

wind reversal is the causal mechanism for seasonal heavy precipitation along the Guinea coastline. As incoming solar radiation comes to a peak over the Sahara Desert, the rapid ascent of air drives very strong surface convergent flow toward this region resulting in the Saharan heat low. Further aloft, this heated air follows a pressure gradient towards the adjacent ocean thus creating a circulation cell. Within this circulation cell, a constant supply of moisture is available for convection over land. This circulation cell is balanced with positive vorticity formation at lower levels and negative vorticity at upper levels, which create cyclonic and anticyclonic systems respectively (Hall & Peyrille, 2006).

1.3 Aerosol-Atmospheric Interactions

The optical properties of aerosols allow for an alteration of Earth's radiation budget through direct interaction with incoming solar radiation (Ramanathan, 2001; Haywood & Shine, 1997) and modification of cloud properties including cloud droplet number concentration (CDNC), radiative effects and lifetime (Twomey et al., 1987). Aerosols have the potential to be transported more than 10,000 kilometers downwind of emission sources (Clarke et al., 2001), where they can alter local radiation budgets and cloud formation processes. Aerosols directly impact the planetary energy balance through absorption, scattering and emission of incoming radiation, this is known as the "direct effect". Some aerosols act as cloud condensation nuclei (CCN), thereby changing cloud particle surface area, influences droplet collisions, and changes the accumulation of liquid water and ice in clouds, and thus alter cloud albedo (the proportion of incident radiation reflected by a cloud top) and lifetime (Ghan et al., 2012). This is the so-called "indirect effect". Some aerosols, particularly black carbon (BC) can absorb shortwave radiation

efficiently and heat the atmosphere leading to cloud dissipation. This is the so-called “semi-direct effect”.

Carbonaceous aerosols in the atmosphere both scatter and absorb radiation. The absorbing component, generally referenced as BC, is mainly soot produced from incomplete combustion. The scattering component is generally referred to as organic carbon (OC) as these aerosols contain organic matter. It should be noted that BC also scatters radiation and act as cloud condensation nuclei (CCN). Observations from Earth observing satellites indicate such carbonaceous aerosols are widespread in the tropics and subtropics. Estimates in the magnitude of radiative forcing by carbonaceous aerosols carry considerable uncertainty. Research has demonstrated that such radiative forcing includes variations in surface solar radiation (Wild, 2012) and the hydrological cycle (Ramanathan et al., 2001). Emissions of BC aerosols also contribute to the global problem of air pollution and its impact on human health. Inhalation of BC is associated with health problems, including respiratory and cardiovascular disease, cancer and even birth defects.

1.4 Research Summary and Thesis Outline

The overall scientific question I propose is: How do variations in aerosols emitted during seasonal biomass burning effect seasonal African climate and dynamics? In order to quantitatively answer this question, I have split my dissertation into 3 main chapters. Here, I will and present and elaborate on questions to be addressed in each chapter:

1. What impacts do fluctuations in aerosols associated with biomass burning and transported from Southern Africa have on West African monsoon (WAM) dynamics? What effects do these

aerosols have on the various cloud types over the Gulf of Guinea and along the coast of West Africa? How do these aerosol-cloud interactions adjust monsoon rains?

2. Can models accurately reproduce observed seasonal fluctuations in biomass burning, resulting aerosol emissions and its effect on WAM dynamics? By which mechanisms do changes in aerosol concentration over the Gulf of Guinea (GoG) suppress precipitation?

3. Can we clearly see a stratocumulus-to-cumulus transition (SCT) region where biomass burning aerosol emissions impact low-level cloud fraction? What are the important mechanisms of biomass burning aerosols possibly impacting the spatial structure of the SCT?

The 2nd chapter of my dissertation is a full preprint as appears in the Journal of Climate. My 3rd chapter, which includes modeling experiments conducted with the help of individuals I have networked with at the National Center for Atmospheric Research (NCAR), is essentially a modeling extension of topic in chapter 2. A great benefit of utilizing model simulations are understanding processes that cannot be obtained solely through observations. For example, we can isolate the change in radiative fluxes solely due to the presence of aerosols. Chapter 4 further looks at changes in large-scale cloud structures throughout the equatorial Atlantic Ocean due to biomass burning aerosols. This chapter is currently in preparation to be submitted to *Atmospheric Research*.

1.5 References

Clarke, A D, Collins, W G, Rasch, P J, Kapustin, V N, Moore, K, Howell, S, & Fuelberg, H E (2001) Dust and pollution transport on global scales: Aerosol measurements and model predictions. *Journal of Geophysical Research: Atmospheres*, *106*(D23), 32555-32569.

Dentener, F., Kinne, S., Bond, T., Boucher, O., Cofala, J., Generoso, S., Ginoux, P., Gong, S., Hoelzemann, J.J., Ito, A. and Marelli, L., 2006. Emissions of primary aerosol and precursor gases in the years 2000 and 1750, prescribed data-sets for AeroCom.

Ghan, S J, Liu, X, Easter, R C, Zaveri, R, Rasch, P J, Yoon, J H, & Eaton, B (2012) Toward a minimal representation of aerosols in climate models: Comparative decomposition of aerosol direct, semidirect, and indirect radiative forcing. *Journal of Climate*, *25*(19), 6461-6476

Hall, N. M., & Peyrillé, P. (2006, December). Dynamics of the West African monsoon. In *Journal de Physique IV (Proceedings)* (Vol. 139, pp. 81-99). EDP sciences.

Haywood, J. M., & Shine, K. P. (1997). Multi-spectral calculations of the direct radiative forcing of tropospheric sulphate and soot aerosols using a column model. *Quarterly Journal of the Royal Meteorological Society*, *123*(543), 1907-1930.

Marlon, J.R., Bartlein, P.J., Carcaillet, C., Gavin, D.G., Harrison, S.P., Higuera, P.E., Joos, F., Power, M.J. and Prentice, I.C., 2008. Climate and human influences on global biomass burning over the past two millennia. *Nature Geoscience*, *1*(10), pp.697-702.

Ramanathan, V C P J, Crutzen, P J, Kiehl, J T, & Rosenfeld, D (2001) Aerosols, climate, and the hydrological cycle. *science*, *294*(5549), 2119-2124

Twomey, S, Gall, R, & Leuthold, M (1987) Pollution and cloud reflectance. *Boundary-Layer Meteorology*, *41*(1-4), 335-348

Wild, M (2012) Enlightening global dimming and brightening. *Bulletin of the American Meteorological Society*, *93*(1), 27-37

Chapter 2: Observed Monsoon Precipitation Suppression Caused by Anomalous Interhemispheric Aerosol Transport

Osinachi Ajoku[1*], Arthur J. Miller[1] and Joel R. Norris[1]

1 Scripps Institution of Oceanography, University of California San Diego, La Jolla, California, USA

Corresponding author address: O. Ajoku, Scripps Institution of Oceanography, University of California San Diego, 9500 Gilman Dr., La Jolla, CA 92093, USA. E-mail: (oajoku@ucsd.edu)

Acknowledgments. This research forms a part of the Ph.D. dissertation of OA, who was supported by a National Science Foundation Graduate Research Fellowship (DGE-1650112) and a San Diego Foundation Fellowship. The National Science Foundation Earth System Modeling Program (OCE1419306) provided additional funding that supported this research. We thank Eric Wilcox, Andi Andreae, Amato Evan and Victor Dike for important discussions and suggestions. We also thank the three referees who provided very important comments that significantly improved our analysis and enhanced the clarity of our results.

1

ABSTRACT

This study uses observations and atmospheric reanalysis products in order to understand the impacts of smoke aerosols advected from the Southern Hemisphere on the dynamics of the West African Monsoon. Seasonal biomass burning and resulting aerosol emissions have been well documented to affect regional weather patterns, especially low-level convection. Out of all monsoon months, precipitation shows the most variability over land during August, in which anomalous smoke aerosol values can increase (decrease) by 33% (29%) in the Northern Gulf of Guinea and precipitation can decrease (increase) by up to ~2.5 mm day^{-1} (~3 mm day^{-1}) along the West African monsoon region accounting for a 17% (18%) change in precipitation. Smoke aerosols produced by biomass burning occurring near Central Africa are advected towards the Gulf of Guinea at elevations around the 850 hPa level. Satellite observations show an increase (decrease) in cloud fraction and optical depth below (above) the 300-hPa level in the Gulf of Guinea and along the West African coastline along with concurrent decreases (increases) in cloud droplet radius during dirty (clean) aerosol episodes. Additional observations of shortwave radiation quantify changes in cloud coverage and monsoon dynamics. On average, reductions in surface shortwave radiation of ~10-15 W m^{-2} occur over the Gulf of Guinea during increased aerosol transport, with aerosols accounting for ~ 33%-50% of that reduction. Reductions in shortwave radiation are associated with decreased convective available potential energy (CAPE). This demonstrates that increased transport of aerosols perturbs surface radiation, convection in the lower troposphere and eventually cloud coverage, potentially leading to the observed monsoon precipitation suppression. In a broader social context, this region houses 200 million people and thus understanding these climate patterns may carry great importance.

Keywords: biomass-burning, West African monsoon, aerosols, climate forcing

2.1 Introduction

Anthropogenic and natural combustion emissions, including biomass burning, are major sources of greenhouse gases such as nitrogen oxide and carbon dioxide, as well as aerosol particles. Aerosols, particulates in the atmosphere, have the potential to be transported more than 10,000 kilometers downwind of emission sources (Clarke et al., 2001), where they can alter local radiation budgets and cloud formation processes. Aerosols directly impact the planetary energy balance through the absorption and scattering of incoming radiation (Ramanathan, 2001; Haywood and Boucher 2000), which is known as the "direct effect". Some aerosols act as cloud condensation nuclei (CCN), thereby influencing cloud droplet size and consequently the likelihood of coalescence and the accumulation of liquid water and ice in clouds, thus altering cloud albedo and lifetime (Albrecht, 1989; Ferek et al., 2000; Ghan et al., 2012). This is the so-called "indirect effect". The direct and indirect effects caused by aerosols might induce changes in convection and precipitation patterns. The change in globally measured radiative forcing from the preindustrial to the present due to interactions between aerosol particles and cloud cover has the largest uncertainty of all anthropogenic factors (Stocker et al., 2013).

Carbonaceous aerosols in the atmosphere both scatter and absorb radiation. The absorbing component, generally referenced as black carbon (BC), is mainly soot produced from incomplete combustion. BC can absorb shortwave radiation efficiently and heat the atmosphere, thus leading to cloud dissipation if the aerosols are co-located with the clouds. This is the so-called "semi-direct effect". The scattering component is generally referred to as organic carbon (OC) since these aerosols contain organic matter. It should be noted that BC also scatters radiation and although initially hydrophobic, becomes hydrophilic when aged and thus can act as CCN (Croft et al., 2005). Observations from Earth observing satellites indicate that carbonaceous aerosols are

widespread with about 80% of biomass aerosols originating in the tropics (Dentener et al., 2006). Estimates of the magnitude of radiative forcing by carbonaceous aerosols carry considerable uncertainty. Radiative forcing by carbonaceous aerosols can alter surface solar radiation (Wild, 2012) and the hydrological cycle (Ramanathan et al., 2001).

Uncertainties of aerosol emissions are large in the tropics, where 50% originate from anthropogenic fires. Smoke emissions from biomass burning account for 20% of the global sum of all aerosol emissions, but smoke emissions in tropical regions account for 12% of the global aerosol burden alone (Dentener et al., 2006; Marlon et al., 2008). Regions with substantial aerosol emissions from biomass burning suffer from frequent drought episodes and other disruptions to the hydrological cycle, with adverse societal impacts that have been widely reported during the last several decades. Africa is the single largest continental source of biomass burning emission and has a vast, complex terrain with stark contrast in geography, most notably the elevation and land cover transitions from southern to central Africa that aid the process of natural fires. African biomass burning peaks during local dry seasons, occurring near savannah-dominated land, and is thus geographically and temporally constrained by spatial and seasonal variations in precipitation. In the Northern Hemisphere, burning is confined between the Sahara Desert to the north and the Congo Rainforest to the south (~5°N-15°N), and in the Southern Hemisphere, burning is confined between the Kalahari Desert to the south and the rainforest towards the north (~10°S-15°S).

Previous studies have demonstrated links between carbonaceous aerosols and changes in local climate. Ramanathan et al. (2005) documented increases in atmospheric stability caused by the presence of BC and OC that significantly impact the intensity of Indian Monsoons. Modeling studies investigating aerosol effects on precipitation have been conducted over East Asia (Liu et

al., 2011; Xie et al., 2016). Such aerosols have been shown to either invigorate or inhibit cloud formation (Koren et al., 2008) and may reinforce existing drought conditions (Rosenfeld et al., 2008b; Zhang et al., 2009). Aerosol loading over West Africa during wet and dry seasons has been linked to correlations in wind intensity (Nwofor et al., 2018). Using direct satellite observations, Tosca et al. (2015) found that a higher smoke burden limits upward vertical motion and increases surface pressure during the African fire season, indicative of convective suppression. A study by Huang et al. (2009a) utilized back trajectory and regression analysis to determine that both dust and smoke contribute to precipitation suppression over the West African Monsoon (WAM) region; however, this study focused on the local dry season in which precipitation is minimal. More so, the mechanisms connecting aerosols and precipitation suppression are not well understood. The misrepresentation of black carbon aerosols across climate models creates uncertainty in our understanding of the mechanisms by which aerosols may impact regional climate. None of the abovementioned studies quantitatively show ways in which smoke aerosols impact the WAM region during the monsoon season.

Recent aerosol aircraft measurement campaigns have been conducted to analyze the potential impacts that smoke emissions from Central Africa have on clouds and precipitation in the tropical Atlantic. NASA's Observations of Aerosols above Clouds and their Interactions (ORACLES; https://espo.nasa.gov/oracles) campaign sampled cloud and aerosol layers in the Southeast Atlantic between peak biomass burning season (Aug-Oct) for 2016-2018 to characterize seasonal offshore aerosol loading and aerosol-cloud interactions. The UK CLARIFY 2016 (Clouds and Aerosol Radiative Impacts and Forcing; Year 2016) campaign took similar samples at St. Helena Island (Zuidema et al., 2016). The Dynamic-Aerosol-Chemistry-Cloud-Interactions in West Africa (DACCIWA) project also took place in the summer of 2016

and involved a campaign near coastal West Africa. Here, the synoptic and mesoscale weather systems accompanying aerosol transport and monsoon dynamics are well documented (Knippertz et al., 2017).

In order to further understand the aerosol-associated changes in WAM dynamics, we examine possible linkages between biomass-burning aerosols and cloud formation and local radiation budgets. Bouniol et al., (2012, their figure 5) analyzed cloud frequency occurrence in a study region encompassing our own during the 2008 monsoon season using CloudSat radar and CALIPSO lidar. Tracing the path that aerosols follow from their source to the WAM, cloud types transition from stratocumulus over the GoG towards tall, cumulonimbus decks over the continent associated with the monsoon (Deetz et al., 2018). This cloud transition may be influenced by the presence of aerosol, so we correspondingly analyze potential impacts that aerosols may have on clouds of various types.

In this study, we show how anomalous aerosol transport may affect meteorological variables associated with monsoon precipitation, including cloud coverage as well as short-wave (SW) radiation budgets. Here, we document regions in Central Africa with maximum aerosol emissions and follow their path across the equator and over the ocean towards the West African coastline. At this location, the potential effects that aerosol loading may have on cloud cover and radiative properties are analyzed. Unlike previous studies, this research focuses on aerosol-cloud-precipitation interactions during the local dry season over aerosol source regions and local monsoon season over impact regions covering a span of 13 years. Utilized datasets and descriptions of methodology are presented in the next section, followed by analyzed results and concluding remarks.

2.2 Datasets and Methods

In order to determine how changes in aerosol loading over source regions impact monsoon precipitation downwind, daily-averaged or time-specific data (GMT) are utilized from a variety of sources (with the exception of fire emissions). Using daily intervals of data allows for a better sampling resolution as well as capturing mesoscale and synoptic-scale weather processes that would not be resolved with monthly data output.

Monthly fire carbon emissions (Giglio et al., 2013) are acquired from the Global Fire Emissions Database (GFED) at 0.25°x0.25° resolution. These data include burn area resulting from small fires and are used only to understand seasonal changes in fire distribution throughout the continent (van der Warf et al., 2017).

Daily aerosol optical depth (AOD) for the years 2003-2015 are obtained from Modern-Era Retrospective analysis for Research and Applications, Version 2 (MERRA-2) at 0.5°x0.625° resolution (GMAO, 2015). The reason for selecting this time period is that it coincides with the launch of the Aqua mission that provides purely observed data onboard NASA's A-train constellation. Like most satellite observations, data are not available for areas outside the satellite swath path. Having missing AOD data can lead to large errors when undergoing statistical analysis. Using reanalysis data reduces such errors as data not captured by observations are assimilated using a numerical algorithm to create a synthesized estimate of the state of the climate system (Bengtsson et al., 2004). Observations, such as the aerosol index and aerosol absorption optical depth obtained from the Ozone Monitoring Instrument (OMI) measurements and aerosol retrievals from the AErosol RObotic NETwork (AERONET) (Buchard, et al., 2015) validated the data obtained from reanalysis used in our study. We note that this study claims that AOD values in Southern Africa biomass burning regions from

MERRA are underestimated.

In order to quantify the magnitude and location of anomalous changes in rainfall, daily data at 1-degree resolution is obtained from the Global Precipitation Climatology Project, Version 1.2 (GPCP 1.2). All the GPCP products are produced by optimally merging precipitation estimates computed from microwave, infrared, sounder data observed on board satellites, and ground-based rain gauge analysis, taking advantage of the strengths of each data type (Huffman et al., 2016). These satellite datasets have been validated against rain gauges on land in West Africa, particularly on sub-monthly time scales (Nicholson et al., 2003).

Daily wind fields (zonal, meridional and vertical), temperature, specific humidity, convective available potential energy (CAPE), sea level pressure and geopotential height data at 0.75° by 0.75° resolution were obtained at multiple pressure levels ranging from the surface to 500hPa from the European Centre for Medium-Range Weather Forecasts (ECMWF) reanalysis product (Berrisford et al., 2011) at a local time of 6 A.M. UTC, which is consistent with the analysis of Tosca et al. (2015). Here, they studied the changes in cloud fraction associated with variability in fire emissions and compared meteorological variables in control and high fire scenes using ECMWF reanalysis at a 6 A.M. local time to better understand the influence of mesoscale dynamics. Furthermore, mid-level clouds have been found to dominate cover over West Africa during the monsoon season early in the morning (Bourgeios et al., 2018).

To analyze the effect of aerosols on cloud cover, we obtained computed, surface radiation fluxes and cloud coverage during the study period from Clouds and the Earth's Radiant Energy System (CERES) data, which is available, daily-averaged, at 1-degree resolution (Doelling et al., 2013; Doelling et al, 2016). This data is broken down into 4 vertical cloud levels (low, mid-low, mid-high and high). Cloud properties are determined using simultaneous measurements by other

EOS and S-NPP instruments such as the Moderate Resolution Imaging Spectroradiometer (MODIS) and the Visible and Infrared Sounder (VIRS). We calculate aerosol forcings by subtracting surface fluxes from computed surface fluxes with aerosols removed in order to gain a better understanding for local radiation budgets. Their computed fluxes are produced using the Langley Fu-Liou radiative transfer model. Here, observed aerosol values are obtained using MODIS and computations are constrained to the observed CERES TOA fluxes.

Our study regions in the northern Gulf of Guinea (GoG) and WAM comprise of the boundaries between 0° -5°N and 10°W-10°E and 5°N-10°N and 10°W-10°E respectively. For each of the 13 years, the 31 days in August were classified into pentiles according to the magnitude of AOD averaged over the study region in the GoG for that day. This pentile sampling is done independently for each month in order to sample many different independent background meteorological states over the entire dataset. (Results using the absolute dirtiest and cleanest days are very similar.) The top and bottom pentiles each had 78 days and are referred to as "clean" (lowest AOD) and "dirty" (highest AOD) days. All dates associated with these dirty and clean days are averaged together to create composites that track how aerosol loading evolves with other meteorological variables of interest. Climatological means are subtracted from composited data to reveal anomalous changes. By utilizing this method, we attempt to determine which variables control or are impacted by variations in aerosol transport. Statistical significance of results was determined by the 95% confidence interval according to a 2-tailed Student's t-test accounting for serial correlation by using the effective sample size, $n(1-r_1)(1+r_1)^{-1}$, where n is the number of days and r_1 is the lag-1 autocorrelation coefficient leading to ~3 day decorrelation time.

2.3 Results

2.3.1 Climatology

African biomass burning peaks during local dry seasons, occurring where tropical rainforests transition into savannah-dominated lands, and is thus geographically constrained by seasonal variations in precipitation. For the current study, maximum aerosol emissions located in this transition zone occur during boreal summer/austral winter (regional dry season in the Southern Hemisphere). **Fig 2.1** shows climatological carbon emissions associated with biomass burning over the period 2003-2015 for the month of August.

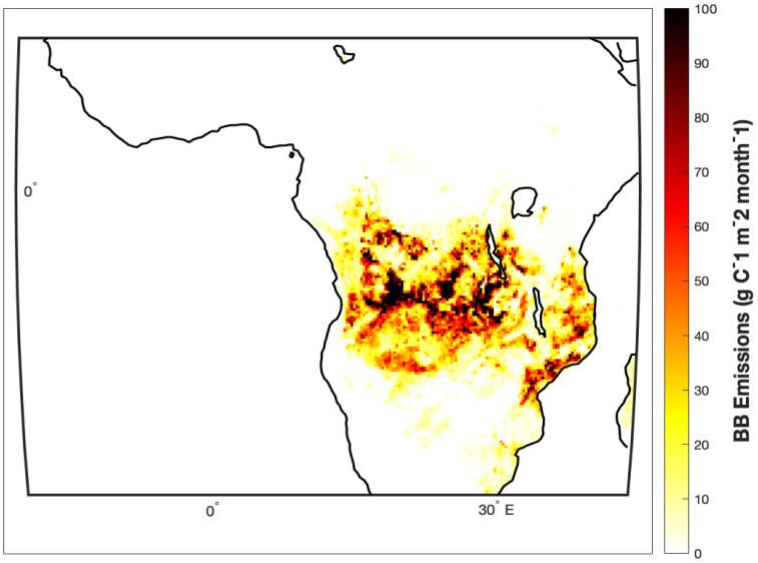

Fig 2.1 Climatological August Biomass Burning Emissions for the years 2003-2015. Units are grams of Carbon m^{-2} $month^{-1}$

The WAM is distinguished by a northward migration of the Intertropical Convergence Zone (ITCZ) and a spatial shift in monsoon onset. Although the WAM occurs during June-September, the present study focuses on August because precipitation variability is largest over land relative to other months. During August, intense precipitation is present in Southern West Africa (**Fig 2.2**). **Fig 2.2** shows 925hPa wind and precipitation climatology for the month of August. The West African westerly jet (WAWJ) is clearly evident at this pressure level (925 hPa) in the areas of deep convection near 8°-11° N. This jet is responsible for transporting low-

level moisture from the GoG toward land and is located at the ~900 hPa level throughout our study region.

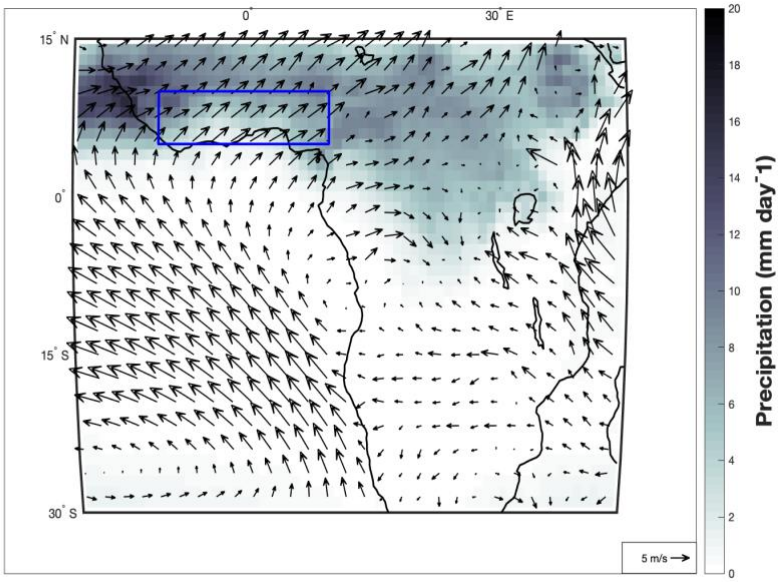

Fig 2.2 925hPa wind and precipitation climatology for the month of August. The box region reflects where precipitation analyses are carried out in subsequent figures

Further south, winds from emission regions can be seen leading into the monsoon flow, which has been documented by reconstruction of the mean meridional circulation over West Africa and the GoG (Hourdin et al., 2010). **Fig 2.3** shows the distribution of aerosol optical depth (AOD), a variable that measures the extinction of incoming solar radiation by airborne particulate matter over the African continent for August averaged during a 13-year observational record. Overlain on top of AOD are climatological winds averaged at 850hPa over the same time period to give an idea as to where smoke aerosols are transported. Winds at this pressure level are used because they represent the conditions immediately above the planetary boundary level (PBL) and have been used in previous studies linking aerosols and precipitation near this region (Huang et al., 2009b, Wilcox et al., 2016). The GoG region is of particular focus because it is adjacent to both the source of aerosol emissions and areas impacted by the WAM.

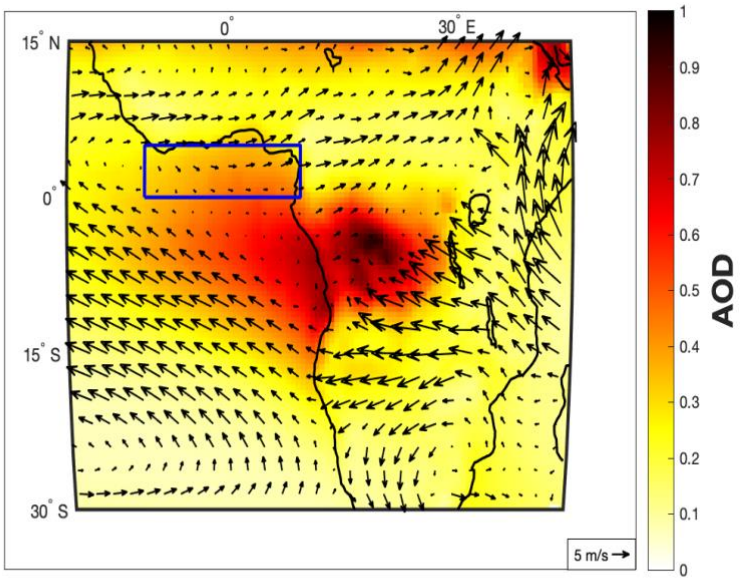

Fig 2.3 850hPa wind and column-integrated AOD climatology for the month of August. The box region reflects where AOD composites are created for analyses carried out in this study

2.3.2 Aerosol-Cloud-SW Radiation Feedback in the WAM Region

Fig 2.4 displays the composite anomalies in AOD and 850hPa winds for dirty (top) and clean (bottom) days. Stippling represents AOD data that is significant at the 5% level, a convention that will be used for data in subsequent figures. It is clearly evident that anomalous transport of aerosols from Central Africa towards the GoG is caused by changes in wind direction and intensity over the source region. Coupled with Africa's complex topography, there exists anomalously higher/lower sea level pressures in Southern Africa that may impact the westward offshore transport of smoke (Adebiyi et al., 2015; Kruger et al., 2010) and these factors lead towards observed, increased aerosol transport (Supplementary figure 1). Within the GoG, AOD values are, on average, ~0.12 +/- 0.018 higher than the climatological value of ~0.36 during episodes of increased transport, accounting for a 33% increase in aerosol presence. In contrast, AOD values are, on average, ~0.11 +/- 0.011 lower during episodes of decreased transport, accounting for a 29% decrease in aerosol presence. We refrain from conducting AOD analysis over the WAM region to avoid possible aerosol washout by climatological precipitation.

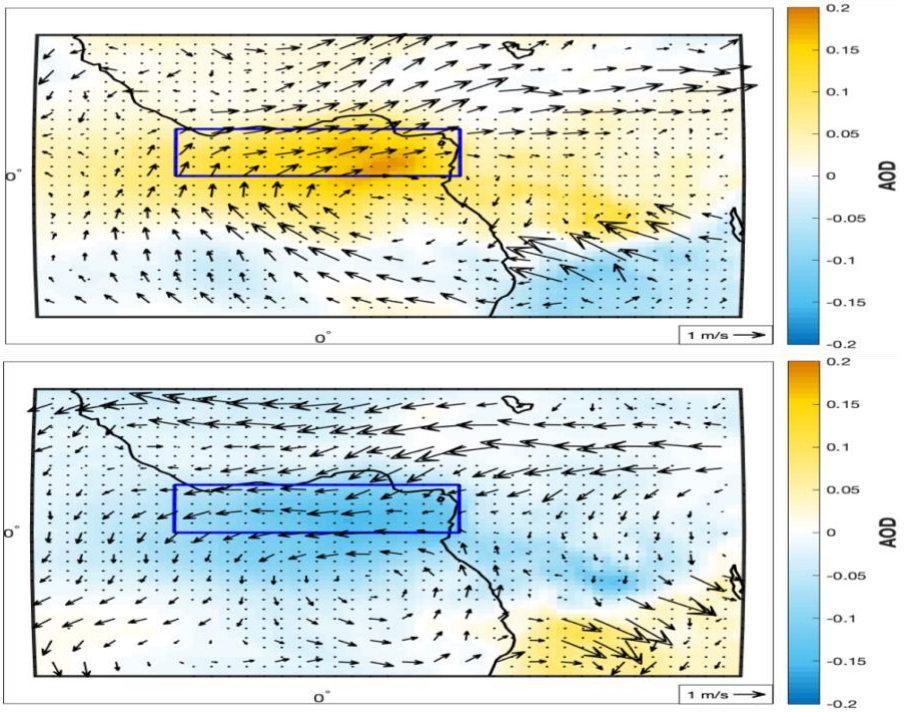

Fig 2.4 AOD and 850hPa wind anomalies for dirty (a) and clean (b) days for the month of August. Stippling represents AOD data that is significant at the 5% level

The presence of increased (decreased) biomass burning aerosols is associated with slight increases (decreases) between ~2%-4% in low-level cloud (surface-700hPa) fraction over our study region in the GoG and Central African interior where aerosols are being transported from (**Fig 2.5**). Considering that the GoG is predominantly covered with lower-level clouds, our results are consistent with Wilcox (2012) and Brioude et al. (2009), who analyzed observations that show that atmospheric warming due to solar absorption by biomass burning aerosols above the cloud layer may enhance the buoyancy of free-tropospheric air above the cloud, inhibit cloud top entrainment and lead to additional cloud thickening in the boundary layer. This may be potentially caused by the semi-direct aerosol effect.

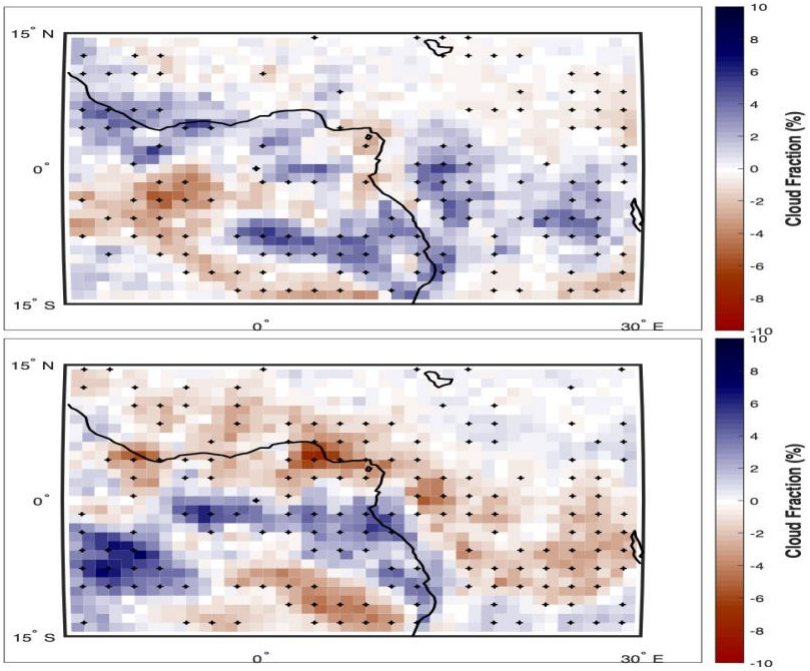

Fig 2.5 Low-level cloud fraction (surface-700hPa) anomalies during dirty (a) and clean (b) days for the month of August. Stippling represents data that is significant at the 5% level

Assuming that aerosols are initially transported around the 850hPa height, aerosol impacts on higher level clouds would be a result of aerosol indirect effects. Therefore, we examine changes in cloud optical depth and cloud water radius (when adequate data is available) in addition to cloud fraction. Looking at mid-low cloud fraction anomalies (700hPa-500hPa), we find increases (decreases) up to 5% for dirty (clean) days respectively between the GoG and the West African coastal region (**Figs 2.6a and 2.**). With an increase in aerosol amount at this particular level, there also exist increases in cloud optical depth (**Fig 2.6b**). Our findings here are in agreement with Kaufman et al. (2005) who they find evidence of a smoke aerosol-induced indirect effect over the eastern Atlantic Ocean during monsoon months for both stratiform and cumulus cloud decks.

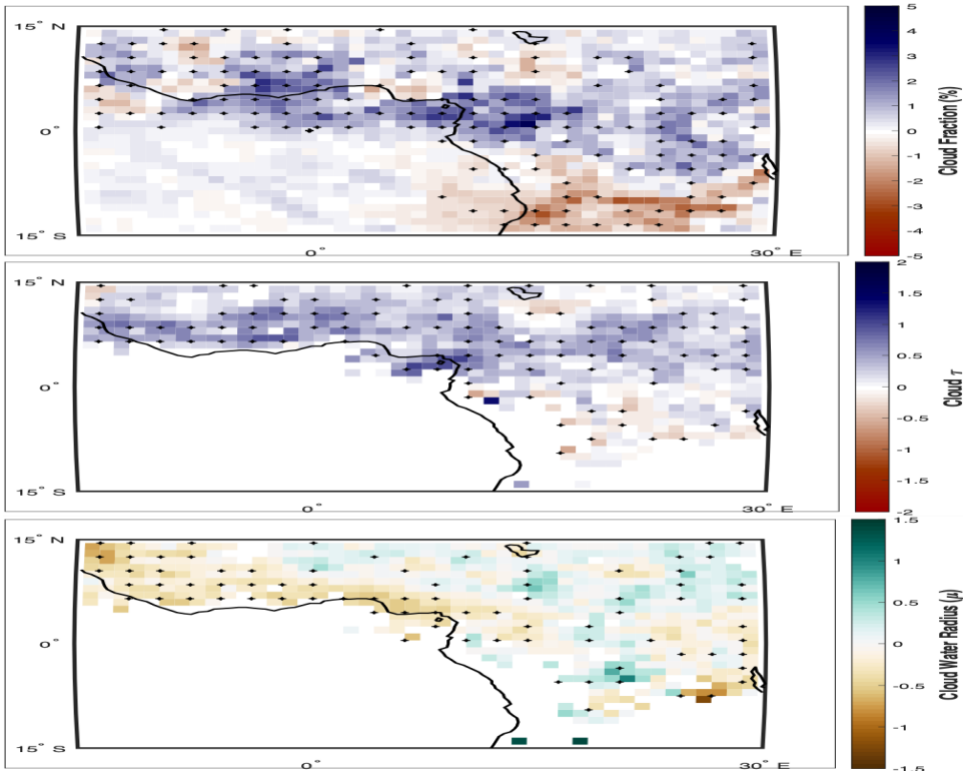

Fig 2.6 Changes in mid-low (700hPa-500hPa) cloud fraction (a), cloud optical depth (b) and cloud droplet radius in units of microns (c) for polluted aerosol conditions. Stippling represents cloud data that is significant at the 5% level

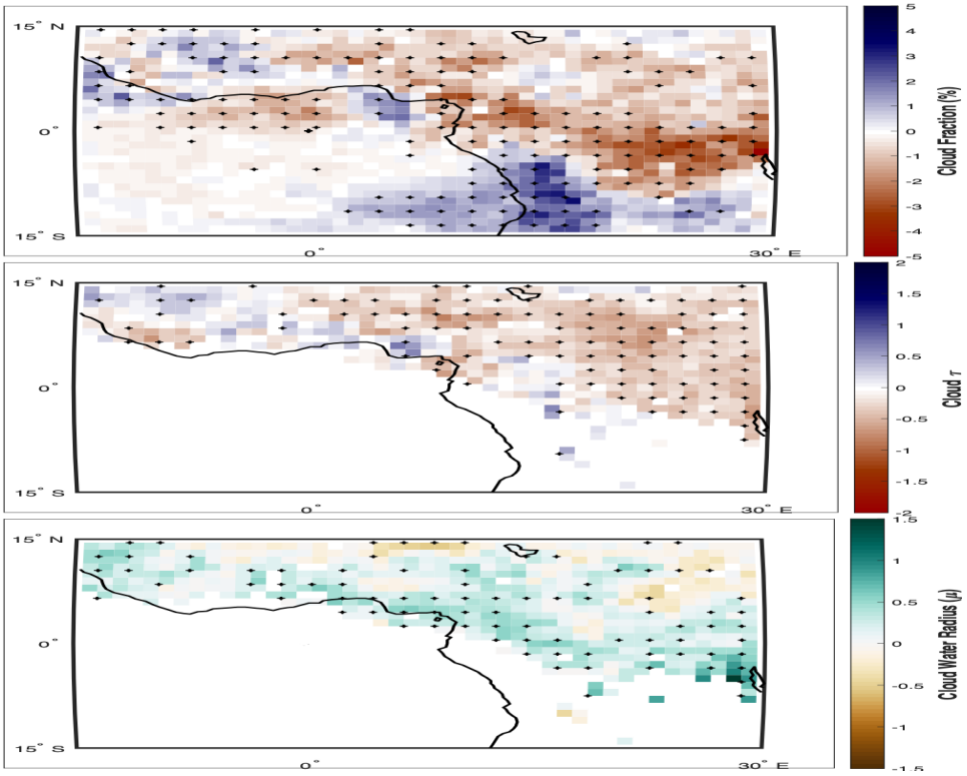

Fig 2.7 Same as figure 6 but under clean aerosol conditions

They attribute increased low-level cloud fraction to dry air entrainment as well. We can see this signal clearly in the GoG on dirty days. The authors correlate increases in cloud coverage and aerosol loading at 3 km with decreases in cloud droplet effective radius (**Fig 2.6c)**. They also find similar results for cumulus clouds that penetrate through the smoke layer. Haywood et al. (2003) found that aerosols over the ocean have a clear separation from the underlying stratiform clouds, whereas over land, biomass-burning aerosols become well mixed up to 500hPa. Over continental air, where deep convection is much stronger than over the ocean, aerosols are lofted into high-level, monsoon strength clouds. For middle high-level clouds (500hPa-300hPa), we find the highest increases in cloud fraction and optical depth over GoG and Southern West Africa (**Fig 2.8**). Contrasting results are found for clean conditions (**Fig 2.9**).

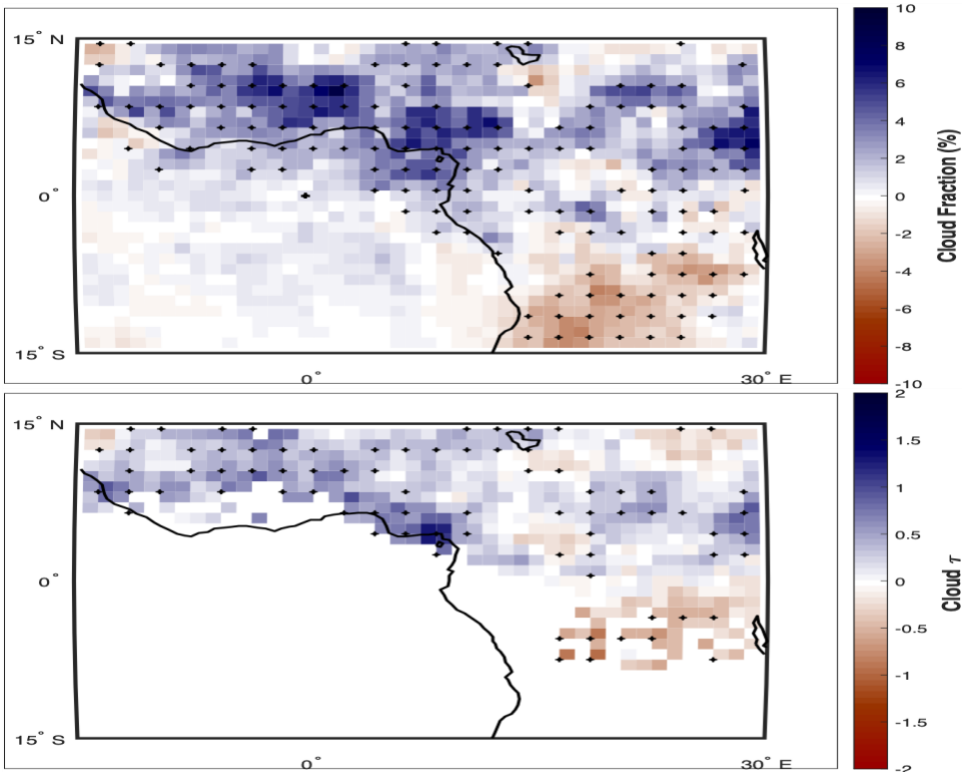

Fig 2.8 Changes in mid-high (500hPa-300hPa) cloud fraction (a) and cloud optical depth (b) during polluted aerosol conditions. Stippling represents cloud data that is significant at the 5% level

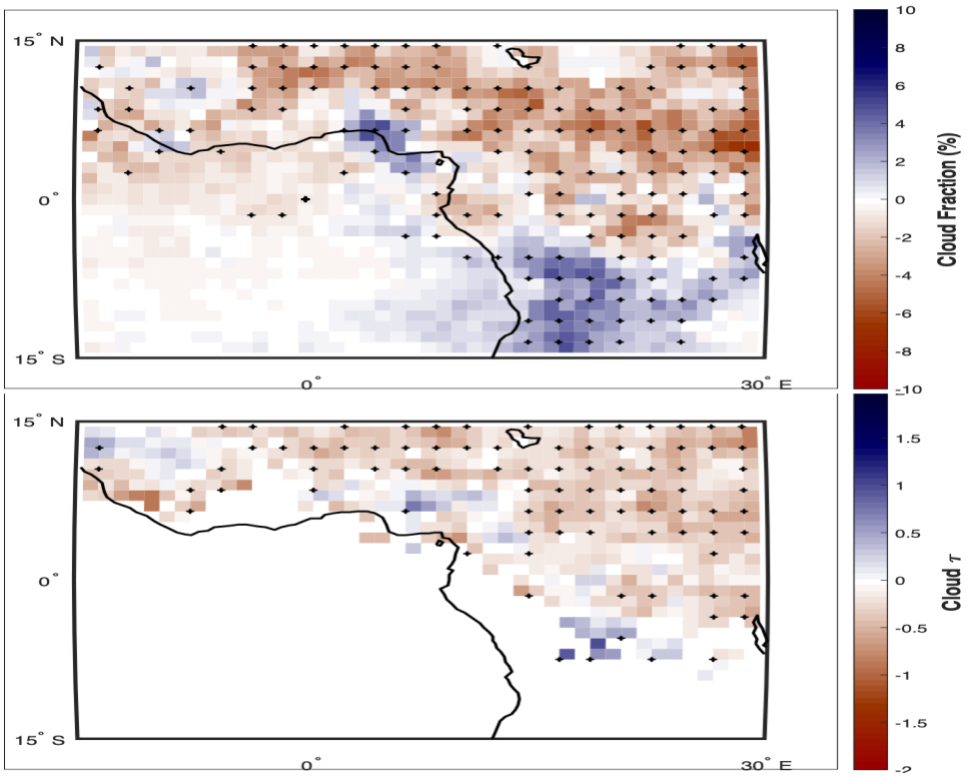

Fig 2.9 Same as figure 8 but under clean aerosol conditions

Changes in the number of absorbing aerosols and cloud fraction lead to further changes in surface heating, which is investigated further by analyzing SW radiation fluxes. **Fig 2.10** shows CERES computed surface SW anomalies during dirty days for the month of August, with the top (bottom) panel represents all-sky (aerosol-only) conditions. At the surface, we find reductions around 10-15 W m^{-2} for all-sky conditions that consist of both clear and cloudy skies, for which ~5 W m^{-2} are due to the direct presence of aerosols. We also find contrasting results for clean days (**Fig 2.11**). A reduction in surface shortwave radiation can decrease surface evaporation and energy available for convection. Therefore, we also explore changes in convective available potential energy (CAPE) during dirty and clean episodes (**Fig 2.12**). When more (less) aerosols are present, a reduction (increase) in CAPE can be seen over our WAM land box and Central Africa where the bulk of monsoon-related precipitation occurs. CAPE reflects the potential vertical speed within an updraft and can be expected to impact the formation of clouds,

especially towering cumulonimbus that reach the tropopause like our current study region. Composite temperature soundings over GoG reveal very little instability (Supplementary figure 2). To complete our analysis of a possible aerosol-cloud-SW radiation feedback, we include changes in high-level (300hPa-tropopause) clouds (**Fig 2.13**). On dirty days, we find reductions in high-level cloud fraction, which is in agreement our previous results showing decreases in surface SW radiation and reduced CAPE. Contrasting results are found on clean days as well.

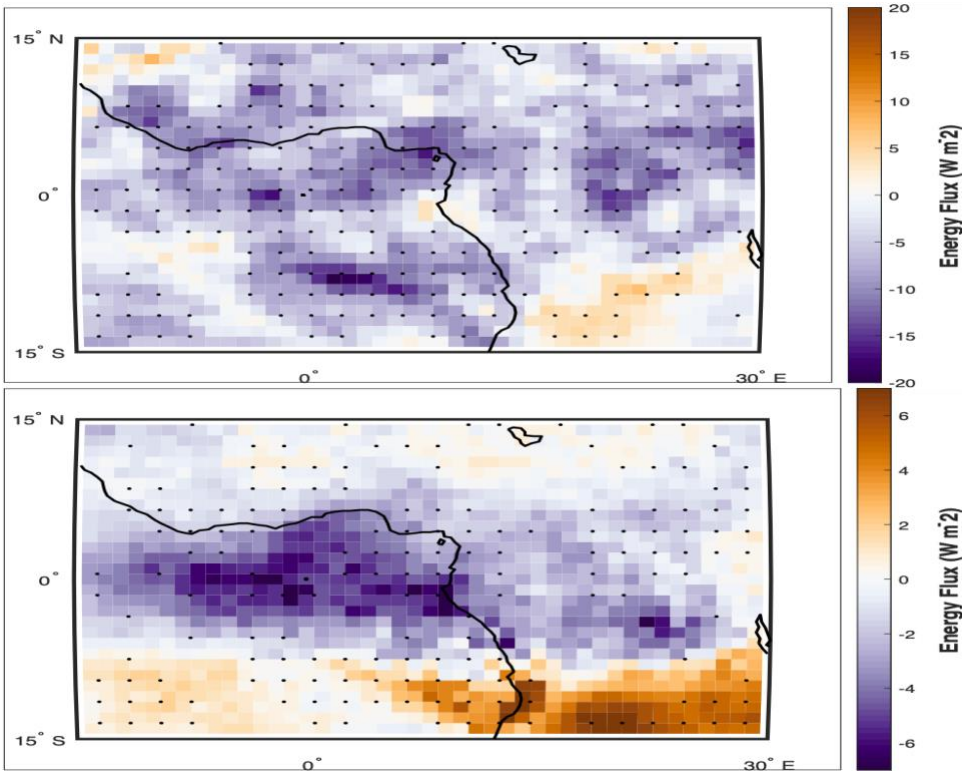

Fig 2.10 CERES computed surface SW anomalies during dirty days for the month of August for all-sky(a) and aerosol-only(b) conditions for polluted days. Stippling represents data that is significant at the 5% level

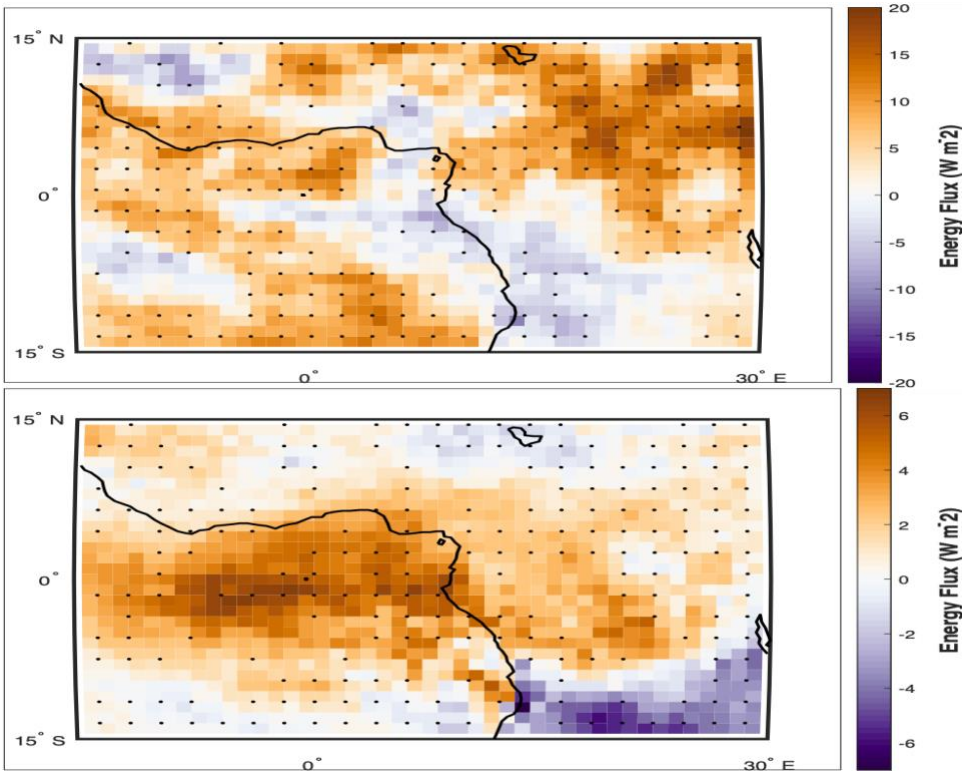

Fig 2.11 Same as figure 10, but with clean days shown

2.3.3 Statistical Relationships between anomalous aerosol transport and the WAM

These AOD, cloud and radiation anomalies within in the GoG, in turn, may potentially impact precipitation in the WAM region. **Fig 2.14** shows precipitation and 925hPa wind anomalies for dirty (top) and clean (bottom) days. Coinciding with dirty days over the GoG is an adjacent decrease in daily precipitation rates along the West African coastline towards its Sub-Saharan interior (Figure 14, box region over West Africa). Decreases of 17% (0.83 mm day^{-1} +/- 0.75 mm day^{-1} on average) relative to a 5.9 mm day^{-1} climatological value can be seen over densely populated countries like Nigeria whose agricultural sector relies on monsoonal rain for annual crop yields. In contrast, increases of 18% (0.91 mm day^{-1} +/- 0.8 mm day^{-1}on average) are associated with clean days over the GoG.

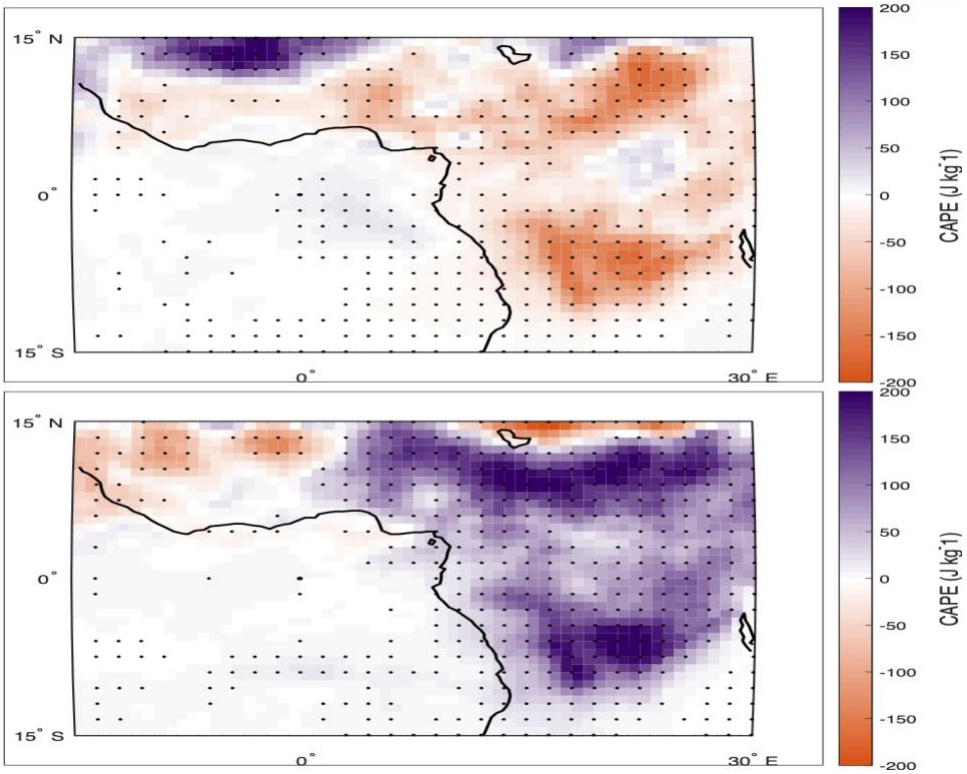

Fig 2.12 Convective available potential energy (CAPE) anomalies for dirty (a) and clean (b) days in the month of August. Stippling represents data that is significant at the 5% level

For further analysis, we compared AOD and precipitation anomalies directly for the month of August during all study years comprising of 403 days by calculating box averages for each day. We use our aforementioned region in the GoG for AOD values, and a region spanning 4.5°N-9.5°N and 9.5°E-9.5°W for precipitation. This boundary encompasses the portion of West Africa that is directly adjacent of the GoG. **Fig 2.15** displays a scatterplot comparing AOD and precipitation rates, providing a good way to visualize how these two variables change together. This fit represents a statistically significant negative relationship and filled circles display where clean and dirty days fall amongst the August spread. For additional context, mean values for each variable are plotted in dotted lines. Previous investigations of relationships between aerosols and precipitation during the Indian summer monsoon are consistent with our results in that increased aerosol is associated with decreased precipitation (Ramanathan et al., 2005;

Shindell et al., 2012).

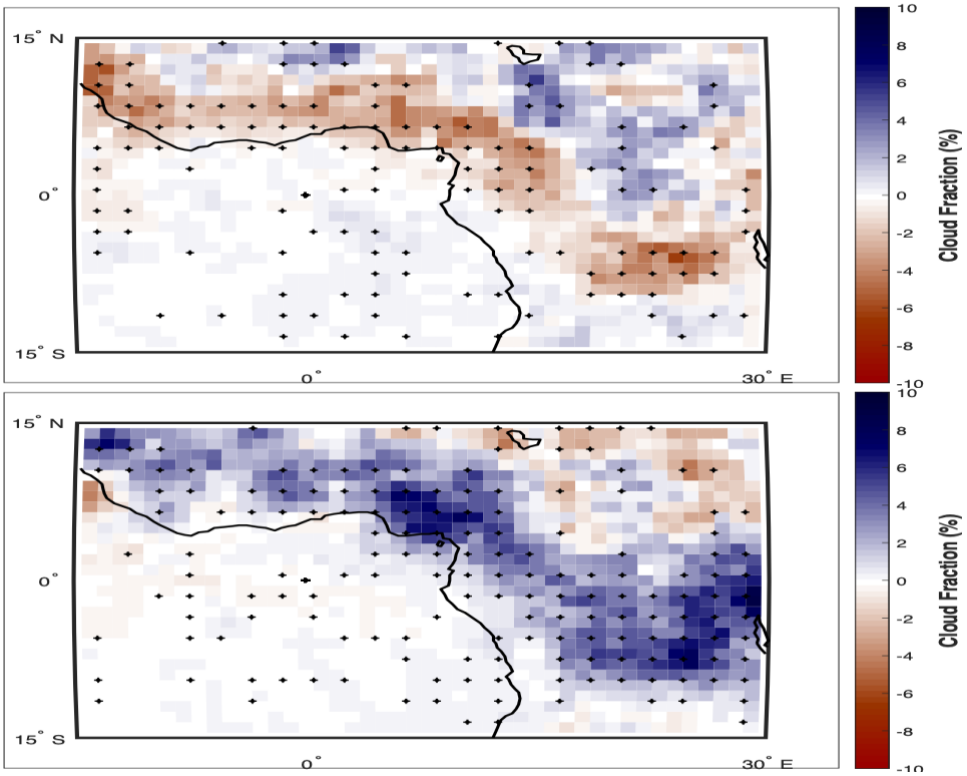

Fig 2.13 High-level cloud fraction (300hPa-tropopause) anomalies during dirty (a) and clean (b) days for the month of August. Stippling represents data that is significant at the 5% level

A potential explanation for the observed precipitation reduction could be simply meteorological variability. What if changes in wind strength, specifically the meridional component can explain the precipitation variability in the WAM region? Ideally, stronger winds from the Gulf of Guinea are indicative of a stronger monsoon flow. If so, the previous connection between aerosols, precipitation, clouds and surface radiation fluxes is merely correlative and not causal. Looking closely at **Fig 2.14** shows stronger meridional winds (925hPa) during dirty days, which would suggest a stronger jet and increased moisture transport, yet there is not an increase in precipitation. Thus, providing good reasoning that local meteorological variability cannot explain changes in aerosol amounts.

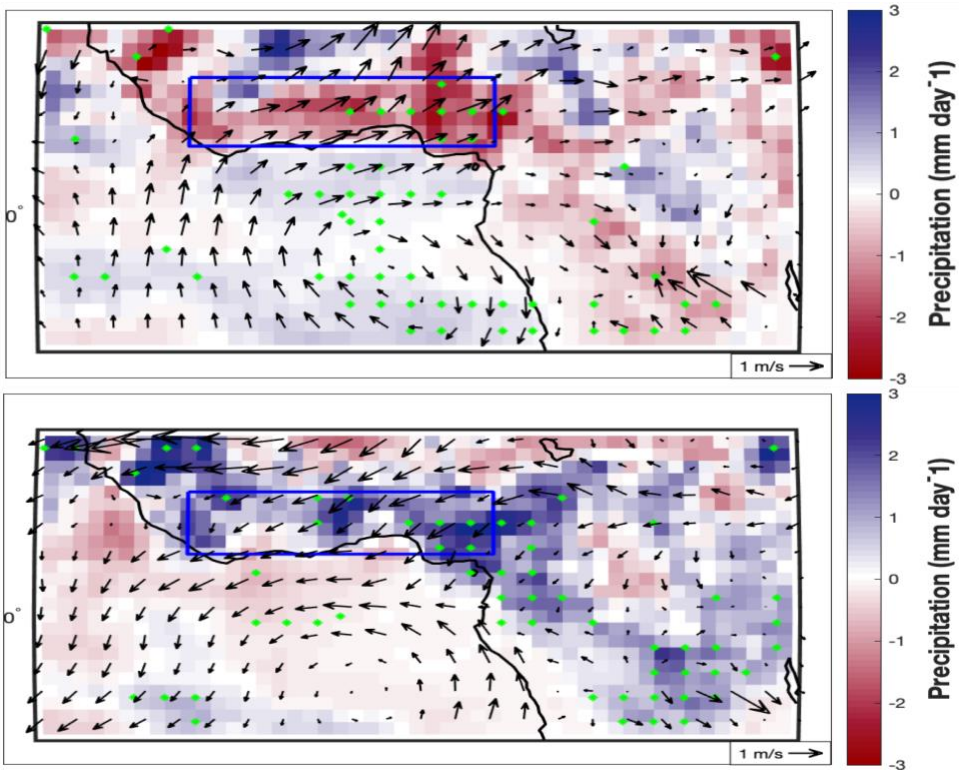

Fig 2.14 Precipitation and 925hPa wind anomalies for dirty (a) and clean (b) days for the month of August. Data significant at the 5% level is shown with filled, green circles. The blue box represents a region downwind of the GoG box highlighting precipitation anomalies

2.4 Conclusion

Variations in wind intensity over source regions of smoke aerosols in tropical Africa leads to anomalous aerosol advection towards the GoG. During the peak in the local monsoon season, we found evidence linking increased aerosol presence with a reduction in precipitation over West Africa. To further understand the possible mechanisms by which this occurs, we analyzed other meteorological variables associated with precipitation.

First, we looked at changes in low level cloud properties associated with dirty and clean aerosol conditions. Throughout our study regions, fine-mode smoke aerosols (Adebiyi et al., 2015) interact with various cloud types and have two different effects on cloud coverage. A

previous study using monthly CALIPSO observations indicated that the peak of smoke aerosols is about 650hPa, which is well above the atmospheric boundary layer (Fig. 1b of Adebiyi and Zuidema, 2018). There is evidence of a semi-direct radiative forcing caused by smoke aerosols in the GoG where low-level clouds dominate the region. At this location, low-level stratocumulus clouds can reside at a lower altitude than smoke aerosols coming from the continent possibly leading to additional cloud coverage. This proposed mechanism for a semi-direct radiative forcing is consistent with the results obtained by Wilcox (2012). Over land, where deep convection is more prevalent, we find evidence for the aerosol indirect effect. Near the West African coastline and Central African interior, we observed increases in mid-level cloud formations during dirty days as shown in **Figure 2.8**. Coupled with an increase in cloud fraction, we find corresponding increases in cloud thickness and decreases in cloud droplet radius. As elegantly noted by Koren et al. (2008), initial cloud fraction plays a critically important role in determining the balance between the two effects. This study further introduces two equations (Eqs. 4-5) representing aerosol direct/indirect effects and its contribution on total cloud fraction by superimposing these two equations (Koren et al. (2008), figure 1). Cloud fields with large cloud fraction will be affected mostly by microphysics, whereas fields with small cloud fraction will be inhibited by aerosol absorption since larger amounts of cloud free sky will be available for aerosol radiative effects to dominate.

The signal for elevated aerosol transport and increased low to mid-level cloud fraction shows itself in the surface SW flux, in which aerosols account for ~33% of the reduction in energy reaching the surface during dirty conditions. With the reduction in SW radiation reaching the surface, we see a corresponding decrease in CAPE which probably promotes a decrease in high-level cloud fraction. We suggest that aerosol radiative effects alter local radiation budgets,

ultimately weakening the energy available for convection and reducing precipitation rates for the month of August in the WAM region.

While this paper proposes a mechanism by which smoke aerosols potentially inhibit monsoon driven precipitation over West Africa, it remains necessary to evaluate how full-physics climate models simulate these aerosol-cloud-precipitation responses over this region, including which aerosol radiative effect is more dominant. Since this research takes a unique approach in linking connections between transport of biomass burning produced aerosols from a source region and monsoon precipitation in another region, there are few related studies for comparison. Additional research will help to clarify the mechanisms and potentially confirm the proposed interactive processes.

Chapter 2, in full, is a reprint of the material as it appears in Climate Dynamics 2020. Ajoku, O., Norris, J. R., & Miller, A. J. (2020). Observed monsoon precipitation suppression caused by anomalous interhemispheric aerosol transport. *Climate Dynamics*, *54*(1-2), 1077-1091. The dissertation author was the primary investigator and author of this paper.

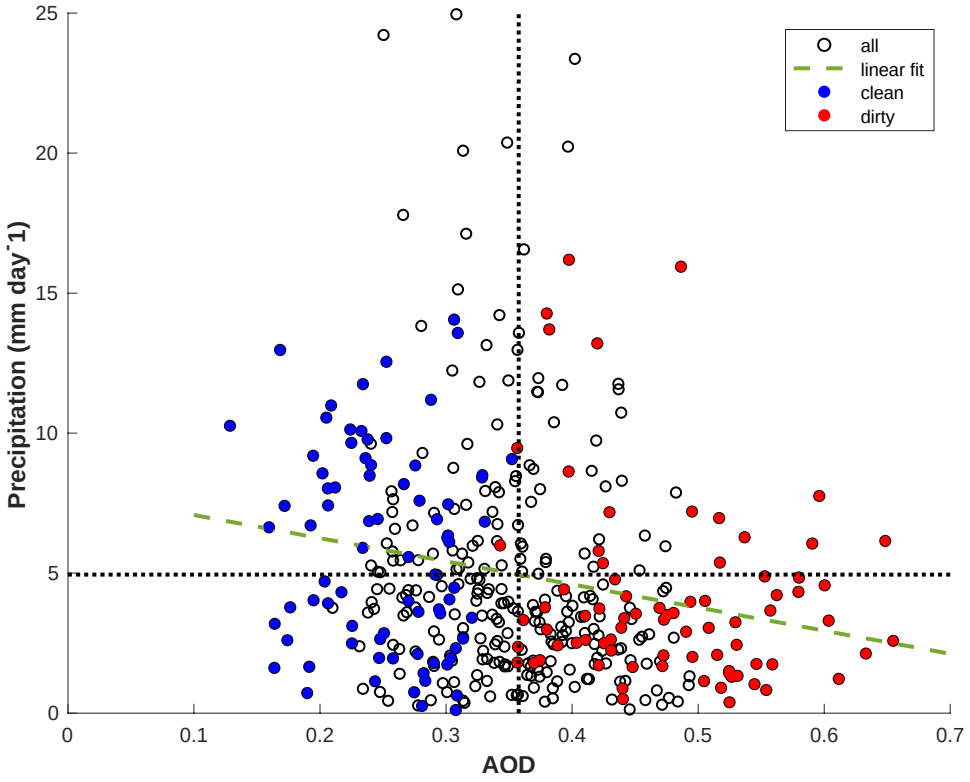

Fig 2.15 Scatterplot of AOD over the Gulf of Guinea study region and precipitation over adjacent land in West Africa for the month of August. Precipitation values are obtained from averaging values in the box shown in figure 14. The red line represents a linear fit of this relationship and dotted circles are mean values for AOD and precipitation. Filled circles reflect data counted during dirty and clean aerosol days

2.5 References

Adebiyi, A A, Zuidema, P, & Abel, S J (2015) The convolution of dynamics and moisture with the presence of shortwave absorbing aerosols over the southeast Atlantic. *Journal of Climate*, *28*(5), 1997-2024

Adebiyi, A. A., & Zuidema, P. (2018). Low cloud cover sensitivity to biomass-burning aerosols and meteorology over the southeast Atlantic. *Journal of Climate*, *31*(11), 4329-4346.

Albrecht, B (1989), Aerosols, cloud microphysics, and fractional cloudiness, Science, 245, 1227-1230, doi:10.1126/science.245.4923.1227

Bengtsson, L, Hagemann, S, & Hodges, K I (2004) Can climate trends be calculated from reanalysis data?. *Journal of Geophysical Research: Atmospheres*, *109*(D11)

Berrisford, P., Dee, D., Poli, P., Brugge, R., Fielding, K., Fuentes, M., Kallberg, P., Kobayashi, S., Uppala, S. and Simmons, A., 2011. The ERA-Interim archive, version 2.0.

Bouniol, D, Couvreux, F, Kamsu-Tamo, P H, Leplay, M, Guichard, F, Favot, F, & O'Connor, E J (2012) Diurnal and seasonal cycles of cloud occurrences, types, and radiative impact over West Africa. *Journal of Applied Meteorology and Climatology*, *51*(3), 534-553

Bourgeois, E., Bouniol, D., Couvreux, F., Guichard, F., Marsham, J.H., Garcia-Carreras, L., Birch, C.E. and Parker, D.J., 2018. Characteristics of mid-level clouds over West Africa. *Quarterly Journal of the Royal Meteorological Society*, *144*(711), pp.426-442.

Brioude, J., Cooper, O.R., Feingold, G., Trainer, M., Freitas, S.R., Kowal, D., Ayers, J.K., Prins, E., Minnis, P., McKeen, S.A. and Frost, G.J., 2009. Effect of biomass burning on marine stratocumulus clouds off the California coast. *Atmospheric Chemistry and Physics Discussions*, *9*(4), pp.14529-14570.

Buchard, V., Da Silva, A.M., Colarco, P.R., Darmenov, A., Randles, C.A., Govindaraju, R., Torres, O., Campbell, J. and Spurr, R., 2015. Using the OMI aerosol index and absorption aerosol optical depth to evaluate the NASA MERRA Aerosol Reanalysis. *Atmospheric Chemistry and Physics*, *15*(10), p.5743.

Clarke, A D, Collins, W G, Rasch, P J, Kapustin, V N, Moore, K, Howell, S, & Fuelberg, H E (2001) Dust and pollution transport on global scales: Aerosol measurements and model predictions. *Journal of Geophysical Research: Atmospheres*, *106*(D23), 32555-32569.

Croft, B., Lohmann, U., & Salzen, K. V. (2005). Black carbon ageing in the Canadian Centre for Climate modelling and analysis atmospheric general circulation model. *Atmospheric chemistry and physics*, *5*(7), 1931-1949.

Deetz, K., Vogel, H., Knippertz, P., Adler, B., Taylor, J., Coe, H., Bower, K., Haslett, S., Flynn, M., Dorsey, J. and Crawford, I., 2018. Numerical simulations of aerosol radiative effects and their impact on clouds and atmospheric dynamics over southern West Africa. *Atmospheric Chemistry and Physics*, *18*(13), pp.9767-9788.

Dentener, F., Kinne, S., Bond, T., Boucher, O., Cofala, J., Generoso, S., Ginoux, P., Gong, S., Hoelzemann, J.J., Ito, A. and Marelli, L., 2006. Emissions of primary aerosol and precursor gases in the years 2000 and 1750, prescribed data-sets for AeroCom.

Doelling, D.R., Loeb, N.G., Keyes, D.F., Nordeen, M.L., Morstad, D., Nguyen, C., Wielicki, B.A., Young, D.F. and Sun, M., 2013. Geostationary enhanced temporal interpolation for CERES flux products. *Journal of Atmospheric and Oceanic Technology*, *30*(6), pp.1072-1090.

Doelling, D R, Sun, M, Nguyen, L. T, Nordeen, M L, Haney, C O, Keyes, D F, & Mlynczak, P E (2016) Advances in geostationary-derived longwave fluxes for the CERES synoptic (SYN1deg) product. *Journal of Atmospheric and Oceanic Technology*, *33*(3), 503-521

Ferek, R.J., Garrett, T., Hobbs, P.V., Strader, S., Johnson, D., Taylor, J.P., Nielsen, K., Ackerman, A.S., Kogan, Y., Liu, Q. and Albrecht, B.A., 2000. Drizzle suppression in ship tracks. *Journal of the Atmospheric Sciences*, *57*(16), pp.2707-2728.

Ghan, S J, Liu, X, Easter, R C, Zaveri, R, Rasch, P J, Yoon, J H, & Eaton, B (2012) Toward a minimal representation of aerosols in climate models: Comparative decomposition of aerosol direct, semidirect, and indirect radiative forcing. *Journal of Climate*, *25*(19), 6461-6476

Giglio, L, Randerson, J T, & van der Werf G R (2013) Analysis of daily, monthly, and annual burned area using the fourth-generation global fire emissions database (GFED4). *Journal of Geophysical Research: Biogeosciences*, *118*(1), 317-328

Global Modeling and Assimilation Office (GMAO)(2015) MERRA-2 tavgM_2d_int_Nx: 2d,Monthly mean, Time-Averaged, Single-Level, Assimilation, Vertically Integrated Diagnostics V5.12.4, Greenbelt, MD, USA, Goddard Earth Sciences Data and Information Services Center (GES DISC), Accessed [July 7, 2017] 10.5067/FQPTQ4OJ22TL

Haywood, J, & Boucher, O (2000) Estimates of the direct and indirect radiative forcing due to tropospheric aerosols: A review. *Reviews of geophysics*, *38*(4), 513-543

Haywood, J M, Osborne, S R, Francis, P N, Keil, A, Formenti, P, Andreae, M O, & Kaye, P H (2003) The mean physical and optical properties of regional haze dominated by biomass burning aerosol measured from the C-130 aircraft during SAFARI 2000. *Journal of Geophysical Research: Atmospheres*, *108*(D13)

Hourdin, F., Musat, I., Guichard, F.S., Ruti, P.M., Favot, F., Filiberti, M.A., Pham, M., Grandpeix, J.Y., Polcher, J., Marquet, P. and Boone, A., 2010. AMMA-model intercomparison project. *Bulletin of the American Meteorological Society*, *91*(1), pp.95-104.

Huang, J, Zhang, C, & Prospero, J M (2009a) African aerosol and large-scale precipitation variability over West Africa. *Environmental Research Letters*, *4*(1), 015006

Huang, J, Zhang, C, & Prospero, J M (2009b) Large-scale effect of aerosols on precipitation in the West African Monsoon region. *Quarterly Journal of the Royal Meteorological Society: A journal of the atmospheric sciences, applied meteorology and physical oceanography*, *135*(640), 581-594

Huffman, G J, Bolvin, D T, & Adler, R F (2016) GPCP version 1.2 one-degree daily precipitation data set. *Research Data Archive at the National Center for Atmospheric Research, Computational and Information Systems Laboratory, Boulder, CO*

Kaufman, Y J, Koren, I, Remer, L A, Rosenfeld, D, & Rudich, Y (2005) The effect of smoke, dust, and pollution aerosol on shallow cloud development over the Atlantic Ocean. *Proceedings of the National Academy of Sciences*, *102*(32), 11207-11212

Knippertz, P., Fink, A.H., Deroubaix, A., Morris, E., Tocquer, F., Evans, M.J., Flamant, C., Gaetani, M., Lavaysse, C., Mari, C. and Marsham, J.H., 2017. A meteorological and chemical overview of the DACCIWA field campaign in West Africa in June–July 2016.

Koren, I, Martins, J V, Remer, L A, & Afargan, H (2008). Smoke invigoration versus inhibition of clouds over the Amazon. *science*, *321*(5891), 946-949

Kruger, A C, Goliger, A M, Retief, J V, & Sekele, S (2010) Strong wind climatic zones in South Africa

Liu, X, Xie, X, Yin, Z Y, Liu, C, & Gettelman, A (2011) A modeling study of the effects of aerosols on clouds and precipitation over East Asia. *Theoretical and applied climatology*, *106*(3-4), 343-354

Marlon, J.R., Bartlein, P.J., Carcaillet, C., Gavin, D.G., Harrison, S.P., Higuera, P.E., Joos, F., Power, M.J. and Prentice, I.C., 2008. Climate and human influences on global biomass burning over the past two millennia. *Nature Geoscience*, *1*(10), pp.697-702.

Nicholson, S.E., Some, B., McCollum, J., Nelkin, E., Klotter, D., Berte, Y., Diallo, B.M., Gaye, I., Kpabeba, G., Ndiaye, O. and Noukpozounkou, J.N., 2003. Validation of TRMM and other rainfall estimates with a high-density gauge dataset for West Africa. Part II: Validation of TRMM rainfall products. *Journal of Applied Meteorology*, *42*(10), pp.1355-1368.

Nwofor, O K, Dike, V N, Lin, Z., Pinker, R T, & Onyeuwaoma, N D (2018) Fine-Mode Aerosol Loading Over a Sub-Sahel Location and Its Relation with the West African Monsoon. *Aerosol Science and Engineering*, *2*(2), 74-91

Ramanathan, V C P J, Crutzen, P J, Kiehl, J T, & Rosenfeld, D (2001) Aerosols, climate, and the hydrological cycle. *science*, *294*(5549), 2119-2124

Ramanathan, V., Chung, C., Kim, D., Bettge, T., Buja, L., Kiehl, J.T., Washington, W.M., Fu, Q., Sikka, D.R. and Wild, M., 2005. Atmospheric brown clouds: Impacts on South Asian climate and hydrological cycle. *Proceedings of the National Academy of Sciences*, *102*(15), pp.5326-5333.

Rosenfeld, D., Lohmann, U., Raga, G.B., O'Dowd, C.D., Kulmala, M., Fuzzi, S., Reissell, A. and Andreae, M.O., 2008. Flood or drought: how do aerosols affect precipitation?. *science*, *321*(5894), pp.1309-1313.

Shindell, D T, Voulgarakis, A, Faluvegi, G, & Milly, G (2012) Precipitation response to regional radiative forcing. *Atmospheric Chemistry and Physics*, *12*(15), 6969-6982

Stocker, T.F., Qin, D., Plattner, G.K., Tignor, M.M., Allen, S.K., Boschung, J., Nauels, A., Xia, Y., Bex, V. and Midgley, P.M., 2014. Climate change 2013: the physical science basis. Contribution of working group I to the fifth assessment report of IPCC the intergovernmental panel on climate change.

Tosca, M G, Diner, D J, Garay, M J, & Kalashnikova, O V (2015) Human-caused fires limit convection in tropical Africa: First temporal observations and attribution. *Geophysical Research Letters*, *42*(15), 6492-6501

Twomey, S, Gall, R, & Leuthold, M (1987) Pollution and cloud reflectance. *Boundary-Layer Meteorology*, *41*(1-4), 335-348

Van Der Werf, G.R., Randerson, J.T., Giglio, L., Van Leeuwen, T.T., Chen, Y., Rogers, B.M., Mu, M., Van Marle, M.J., Morton, D.C., Collatz, G.J. and Yokelson, R.J., 2017. Global fire emissions estimates during 1997-2016. *Earth System Science Data*, *9*(2), pp.697-720.

Wilcox, E M (2012) Direct and semi-direct radiative forcing of smoke aerosols over clouds. *Atmospheric Chemistry and Physics*, *12*(1), 139-149

Wilcox, E M, Thomas, R M, Praveen, P S, Pistone, K, Bender, F A M, & Ramanathan, V (2016) Black carbon solar absorption suppresses turbulence in the atmospheric boundary layer. *Proceedings of the National Academy of Sciences*, *113*(42), 11794-11799

Wild, M (2012) Enlightening global dimming and brightening. *Bulletin of the American Meteorological Society*, *93*(1), 27-37

Xie, X, Wang, H, Liu, X, Li, J, Wang, Z, & Liu, Y (2016) Distinct effects of anthropogenic aerosols on the East Asian summer monsoon between multidecadal strong and weak monsoon stages. *Journal of Geophysical Research: Atmospheres*, *121*(12), 7026-7040

Zhang, Y., Fu, R., Yu, H., Qian, Y., Dickinson, R., Silva Dias, M.A.F., da Silva Dias, P.L. and Fernandes, K., 2009. Impact of biomass burning aerosol on the monsoon circulation transition over Amazonia. *Geophysical Research Letters*, *36*(10).

Zuidema, P, Redemann, J, Haywood, J, Wood, R, Piketh, S, Hipondoka, M, & Formenti, P (2016) Smoke and clouds above the southeast Atlantic: Upcoming field campaigns probe absorbing aerosol's impact on climate. *Bulletin of the American Meteorological Society*, *97*(7), 1131-1135

Chapter 3: Model Evaluation of Aerosol-Induced Monsoon Suppression Using Community Earth System Model Version 2

Osinachi F. Ajoku[1*], Arthur J. Miller[1], Joel R. Norris[1] and Rebecca Buchholz[2]

1 Scripps Institution of Oceanography, University of California San Diego, La Jolla, California, USA

2 National Center of Atmospheric Research, Atmospheric Chemistry Observations and Modeling, Boulder, CO USA

Corresponding author: Osinachi Ajoku (oajoku@ucsd.edu)

Key Points:

- Increases in the loading of biomass burning over the equatorial Atlantic is associated with altered climatic conditions.
- Model simulations show that changes in shortwave cloud radiative effects drive most of the precipitation changes along the Guinea coastline

Abstract

Physical mechanisms underlying aerosol-induced suppression over West Africa are explored using the Community Earth System Model version 2 (CESM 2). Extending upon previous research, model simulations forced with specified dynamics and free-running aerosols reveal drier atmospheric conditions associated with dirty aerosol conditions. We find +/- 3%

changes in convective cloud cover between 5N-10N that is responsible for the bulk of precipitation changes. Model simulated changes in shortwave fluxes dominate the radiation response. Along the Guinea coastline, we find +/- 20 W m^{-2} changes in surface shortwave cloud radiative effects. Changes in radiation due to black carbon (BC) are negligible or opposite in sign relative to cloud radiative effects. During dirty conditions, increased stability (atmospheric warming and surface cooling) leads to 15-25 J kg^{-1} reductions in Convective Available Potential Energy and 600-meter declines in cloud top height along the Guinea coastline. Changes in cloud droplet number concentration ranging from 2-7 cm^{-3} bounded below 700mb and average droplet effective radius ranging from 0.2-0.7 microns below 600mb accompany such precipitation reductions (~2.5 mm day^{-1}). Our model simulations show that aerosol semidirect and indirect effects interact together to alter cloud formation processes and ultimately the precipitation response. These results are consistent with the types of responses that we have surmised using observations alone.

3.1 Research Background

The influence of aerosols on rain-bearing clouds represents one of the most uncertain climate forcings (Myhre et al. 2013). Fires account for 20% of the global aerosol emissions, with about 80% of biomass burning aerosols originating in the tropics (Dentener et al., 2006). Biomass burning aerosols have been shown to influence clouds, rainfall and monsoon onsets over Asia and South America (e.g. Chung and Ramathan 2006; Zhang et al. 2009). However, much less attention has been given to its influence on rainfall and monsoon onset over Africa. Africa is an important global source of aerosols that has far reaching influence, including on rainfall over the Sierras in California (e.g., Creamean et al. 2013) as well as a more regional influence (Randles & Ramaswamy, 2010). Rainfall plays a central role in food production, sustaining the ecosystem and wildlife, and ultimately in determining wildfires and aerosol emissions.

Physical properties within each aerosol allow for an interaction with incoming shortwave (SW) radiation, either through scattering or absorbing (aerosol direct effect). Generally, the smaller the size of a particle, the weaker its ability to scatter radiation (Petty, 2006). Thus, fine-mode biomass burning-produced aerosols such as black carbon (BC) act as an efficient absorber of SW radiation. In addition, such properties allow for a warming of the lower atmosphere coupled with diminished radiation reaching the surface. These combined effects result in stability of the atmosphere and an alteration of the hydrological cycle (Ramanathan & Carmichael, 2008).

Although aerosols affect clouds and precipitation in complex ways involving several competing processes, a pattern is emerging: aerosols tend to invigorate clouds and rainfall under

humid, thermodynamically less stable and moderately polluted conditions, but tend to suppress clouds and rainfall under dry, stable conditions with high vertical wind shear and heavy pollution (Altaratz et al. 2014; Rosenfeld et al. 2014; Chakraborty et al., 2016, 2018). This is because a relatively humid and unstable environment leads to clouds with greater cloud water path (CWP), which create a favorable condition for the aerosol indirect (microphysical) effect which invigorates shallow convection. In contrast, a relatively dry and stable environment tends to produce clouds with lower CWP, and so promotes the aerosol semi-direct (thermodynamic) effect. Altaratz et al. (2014) and Rosenfeld et al. (2014) further suggest that entrainment of dry ambient air would enhance evaporation of cloud droplets, especially the smaller droplets that are increased by aerosols. Note that biomass burning-produced aerosols are transported within dry air masses. In contrast, the entrainment of humid ambient air would reduce evaporation of cloud droplets, allowing smaller cloud droplets to rise to the freezing level and provide more latent heating, invigorating updrafts and convective anvils. The change of latent and radiative heating, can, in turn, affect monsoon circulation.

Given the strong rainfall variability over tropical-subtropical Africa (e.g., Maley 1982) and the coupling between rainfall over the Guinea coastline and aerosol emissions over the Gulf of Guinea (Ajoku et al. 2020), it is imperative to understand the physical mechanisms by which shortwave (SW) radiation absorbing biomass burning aerosols such as BC may impede precipitation processes. In a broader context, there are two basic scenarios: A) Large-scale meteorology controls both the precipitation changes and the distribution of aerosols, with no significant effects of the aerosols in controlling the precipitation changes; and B) Large-scale meteorology advects the aerosols and the aerosols then help to control precipitation changes. The aerosols may reduce the precipitation in three ways; i) direct radiative forcing that cools the

surface and warms the atmosphere, thereby increasing stability and decreasing CAPE; ii) indirect radiative forcing that changes cloud radiative properties such that the surface is cooled, the atmosphere is stabilized and CAPE decreases, or iii) inducing microphysical changes that suppress precipitation apart from the meteorological changes. A complete understanding of all these effects using observations alone is not possible with our current measuring strategies and observations. So, we turn to implementing climate model simulations to attempt to address key parts of the process.

Climate models can be used in many ways to address these issues. One could study long free-running simulations with aerosol emissions specified at the surface in tropical Africa, and then extract anomalies over the target area for clean and dirty days as Ajoku et al. (2020) did using observations. We did not have any daily-sampled runs available to address the problem in this way. In addition, these runs would not be directly comparable to observations since they generate their own random states. A second approach is to initialize the model using observations and run the model forward with specified surface emissions to allow fully-coupled behavior that, at least for a short time period (~days to weeks), can follow observed meteorological conditions. Random variability in the atmosphere will obscure the signal so that ensembles of these initial-condition runs would be needed to gain significance. A third approach is to use a constrained model run where the climate model is partly nudged to observed fields (e.g., wind, temperature) with the specified aerosol emissions being advected by the mereology and affecting the radiation budget and the cloud properties downstream over the GoG. This approach allows direct comparison with the observed features but includes the imprint of the effects of observed rainfall (i.e., the changes in winds and temperature associated with observed convection), which itself

may have been influenced by observed aerosols. This does allow us, however, to study the impact of the aerosols on the radiative properties of the system locally in the GoG.

Following the research published in Ajoku et al. [2020], we use the latter two climate modeling approaches in this study to examine aerosol-cloud-precipitation responses in the GoG. First, we examine a climate model constrained to follow the observed wind and temperature fields with specified surface emissions of aerosols. How well can the climate model represent the observed distributions of aerosols over the GoG that were studied by Ajoku et al. (2020). Do these runs generate a radiative response in aerosols that is consistent with precipitation-altering mechanism invoked by Ajoku et al (2020) using observations alone?

Second, we execute free-running initial condition simulations for two key years, 2006 and 2012, which correspond to strong dirty conditions and sharply clean conditions. We compare the subsequent freely-evolving atmosphere-cloud-aerosol-radiation feedbacks over the GoG in these two years to better isolate the full effects of aerosols on the cloud properties, radiative budget, and precipitation field. How well do these initial-condition climate model runs correspond to the observed monsoon response as seen in observational data? For insight, we additionally execute diagnostic "double radiation" calls within these simulations, with the BC forcing effect turned off to determine its simultaneous effect on the radiation budget. Does BC primarily affect the monsoon response through the direct effect, the indirect effect or the cloud microphysics effect of its presence. We first give a detailed explanation of the model and our modeling strategy in the section 2. The results are presented in section 3. Finally, we give a summary of results in the section 4.

3.2 Modeling Methodology

3.2.1 Model Description

The model simulations for this research were conducted using a beta version of Community Earth System Model version 2 (CESM 2) provided by the National Center for Atmospheric Research (NCAR). CESM is a state-of-the-art, fully coupled, global climate model (GCM) capable of simulating Earth's climate through various temporal scales. The atmospheric portion of CESM, referred to as the Community Atmospheric Model (CAM) includes substantial improvements in most atmospheric physics parameterizations.

The Cloud Layers Unified by Binomials (CLUBB) scheme is a prognostic moist turbulence scheme that aids the model in simulating cloud microphysics, boundary layer turbulence and shallow convection (Gettleman & Morrison, 2015). A two-moment prognostic microphysics (MG2) interacts with the Modal Aerosol Module (MAM4) aerosol microphysics scheme to calculate condensate mass fractions and number concentrations. Danasaboglu et al. [2020] provides an overview of CESM 2 in which they detail improvements and biases compared to its predecessor. In particular, this release improves on the low AOD biases over central Africa, which is crucial for this research.

CESM 2 is configured using Community Atmosphere Model version 6 (CAM6) with comprehensive tropospheric and stratospheric chemistry representation, otherwise known as CAM-chem (Emmons et al., 2020). The chemical mechanism in CAM-chem is based on the

chemical transport model, Model for Ozone And Related chemical Tracers (MOZART) with chemistry coupled to MAM4 that can distinguish between fine mode and coarse mode aerosols. CAM-chem can be run either as a free-running model in which meteorology is internally produced by the model physics or run with specified dynamics (SD) configurations, whereby certain prognostic variables are nudged toward target fields such as reanalysis with the aim of creating reproducible meteorological conditions. Tilmes et al., [2019] provides an overview of the climate forcing and trends of organic aerosols (OA) under various atmospheric configurations and OA schemes.

Table 3.1 List of model output variables from CAM-chem SD and hybrid branch runs (in italics). Variables with an asterisk were used in the double radiation call.

Name	**Long name**
bc_a1	Fine mode BC concentration
CLDHGH	Vertically-integrated high cloud
CLDHGT	Cloud top height
CLDLIQ	Grid box averaged cloud liquid amount
CLDLOW	Vertically-integrated low cloud
CLDMED	Vertically-integrated mid-level cloud
CLOUD	Cloud fraction
CONCLD	*Convective cloud cover*
FLNT*	Net longwave flux at top of model
FLNTC*	Clear sky net longwave flux at top of model
FLUT*	Upwelling longwave at top of model
FSDS*	Downwelling solar flux at surface
FSDSC*	Clear sky downwelling solar flux at surface
FSNS*	Net solar flux at surface
FSNSC*	Clear sky downwelling solar flux at surface
H2O	Water vapor concentration

PRECT	Total precipitation (convective and large-scale), liquid + ice
Q	Specific humidity
T	Temperature
U	Zonal wind
V	Meridional wind
AREL	*Average Droplet Effective Radius*
AWNC	*Average cloud water number concentration*
CAPE	*Convective available potential energy*
*LWCF**	*Net Longwave cloud forcing*
OMEGA	*Vertical velocity*
*SWCF**	*Net Shortwave cloud forcing*

3.2.2 Model Experiments

We employ CAM6-chem with SD using Modern-Era Retrospective analysis for Research and Applications, Version 2 (MERRA2) meteorological fields for detailed comparisons to Ajoku et al. [2020] at the standard horizontal resolution of 1 degree. A full list of input fields required for SD can be found in table 2 of Lamarque et al., [2012]. This model was utilized for the years 2002-2015 using compset FCSD and tested resolution f09_f09_mg17(1-degree horizontal resolution). SD compsets use CMIP6 emissions, observed sea surface temperatures (SSTs), observed sea ice values and are set up to be nudged to winds, temperature and surface fluxes with a 50-hour relaxation (1%) timescale to simulate historical variability and run on 56 vertical levels. Biogenic emissions are calculated online in the coupled Community Land Model (CLM) using the Model of Emissions of Gases and Aerosols from Nature version 2.1 (MEGAN 2.1). A detailed description of CESM2/CAM-chem and its configurations can be found in Emmons et al., [2020]. The user namelist was edited as to modify output variables and provide model output

on a daily frequency. RB designed and executed the SD model simulation. This simulation is used in order to constrain known variability within atmospheric circulation and better isolate chemical processes.

The data analysis conducted in this study and the overall study region is similar to preceding work and can be found under section 2 of Ajoku et al., [2020]. In addition to the SD run described above, initial condition (IC) runs with the freely evolving climate model were conducted to simulate high (2006) and low (2012) aerosol optical depth (AOD) years within our study region (**Fig. 3.1**). In each IC run, the model is initialized for July of the simulated year using initialization datasets from our SD run and run without any nudging for 2 months with the same aerosol emissions. Since the model is free-running, meteorology may not be specific to those years but emissions will be since they are prescribed. For each IC case, we also compute parallel diagnostic (known as a "double radiation" call) of the impacts of BC on SW radiation. This additional evaluation of the radiation budget excludes interactions with BC aerosols and, by differencing the two runs, allows us to look more closely at changes in energy fluxes due to BC. **Table 3.1** lists the model output variables used in this study. OFA conducted the hybrid runs with the guidance of RB. The data analysis conducted in this study and the overall study region is similar to preceding work and can be bound under section 2 of Ajoku et al. [2020].

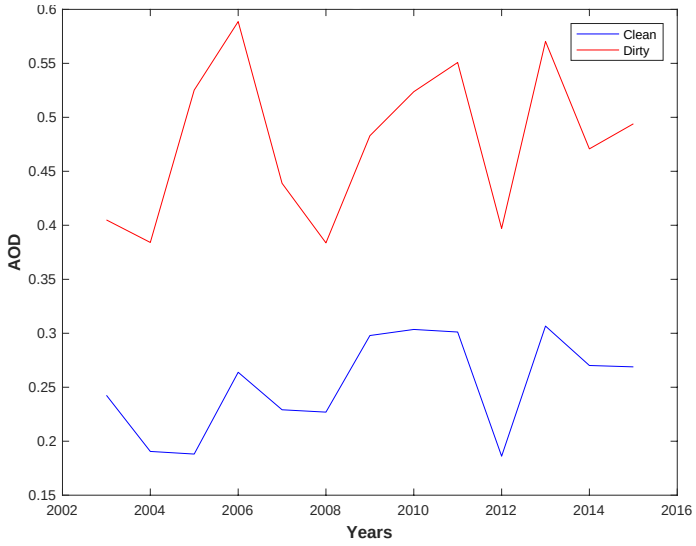

Figure 3.1 Box-averaged AOD during dirty and clean conditions over the Gulf of Guinea for the month of August from MERRA2 reanalysis.

3.3 Results

3.3.1 Aerosol-Cloud-Precipitation Reproducibility

The first focal point of this work is to see how well CAM-chem with SD can reproduce the main results obtained in Ajoku et al., [2020]. In particular, we evaluated aerosol concentration, corresponding cloud structure and resulting precipitation response. We found that this model is able to properly reproduce aerosol transport from central Africa towards the Gulf of Guinea. Changes in fine mode BC concentration are controlled by increased surface wind convergence or divergence over the GoG and result in a dry mixing ratio ~ +/- 2.5×10^{-9} kg kg^{-1} relative to a mean value ~1.5×10^{-8} kg kg^{-1} (**Figure 3.2**). We can clearly see that during increased aerosol loading over the GoG, there is a deficit present over central Africa indicating that wind intensity over the BC source region is the dominant driver of advection.

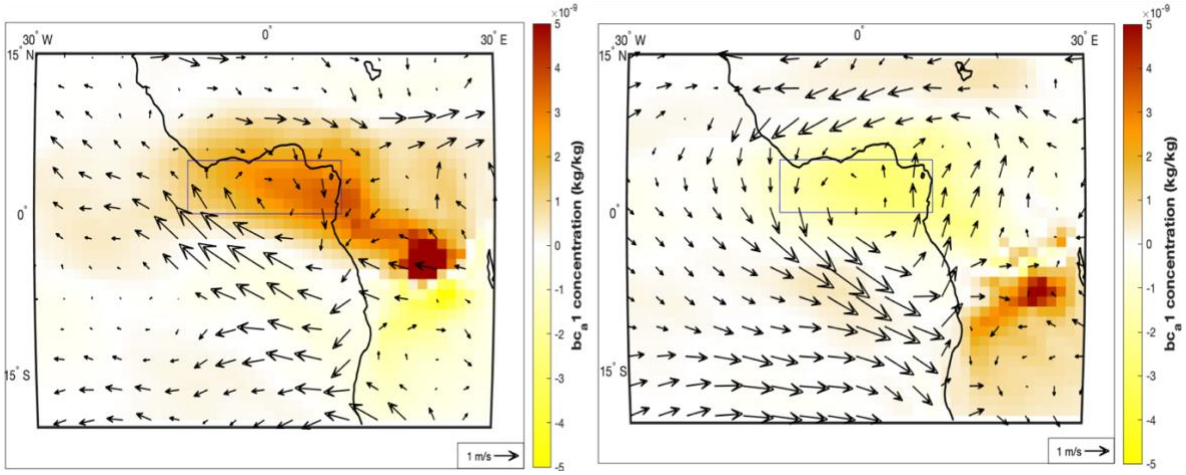

Figure 3.2 Fine mode BC concentration and 857mb wind anomalies for dirty (left) and clean (right) conditions. Rectangular box reflects the area used to average fine mode BC values and create data composites

Analysis of the low cloud model response found here is in contrast to results found in our previous study. Initially in observations, we found 2-4% changes in low-level cloud cover (surface-700mb) throughout the GoG and adjacent land with increasing aerosol values using data from the Clouds and the Earth's Radiant Energy System (CERES) catalog. Note that satellite observations of low clouds are obscured by high clouds and can lead to uncertainty in measurements. Here, we find 4-6% changes in coverage and they are solely concentrated over the GoG and Guinea coastline (**Figure 3.3b and 3.3c**). During dirty conditions, we find decreases in low cloud fraction within the GoG and Guinea coastline, which are the opposite sign to those that we see with CERES data (**Figure 3.4**). However, these results are in agreement with Tosca et al. [2014] and Allen et al. [2019]. With less aerosols present, we see increases in low cloud fraction. However, our model results are in agreement with the overall change in high level cloud fraction (400mb-tropopause) that we found in observations. Most of the changes we see in

high level clouds during dirty conditions (**Figure 3.3e**) occur over land as that is where the bulk of clouds reside normally (**Figure 3.3d**) as well as it being the source of the aerosols.

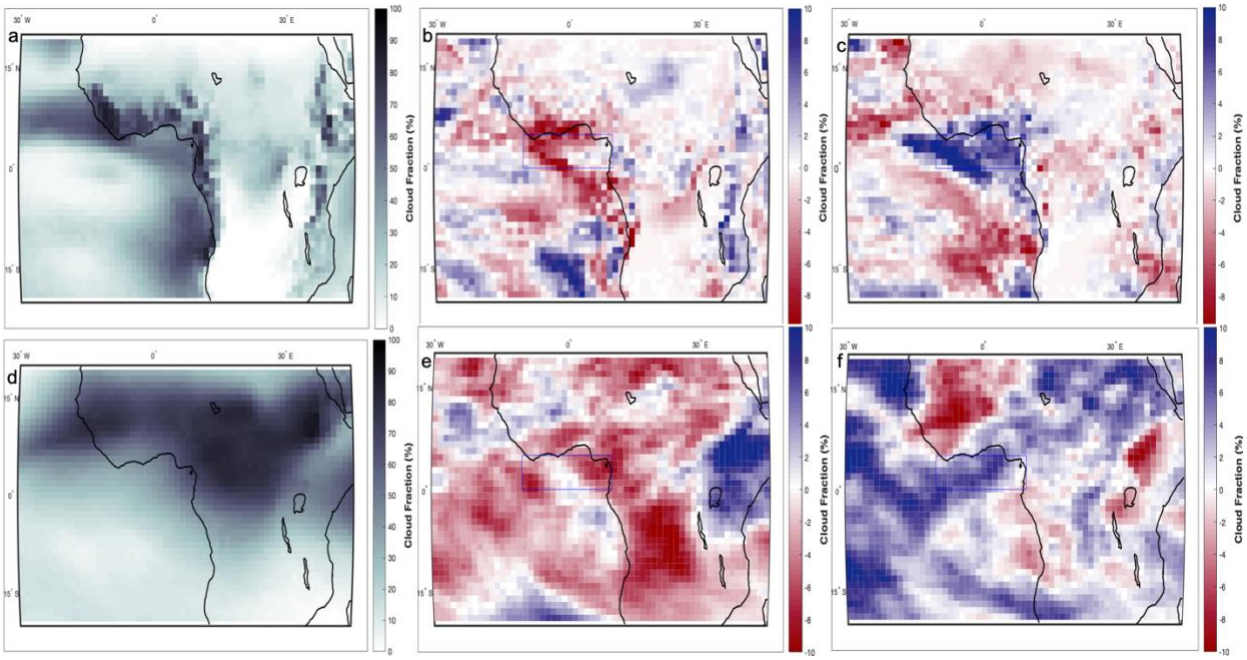

Figure 3.3 Simulated vertically integrated cloud fraction and aerosol-associated changes. Top panel represents climatological low cloud fraction (a) and anomalies for dirty(b) and clean(c) conditions in the GoG. Bottom panel represents climatological high cloud fraction (d) and anomalies for dirty(e) and clean(f) conditions in the GoG.

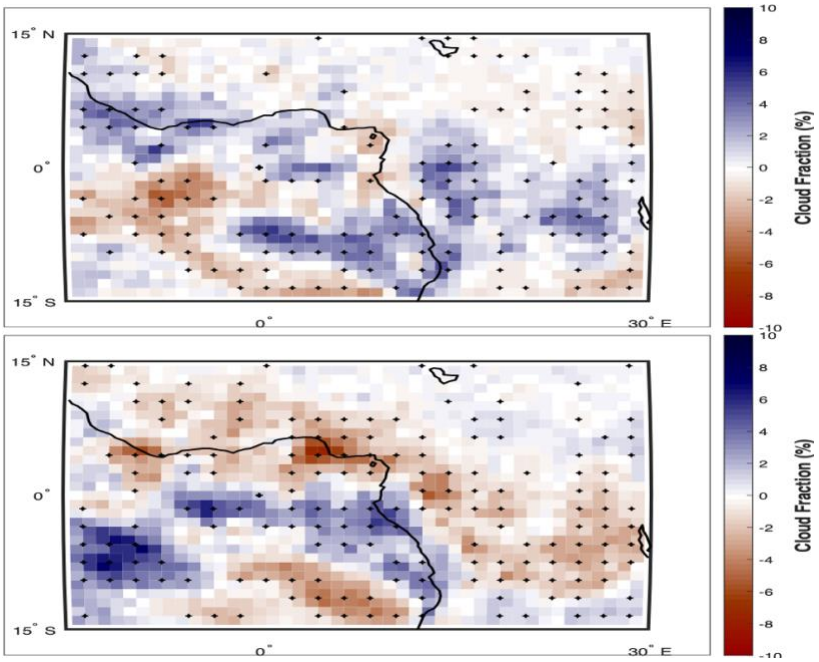

Figure 3.4 Observed, vertically integrated low cloud fraction for dirty(top) and clean(bottom) conditions as shown in Ajoku et al. (2020).

CAM-chem runs with SD include a modification to the Zhang and McFarlane technique that improves convective precipitation (Yang et al., [2013]). Our model simulation correctly captures the basic structure of observed precipitation changes over the Guinea coastline for both aerosol conditions (**Figure 3.5**). Values of precipitation rate anomalies match well with our previous study ranging ~+/-2.5 mm day^{-1} over densely populated Nigeria (**Figure 3.6)**. We note a slight northward shift in anomalous cyclonic/anticyclonic winds compared with our analysis using ERA-Interim global atmospheric reanalysis. This can be contributed to a difference in temporal sampling. In our previous study, we used winds from 6 A.M. while we used daily averaged in the current study to be consistent with the analysis of Tosca et al. [2015]. The daytime warming allows for a stronger monsoonal flow within the diurnal cycle that is captured in the model. Out model results show that during dirty aerosol conditions, decreases throughout the cloud column over the Guinea coastline leads to a decrease in precipitation rates. In addition,

we note an increase in precipitation further North in both models and observations, which is in agreement with Zhang et al., [2008] who find similar results of a northern latitudinal shift of precipitation maximum while modeling the direct radiative forcing of carbonaceous aerosols in East Asia.

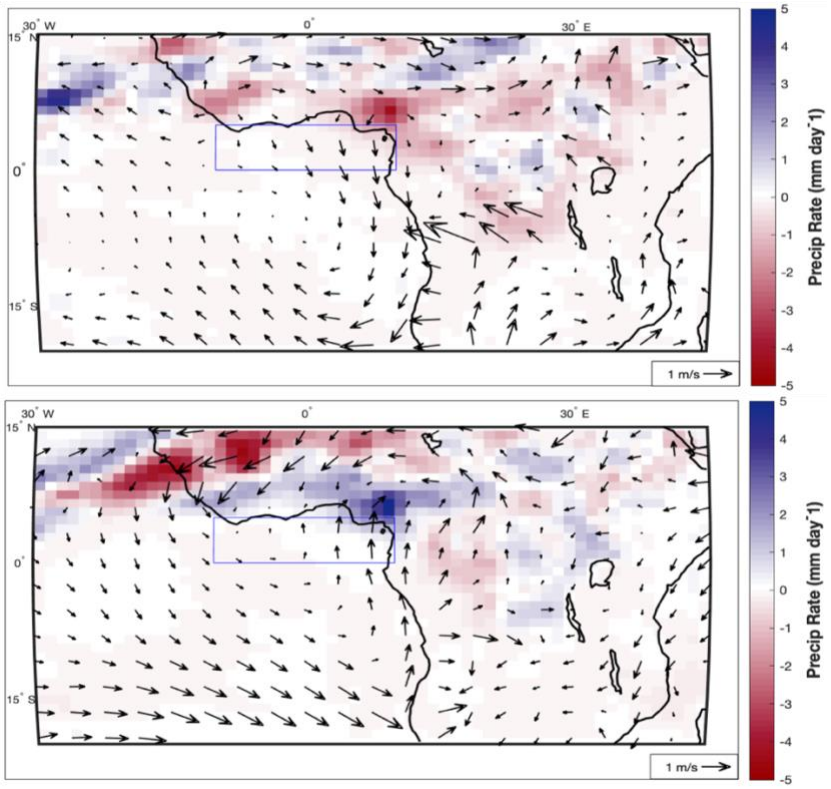

Figure 3.5 Simulated precipitation and 932mb wind anomalies for dirty(top) and clean(bottom) conditions.

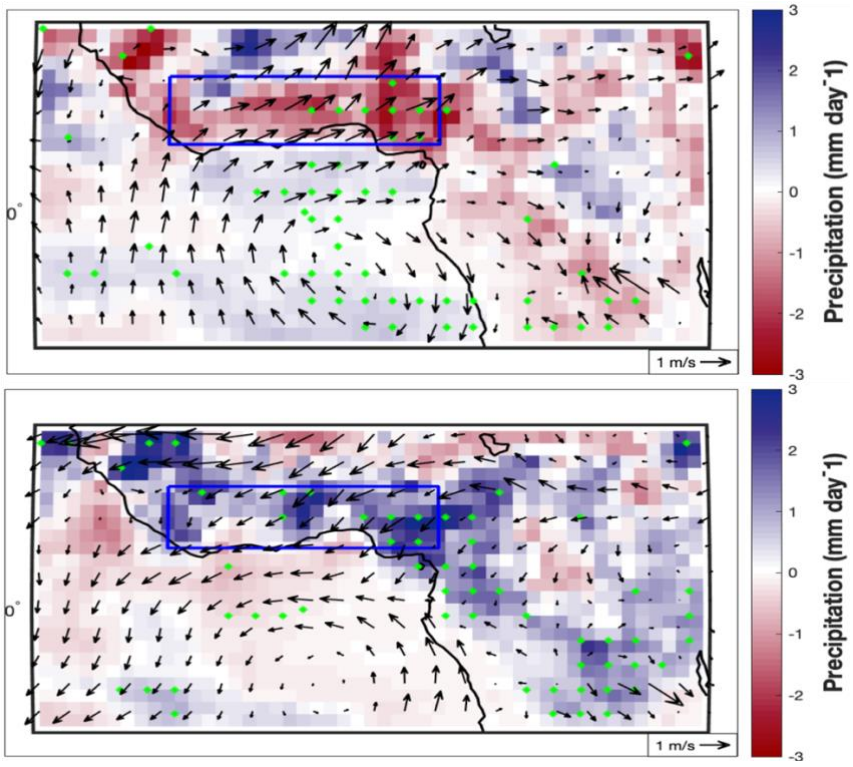

Figure 3.6 Observed precipitation and 925mb wind anomalies from ERA-Interim reanalysis for dirty(top) and clean(bottom) conditions, as presented in Ajoku et al. (2020).

3.3.2 Vertical BC Aerosol and Cloud Structure in CESM 2

Now that we have shown that aerosol-cloud-precipitation interactions are in agreement between observations/reanalysis data and model simulations, we can look more closely at the mechanisms driving these responses. The vertical structure of aerosols is not easy to assess from observations alone, but we can examine the model fields to determine this. Zonally averaged fine mode BC concentrations (**Figure 3.7**) allow us to see that the largest changes occur over the GoG between 700mb-850mb. Peaks in fine mode BC anomalies of ~ $2x10^{-10}$ kg kg^{-1} (per kg of dry air) occur near 750mb. As expected from the precipitation fields, changes in aerosol loading

are accompanied with drier/wetter atmospheric conditions aloft (**Figure 3.8**). Increases in wind intensity over BC source regions (**Figure 3.2a**) advect dry, continental air into the GoG. To illustrate, decreases in cloud liquid amount and water vapor concentration during dirty conditions (**Figure 3.8a** & **3.8c**) match the location of maximum fine mode BC concentration anomalies. Further inland, ~15°N, we note a change in sign of water vapor concentration (**Figure 3.8c** & **3.8d**) that is similar to precipitation rates (**Figures 3.5** & **3.6**).

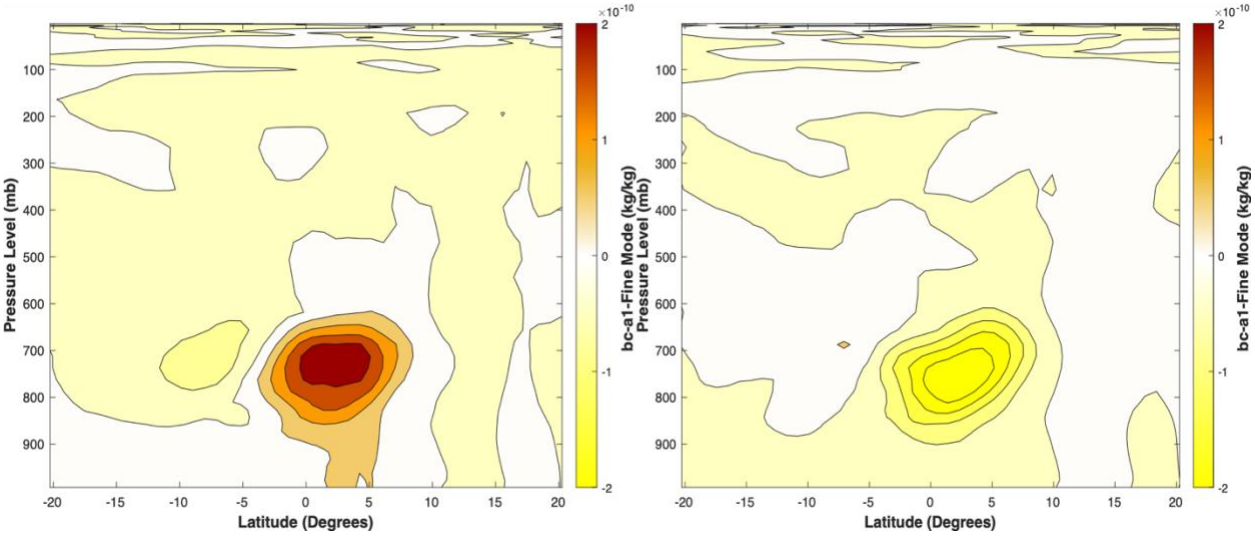

Figure 3.7 Zonal average fine-mode BC concentration anomalies for dirty(left) and clean(right) conditions. Data is averaged between 10°W and 10°E and is the same for all subsequent zonally-averaged figures

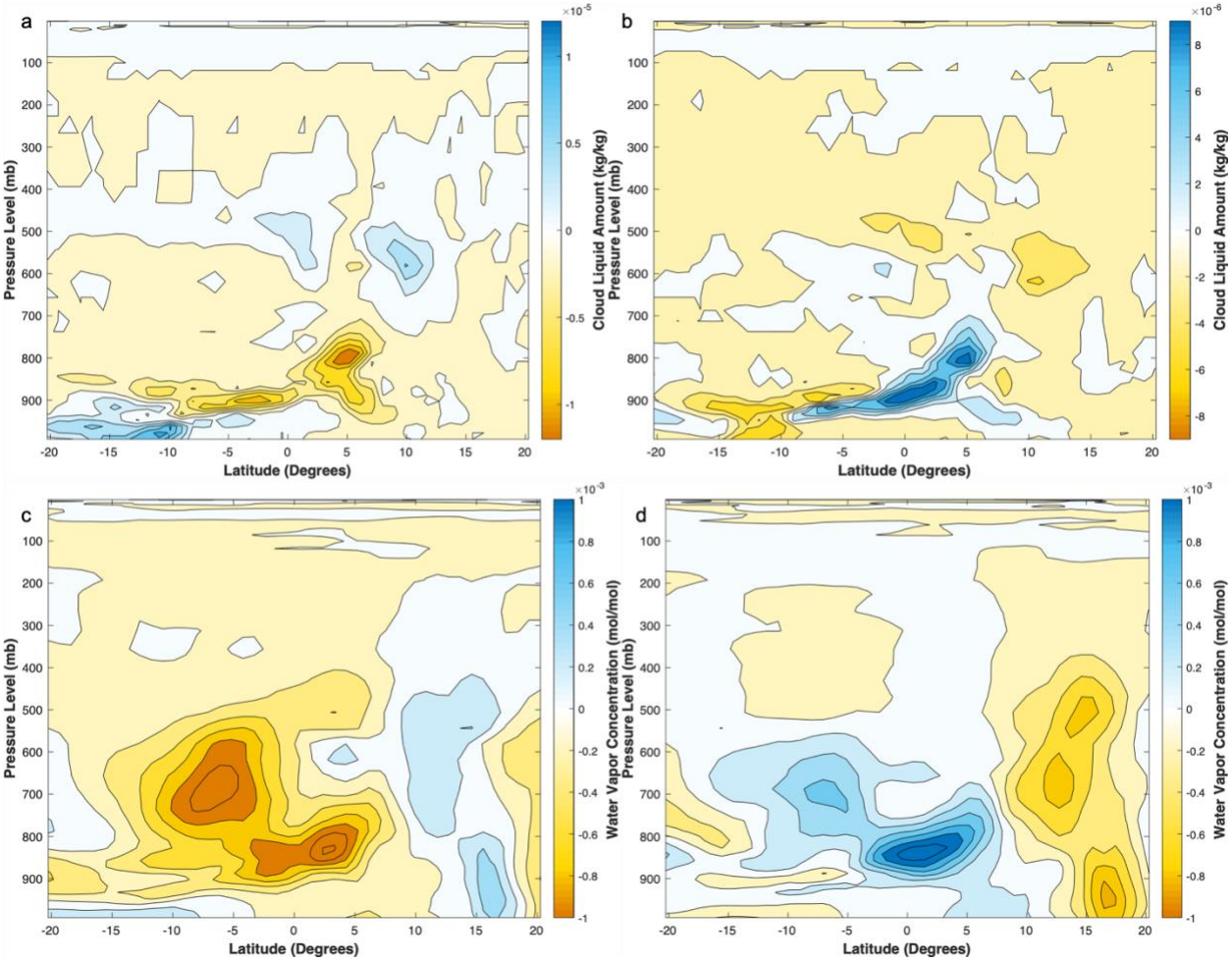

Figure 3.8 Zonal averages of atmospheric water quantities. Anomalous changes in cloud liquid amount and water vapor concentration during dirty (a & c) and clean (b & d) conditions

Figure 9 establishes that the preceding changes we have shown in atmospheric water quantities reflects the model's simulated cloud structure. With less or more cloud liquid and water vapor available for condensation, low-level clouds (surface-700mb) do not develop as much over water which leads to a decrease in deep convective clouds over land. Note that the Guinea coastline begins at approximately 7°N. Over land, we see somewhat different behavior in mid-troposphere (~500mb) cloud cover changes. Between 12°N and 17°N, these changes are most apparent and coincide with the location of the African easterly jet, which is a consequence

of the reversal in meridional temperature gradients between the GoG and African continent coupled with corresponding strong easterly geostrophic flow in boreal summer.

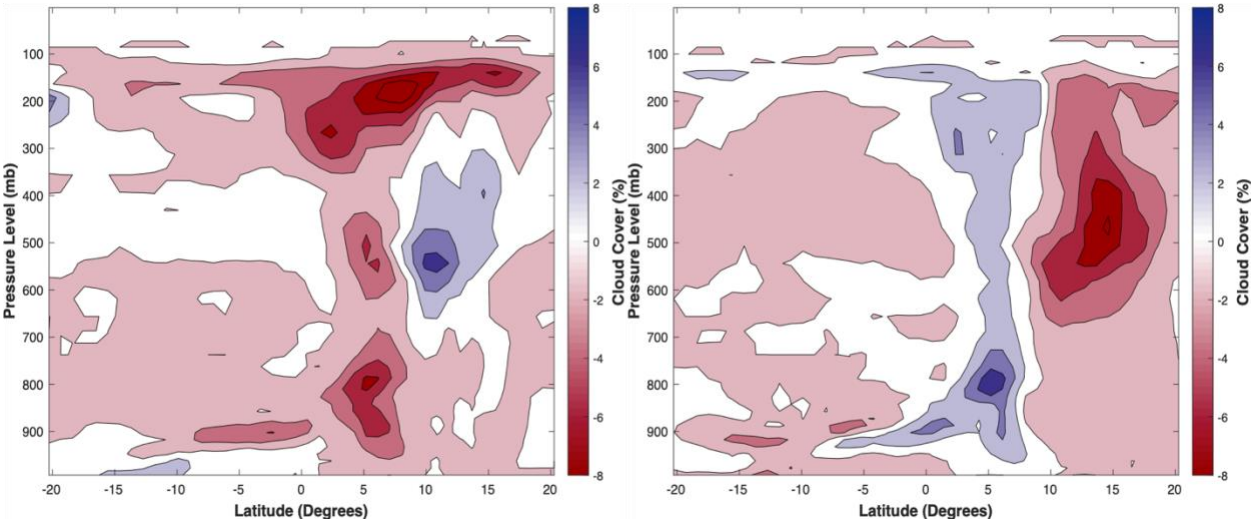

Figure 3.9 Zonal average cloud fraction anomalies for dirty(left) and clean(right) conditions

CESM 2 allows us to also look at the vertical structure of convective cloud cover, the portion of a cloud responsible for producing precipitation within the model. Regardless of background aerosol conditions, the largest of the changes in convective cloud cover (~3%) occur below 400mb over land, below the location of high-level cloud formations (**Figure 3.10**) and reflect anomalous changes we see in cloud top height along the Guinea coastline (**Figure 3.11**). We identify decreases in cloud top heights up to 600m during dirty conditions and increases up to 1km during clean conditions, with the extremes located over Nigeria. The changes seen in cloud top height are likely a byproduct of weakened deep convection over the Guinea coastline as shown in **figures 3.9** & **3.10**.

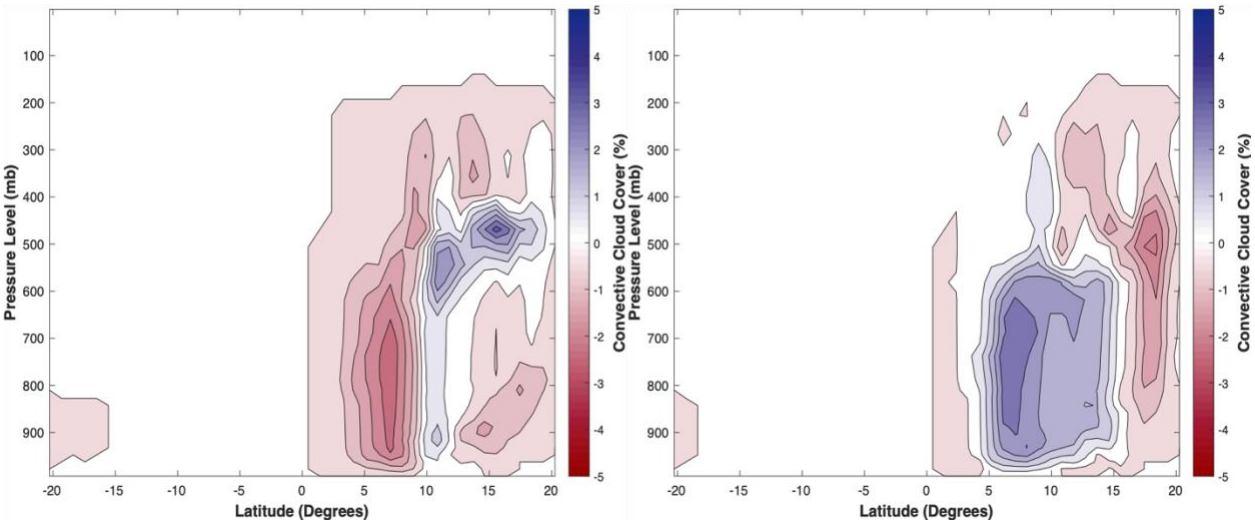

Figure 3.10 Zonal average convective cloud cover anomalies for 2006 (high AOD year) during dirty(left) and clean(right) conditions

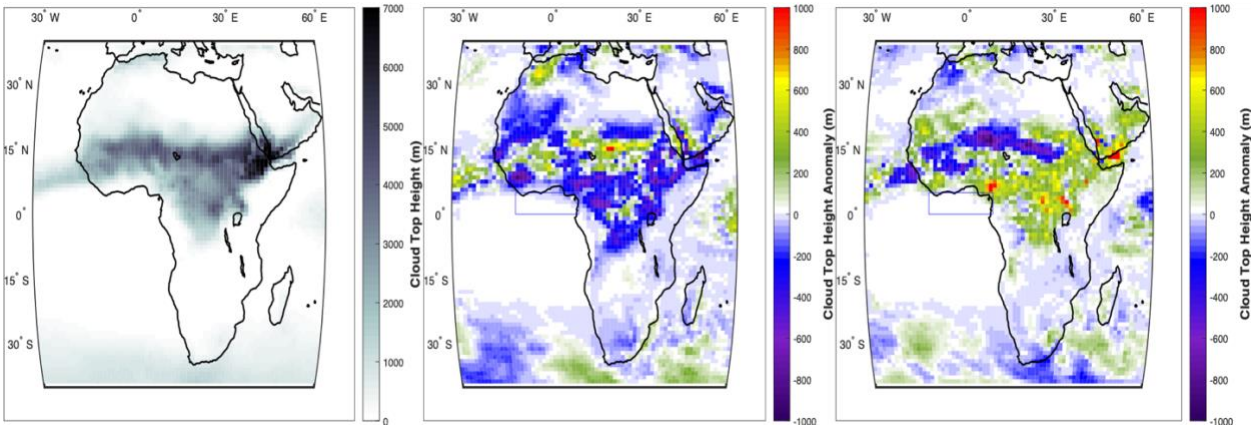

Figure 3.11 Model Simulated cloud top height climatology (left) and anomalous changes during dirty (middle) and clean(right) conditions

3.3.3 Aerosol Radiative and Cloud Microphysical Impacts

With a better picture of the vertical cloud structure and convective development in our study region, we can now look at the impacts of clouds and BC aerosols on local radiation budgets. It is widely known that BC leads to an absorption of SW radiation in the atmosphere and surface cooling, particularly over land (Ramanathan et al. 2001; Wang 2004). **Figure 3.12** highlights changes in surface SW fluxes for all-sky conditions and the portion due to the SW cloud radiative effect (CRE), which is the difference between clear-sky and all-sky values. Increased BC transport, which is escorted with drier air and less cloud development, allows more SW radiation to reach the surface unattenuated (**Figure 3.12a** & **3.12c**). On average, there is an increase of about 10 W m^{-2} reaching the surface along the Guinea coastline during all-sky conditions, with a cloud radiative effect averaging ~ +20 W m^{-2}. Similar results, with opposite sign, are obtained during clean conditions as well (**Figure 3.12b** & **3.12d**), meaning that there is less incoming solar radiation reaching the surface. The signs of downwelling surface SW flux anomalies reflect whether the CRE has a warming or cooling effect on the climate. In the case of dirty conditions, decreases in cloud coverage lead to regional atmospheric warming.

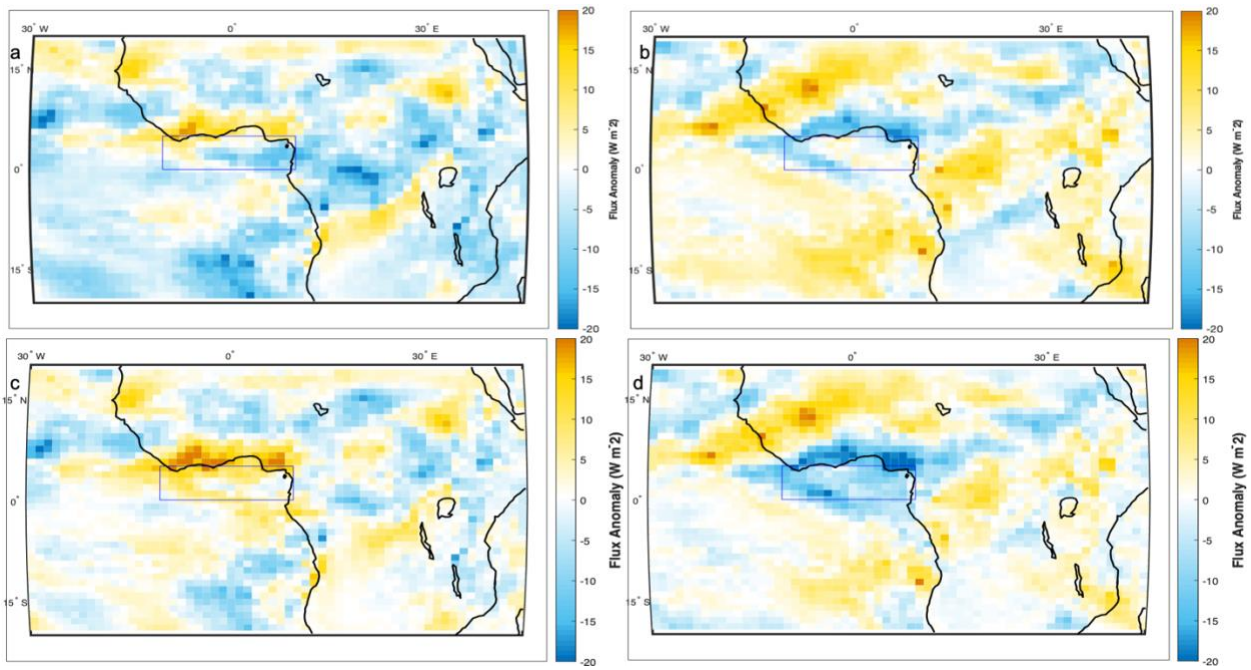

Figure 3.12 Model simulated surface SW flux anomalies under all-sky conditions (a & b) and corresponding SW cloud radiative effects (c &d). Panels a & c reflect dirty conditions and panels b & d clean conditions. *A positive(negative) anomaly symbolizes more(less) SW radiation reaching the surface*

A double radiation call utilized in our hybrid runs allow for us to compute changes in net shortwave cloud forcing (SWCF) due to the presence of BC (**Figure 3.13**). Accounting for the changes in albedo with anomalous cloud coverage, SWCF values are about twice as large as surface SW CRE along the Guinea coastline (+/- 40 W m^{-2}). A net positive cloud forcing anomaly means that increases in radiation reaching the surface outweighs the portion reflected or emitted back into space. Our results show that the portion of SWCF due to BC present is negligible compared with the contribution of all aerosols (**Figure 3.13 c** & **d**) except for countries along the central African coastline such as Gabon, Equatorial Guinea and the Republic of Congo. Over the GoG, BC accounts for a negative SWCF during dirty conditions due to its ability to absorb radiation that would otherwise reach the surface. However, changes in BC-only SWCF during clean conditions (**Figure 3.13d**) over the Guinea coastline make up ~50% of the

net reduction. Less BC aerosols favor cloud development and thus more SW radiation reflects back into space (negative SWCF). In comparison with longwave cloud forcing's (LWCF), values are smaller in magnitude and BC accounts for less than 1 W m^{-2} change throughout our study region (**Figure 3.14**). Net CRE along the Guinea coastline remains positive during dirty conditions and we attribute it to the dominant surface SW CRE associated with low-level cloud changes and a weakened deep-level convection. Positive forcing values near the central African coastline in Figure 13c are in agreement with BC semi-direct effect calculated in Tegen & Heinhold [2018].

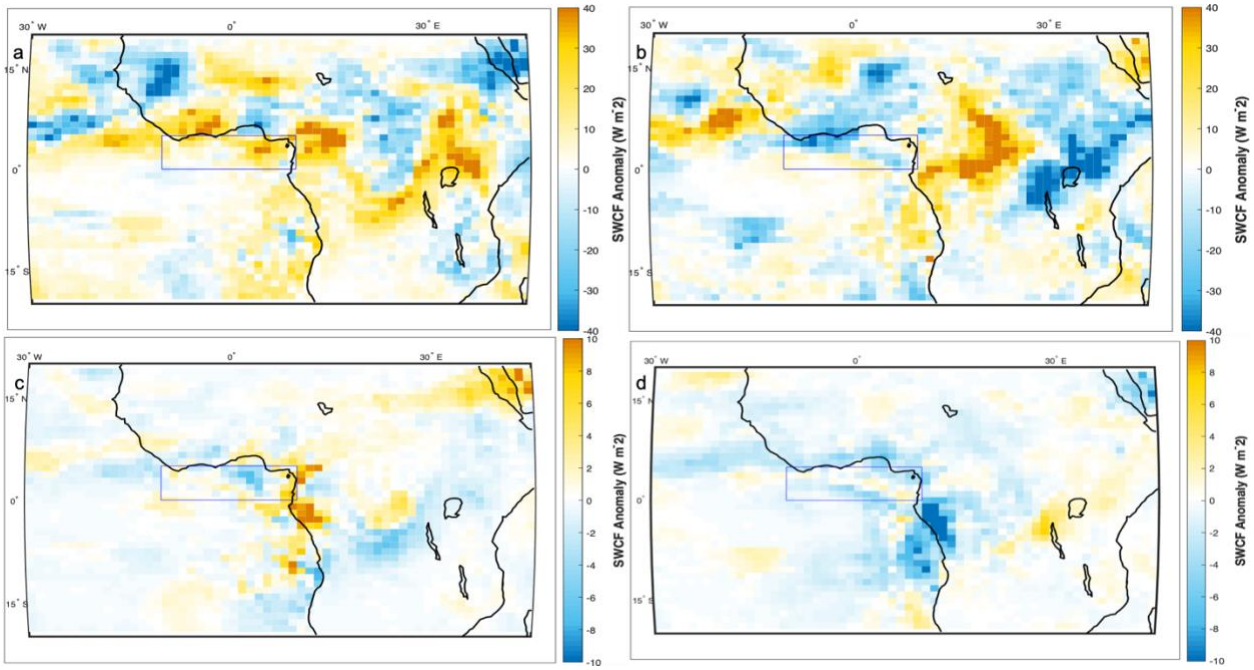

Figure 3.13 Model simulated shortwave cloud forcing (SWCF) for August 2006 (High AOD year) with all aerosols present (a & b) and only BC present (c & d). Panels a & c reflect dirty conditions and panels b & d reflect clean conditions. These values represent a balance at the top of the atmosphere *with positive(negative) anomalies representing less(more) SW radiation reflected back into space.*

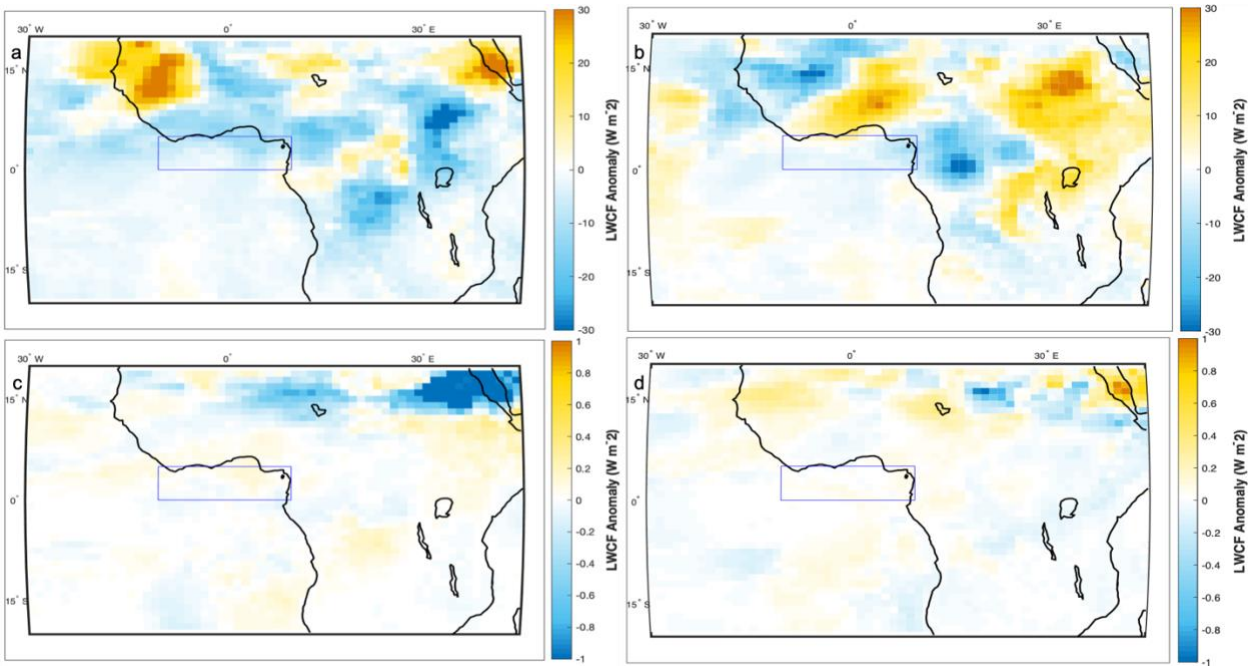

Figure 3.14 Same as figure 3.12 but for longwave cloud forcing. These values represent a balance at the top of the atmosphere

Figure 3.15 shows changes in cloud droplet number concentration (CDNC) for each aerosol background. An increase(decrease) in aerosol presence creates more(less) cloud droplets. Knowing that most of the clouds responsible for convective rain occurs between 5°N-10°N (Figure 10), we see changes in ranging 2-7 cm^{-3} that coincide with the largest change in cloud fraction and SWCF. Changes in CDNC are found below 700mb, the location of low-level clouds. In addition, the impact on cloud droplet effective radius can be seen from 900mb-600mb (**Figure 3.16**). Decreases ranging from 0.2-0.7 microns during dirty days and increases of 0.2-0.9 microns for clean days coupled with the aforementioned changes in CDNC and precipitation display the traditional aerosol indirect effect (Albrecht 1989; Ghan et al. 2012). South of 5°N, decreases in CDNC during dirty conditions are possibly an artifact of decreased low-cloud fraction whereas over land, these cloud fraction decreases are coupled with increases CDNC reflecting aerosol indirect effects.

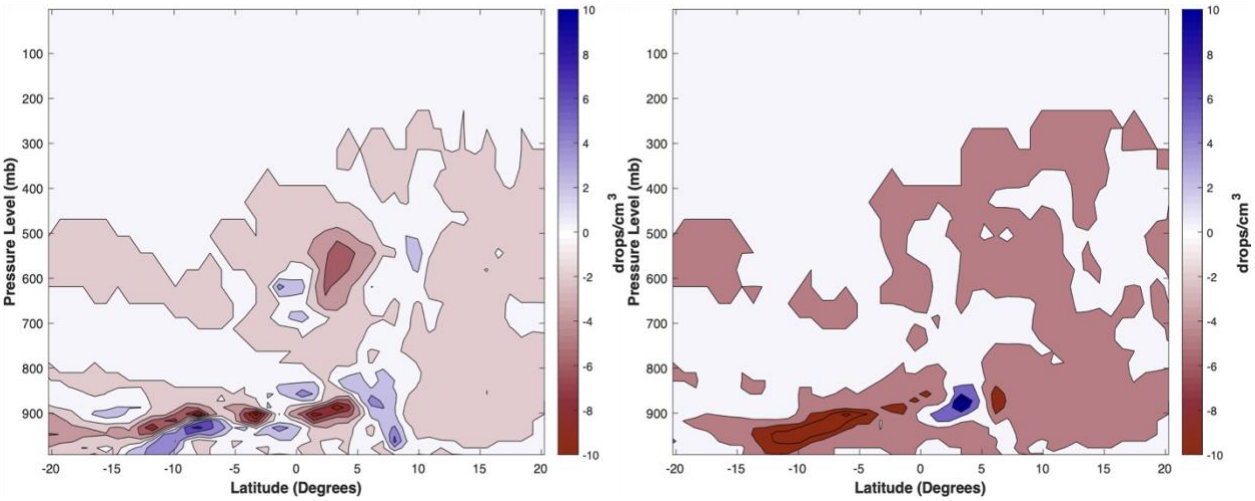

Figure 3.15 Zonal average cloud droplet number concentration (CDNC) anomalies for dirty(left) and clean(right) conditions

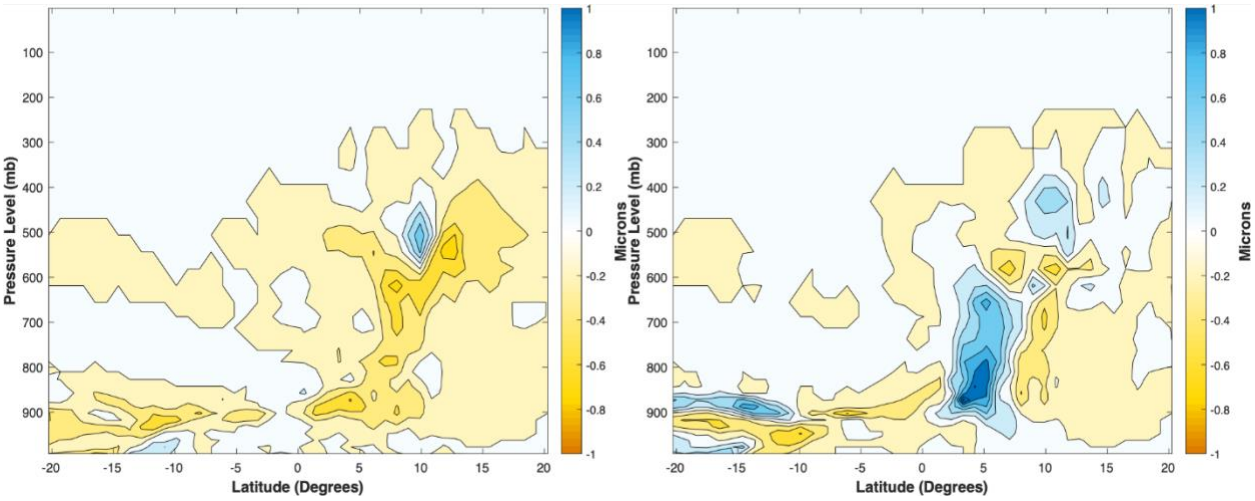

Figure 3.16 Zonal average droplet effective radius anomalies for dirty(left) and clean(right) conditions

3.3.4 BC Radiation-Thermodynamic Feedback

Observational evidence has linked fire aerosols emitted during local biomass burning seasons to reductions of cloud fraction in the African tropics (Tosca et al. 2014). This inverse

relationship between cloud fraction and smoke aerosol amount reflects aerosol semidirect effects. Feingold et al. [2005] and Ackerman et al. [2000] describe this effect as aerosols simultaneously cooling the surface and warming the atmosphere, which stabilizes the atmosphere and inhibits cloud growth. Such atmospheric stability/instability is outlined in **Figure 3.17**. During dirty conditions, temperature anomalies of +0.3 K between 750mb-850mb and -0.3K below 900mb display this vertical stratification over the GoG, where the largest fine mode BC anomalies occur. When conditions are in a clean state, temperatures are 0.3K-0.5K cooler. These changes in vertical stability influences turbulence and thus the convective available potential energy (CAPE). The calculation of CAPE assumes an entraining plume to provide in-cloud temperature and humidity profiles which are then used to calculate buoyancy(updraft). During dirty days, increased atmospheric stability is accompanied with a reduction in CAPE (**Figure 3.18**, left) between 15-25 J kg^{-1} along the Guinea coastline. Increases between 15-45 J kg^{-1} are shown during clean conditions (**Figure 3.18**, right). Our modeled values of CAPE are within agreement with values obtained in Ajoku et al. [2020] and are a reflection of the changes we see in cloud top height (**Figure 3.11**).

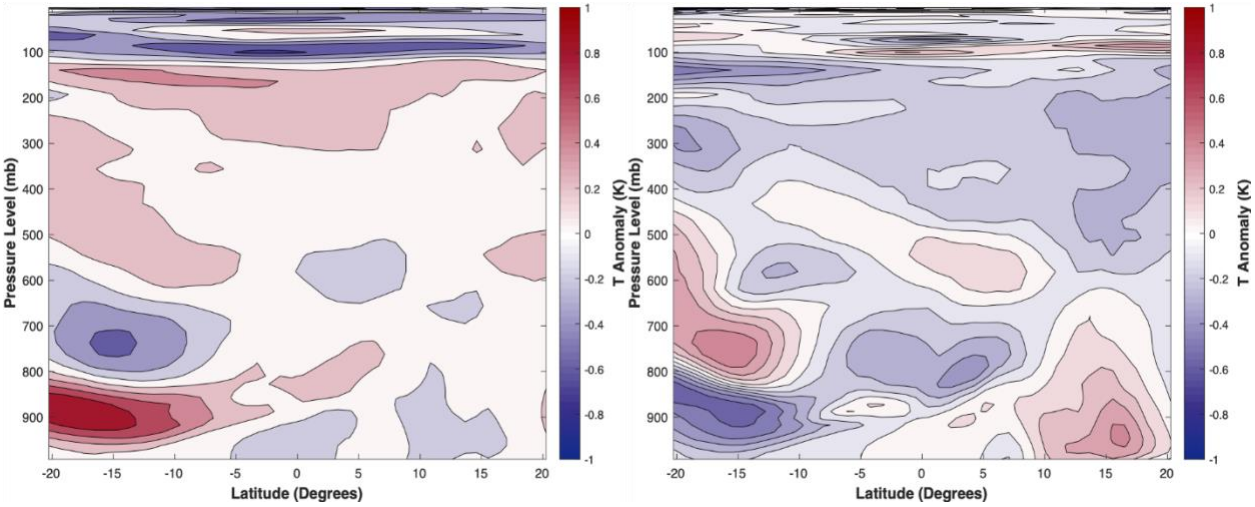

Figure 3.17 Zonal average temperature anomalies for dirty(left) and clean(right) conditions

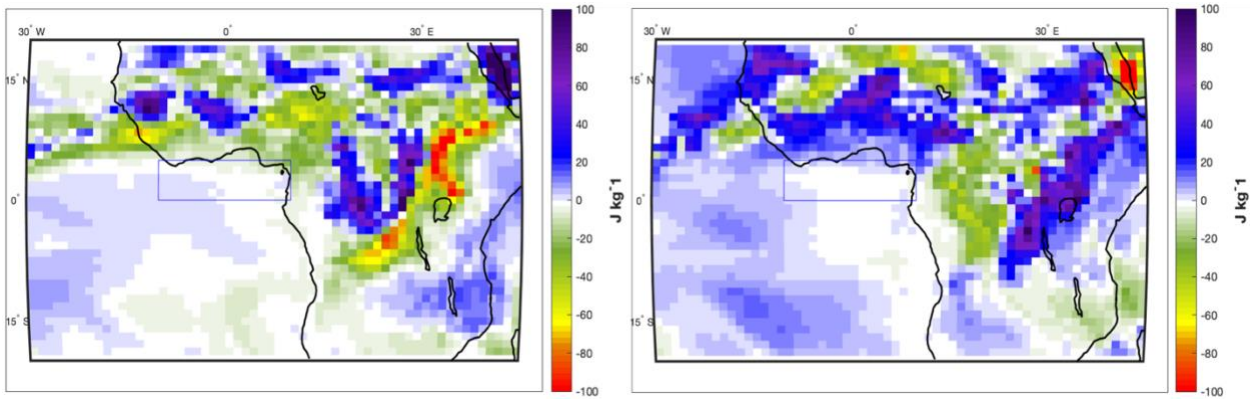

Figure 3.18 Anomalous changes if convective available potential energy (CAPE) for dirty(left) and clean(right) conditions *in the year 2006*.

3.4 Conclusion

During the southern African dry season, plumes of biomass burning aerosols are advected throughout the Atlantic Ocean toward the Guinea coastline. We have demonstrated the reproducibility of aerosol-cloud-precipitation interactions obtained in Ajoku et al. [2020] using CESM 2. Changes in wind intensity over biomass burning-produced aerosols influences the

amount of loading toward the adjacent Atlantic. Dirty conditions in Figure 2 are associated with increased convergence along the Guinea coastline (Heinold et al., [2011]). As these aerosols make their way towards the GoG, they mix into the boundary layer and exert radiative influences that enhance the evaporation of clouds (Hill and Dobbie, 2008) and change cloud microphysical properties (Feingold et al. 2010; Gordon et al. 2018) which impact overall precipitation.

Model simulations reveal the presence of fine mode BC vertically up to about 700mb, higher than our previous assumption of 850mb. We associate increases in BC aerosols with drier atmospheric conditions and less cloud liquid water availability throughout the equatorial Atlantic. Mixtures of aerosols and drier air within the boundary leads to decreased low-cloud fraction and limits deep convection over land associated with the West African monsoon. Reductions in cloud development yields a positive SW CRE up to 20 W m^{-2} (twice as much as LW CRE) and SWCF ~40 W m^{-2} along the Guinea coastline (heavily outweighing changes in LWCF), with the contribution of BC to this forcing being minimal. Because the isolated direct effect of BC is so minimal, we attribute cloud reductions to a positive aerosol semidirect effect that is in agreement with Tegen and Heinold [2018]. Variables describing cloud microphysical effects in cloud droplet number concentration and droplet effective radius are mainly restricted to below 700mb. Together, increased aerosol loading, and cloud fraction reductions warm the lower troposphere and cool the surface, which reinforces reductions in turbulence and convection (Tosca et al. 2015).

There are always uncertainties associated with using a GCM to reproduce meteorological observations, especially when relying on internal model physics. An important uncertainty to be considered for future work are the pseudo-radiative effects potentially caused by temperature nudging (He et al., 2017). Additional free-running models coupled with observations as initial

conditions and varying SD relaxation times can give more insight to potential biases that are possibly missed with the research strategy employed and discussed here.

Chapter 3, in part is currently being prepared for submission for publication of the material. Ajoku, Osinachi; Miller, Arthur; Norris, Joel; Buchholz, Rebecca. The dissertation author was the primary investigator and author of this material.

3.5 References

Ajoku, O., Norris, J. R., & Miller, A. J. (2020). Observed monsoon precipitation suppression caused by anomalous interhemispheric aerosol transport. *Climate Dynamics*, *54*(1-2), 1077-1091.

Albrecht B (1989) Aerosols, cloud microphysics, and fractional cloudiness. Science 245:1227–1230. https://doi.org/10.1126/scien ce.245.4923.1227

Allen, R.J., Amiri-Farahani, A., Lamarque, J. *et al.* Observationally constrained aerosol–cloud semi-direct effects. *npj Clim Atmos Sci* **2,** 16 (2019). https://doi.org/10.1038/s41612-019-0073-9

Altaratz, O., et al. "Cloud invigoration by aerosols—Coupling between microphysics and dynamics." *Atmospheric Research*140 (2014): 38-60.

Chakraborty, S., R. Fu, S. T. Massie, et al. (2016), Relative influence of meteorological conditions and aerosols on the lifetime of mesoscale convective systems, *P Natl Acad Sci USA*, *113*(27), 7426-7431.

Chakraborty, Sudip, et al. "On the role of aerosols, humidity, and vertical wind shear in the transition of shallow-to-deep convection at the Green Ocean Amazon 2014/5 site." *Atmospheric Chemistry and Physics (Online)* 18.15 (2018).

Creamean, J. M., et al. (2013), Dust and Biological Aerosols from the Sahara and Asia Influence Precipitation in the Western U.S., *Science*, *339*(6127), 1572-1578.

Danabasoglu, G., Lamarque, J.F., Bacmeister, J., Bailey, D.A., DuVivier, A.K., Edwards, J., Emmons, L.K., Fasullo, J., Garcia, R., Gettelman, A. and Hannay, C., 2020. The community earth system model version 2 (CESM2). *Journal of Advances in Modeling Earth Systems*, *12*(2), p.e2019MS001916.

Dentener, F., Kinne, S., Bond, T., Boucher, O., Cofala, J., Generoso, S., Ginoux, P., Gong, S., Hoelzemann, J.J., Ito, A. and Marelli, L., 2006. Emissions of primary aerosol and precursor gases in the years 2000 and 1750, prescribed datasets for AeroCom.

Emmons, L.K., Schwantes, R.H., Orlando, J.J., Tyndall, G., Kinnison, D., Lamarque, J.F., Marsh, D., Mills, M.J., Tilmes, S., Bardeen, C. and Buchholz, R.R., 2020. The Chemistry Mechanism in the Community Earth System Model version 2 (CESM2). *Journal of Advances in Modeling Earth Systems*, *12*(4), p.e2019MS001882.

Feingold, G., Koren, I., Wang, H., Xue, H., and Brewer, W. A.: Precipitation-generated oscillations in open cellular cloud fields, Nature, 466, 849–852, https://doi.org/10.1038/nature09314, 2010.

Gettelman, A. and H. Morrison, Advanced Two-Moment Microphysics for Global Models. Part I: Off line tests and comparisons with other schemes. J. Climate, 28, 1268-1287. doi: 10.1175/JCLI-D-14-00102.1, 2015.

Ghan SJ, Liu X, Easter RC, Zaveri R, Rasch PJ, Yoon JH, Eaton B (2012) Toward a minimal representation of aerosols in climate models: comparative decomposition of aerosol direct, semidirect, and indirect radiative forcing. J Clim 25(19):6461–6476

Gordon, H., Field, P. R., Abel, S. J., Dalvi, M., Grosvenor, D. P., Hill, A. A., Johnson, B. T., Miltenberger, A. K., Yoshioka, M., and Carslaw, K. S.: Large simulated radiative effects of smoke in the south-east Atlantic, Atmos. Chem. Phys., 18, 15261–15289, https://doi.org/10.5194/acp-18-15261-2018, 2018.

He, J., Glotfelty, T., Yahya, K., Alapaty, K., & Yu, S. (2017). Does temperature nudging overwhelm aerosol radiative effects in regional integrated climate models?. *Atmospheric Environment*, *154*, 42-52.

Heinold, B., Tegen, I., Bauer, S., Wendisch, M. Regional modelling of Saharan dust and biomass-burning smoke. *Tellus B* **2011**, *63*, 800–813.

Hill, A. A. and Dobbie, S.: The impact of aerosols on non-precipitating marine stratocumulus. II: The semi- direct effect, Q. J. Roy. Meteor. Soc., 134, 1155–1165, https://doi.org/10.1002/qj.277, 2008.

Lamarque, J.F., Emmons, L.K., Hess, P.G., Kinnison, D.E., Tilmes, S., Vitt, F., Heald, C.L., Holland, E.A., Lauritzen, P.H., Neu, J. and Orlando, J.J., 2012. CAM-chem: Description and evaluation of interactive atmospheric chemistry in the Community Earth System Model. *Geoscientific Model Development*, *5*(2), p.369.

Maley, Jean. "Dust, clouds, rain types, and climatic variations in tropical North Africa." *Quaternary Research* 18.1 (1982): 1-16.

Myhre, G., D. Shindell, F.-M. Bréon, W. Collins, J. Fuglestvedt, J. Huang, D. Koch, J.-F. Lamarque, D. Lee, B. Mendoza, T. Nakajima, A. Robock, G. Stephens, T. Takemura and H. Zhang, 2013: Anthropogenic and Natural Radiative Forcing. In: Climate Change 2013: The Physical Science Basis. Contribution of Working Group I to the Fifth Assessment Report of the

Intergovernmental Panel on Climate Change [Stocker, T.F., D. Qin, G.-K. Plattner, M. Tignor, S.K. Allen, J. Boschung, A. Nauels, Y. Xia, V. Bex and P.M. Midgley (eds.)]. Cambridge University Press, Cambridge, United Kingdom and New York, NY, USA.

Petty, G.W., 2006: *A First Course in Atmospheric Radiation*, Sundog Publishing, 472 pp.

Randles, C. A., and Venkatachalam Ramaswamy. "Direct and semi-direct impacts of absorbing biomass burning aerosol on the climate of southern Africa: A Geophysical Fluid Dynamics Laboratory GCM sensitivity study." *Atmospheric Chemistry and Physics* 10.20 (2010): 9819.

Rosenfeld, D., Andreae, M.O., Asmi, A., Chin, M., de Leeuw, G., Donovan, D.P., Kahn, R., Kinne, S., Kivekäs, N., Kulmala, M. and Lau, W., 2014. Global observations of aerosol-cloud-precipitation-climate interactions. *Reviews of Geophysics*, *52*(4), pp.750-808.

Tegen, I., & Heinold, B. (2018). Large-scale modeling of absorbing aerosols and their semi-direct effects. *Atmosphere*, *9*(10), 380.

Tilmes, S., Hodzic, A., Emmons, L.K., Mills, M.J., Gettelman, A., Kinnison, D.E., Park, M., Lamarque, J.F., Vitt, F., Shrivastava, M. and Campuzano Jost, P., 2019. Climate forcing and trends of organic aerosols in the Community Earth System Model (CESM2). *Journal of Advances in Modeling Earth Systems*.

Tosca, M. G., D. J. Diner, M. J. Garay, and O. V. Kalashnikova (2014), Obser- vational evidence of fire-driven reduction of cloud fraction in tropical Africa, *J. Geophys. Res. Atmos.*, *119*, 8418–8432, doi:10.1002/2014JD021759.

Tosca, M G, Diner, D J, Garay, M J, & Kalashnikova, O V (2015) Human-caused fires limit convection in tropical Africa: First temporal observations and attribution. *Geophysical Research Letters*, *42*(15), 6492-6501

Wang, C.: A modeling study on the climate impacts of black carbon aerosols, J. Geophys. Res., 109, D03106, doi:10.1029/2003JD004084, 2004.

Yang, B., Qian, Y., Lin, G., Leung, L.R., Rasch, P.J., Zhang, G.J., McFarlane, S.A., Zhao, C., Zhang, Y., Wang, H. and Wang, M., 2013. Uncertainty quantification and parameter tuning in the CAM5 Zhang-McFarlane convection scheme and impact of improved convection on the global circulation and climate. *Journal of Geophysical Research: Atmospheres*, *118*(2), pp.395-415.

Zhang, H., Z. L. Wang, P. W. Guo, and Z. Z. Wang, 2009: A modeling study of the effects of direct radiative forcing due to carbonaceous aerosol on the climate in East Asia. Adv. Atmos. Sci., 26(1), 57–66, doi: 10.1007/s00376-009-0057-5.

Zhang, Y., Fu, R., Yu, H., Qian, Y., Dickinson, R., Silva Dias, M.A.F., da Silva Dias, P.L. and Fernandes, K., 2009. Impact of biomass burning aerosol on the monsoon circulation transition over Amazonia. *Geophysical Research Letters*, *36*(10).

Chapter 4: Impacts of Aerosols Produced by Biomass Burning on the Stratocumulus-to-Cumulus Transition in the Equatorial Atlantic

Osinachi F. Ajoku[1*], Arthur J. Miller[1], and Joel R. Norris[1]

1 Scripps Institution of Oceanography, University of California San Diego, La Jolla, California, USA

Corresponding author: Osinachi Ajoku (oajoku@ucsd.edu)

Key Points:

- Transport of biomass burning aerosols within the equatorial Atlantic impact the stratocumulus to cumulus transition.
- Aerosol radiative effects alter lower tropospheric stability and moisture availability throughout the tropical and subtropical Atlantic.

Abstract

The impact of aerosols produced by biomass burning on the stratocumulus-to-cumulus transition (SCT) in the equatorial Atlantic is studied using satellite-based and reanalysis data for the month of June. The month of June is highlighted because it represents monsoon onset as well as the largest sea surface temperature gradient in the summer, which is the peak season of tropical African biomass burning. Boundary layer deepening and increasing temperatures put the location of the SCT within the Gulf of Guinea. Satellite retrievals indicate that the bulk of aerosols occurs at 1500m in altitude, either above or below the boundary layer depending on latitudinal position. Changes in smoke loading over the Gulf of Guinea due to greater transport from regions of biomass burning leads to increased low-level cloud cover and lower surface temperatures when aerosol optical depth anomalies exceed 0.1. Similar results opposite in sign are obtained during lesser transport. Further south, we find significant changes to cloud top height, tropospheric stability and moisture availability near maximum aerosol loading. These effects combine to extend the SCT in space during increased aerosol loading episodes.

4.1 Background/Introduction

Differential heating due to Earth's axial tilt causes excess energy in the form of shortwave radiation in the tropics that must be transported poleward. This sets up regions with considerable meridional sea surface temperature (SST) gradients. In addition, locations with eastern boundary currents that transport cooler waters equatorward coupled with large-scale subsidence are dominated by persistent stratocumulus decks [*Klein and Hartmann*, 1993]. As these decks follow the mean trade wind circulation equatorward, the cloud regime transitions from predominantly stratocumulus to trade cumulus [*Bretherton*, 1992; *Bretherton and Wyant*, 1997; *Bretherton et al.*, 1999; *Teixeira et al.*, 2011]. A better understanding of this

Stratocumulus-to-Cumulus transition (SCT) is important for modelling cloud interactions in a changed climate. As tropical regions are projected to expand under various modelled scenarios, so will corresponding subtropical dry zones which heavily influence the location of persistent stratocumulus decks [*Allen and Ajoku*, 2016].

Factors that may potentially influence this transition have been studied using both observations [*Albrecht et al.*, 1995; *Albrecht et al.*, 2019; *Wood et al.*, 2018] and model simulations [*Chung et al.*, 2012; *Sandu and Stevens*, 2011]. The major factors controlling cloud coverage and structure in these transition regions are lower tropospheric static stability (LTS) [*Wood and Bretherton*, 2006] and the typical advection of a cloud system over increasing SST. Specifically, increases in LTS create a stronger cap of the planetary boundary layer, allowing for greater low-level cloud coverage and hindering deep-cloud formation while the abovementioned cloud advection lead to larger surface latent heat fluxes, buoyancy fluxes and boundary layer deepening. In essence, the boundary layer deepens due to a weakening of LTS.

Aerosols alter earth's radiation budget in three different ways, all of which can contribute to changes in cloud properties. First, aerosols directly impact the planetary energy balance through the absorption and scattering of incoming radiation [*Ramanathan*, 2001; *Haywood and Boucher* 2000], which is known as the "direct effect". Second, some aerosols act as cloud condensation nuclei (CCN), thereby influencing cloud droplet size and consequently the likelihood of coalescence and the accumulation of liquid water and ice in clouds, thus altering cloud albedo and lifetime [*Albrecht*, 1989; *Ferek et al.*, 2000; *Ghan et al.*, 2012]. This is the so-called "indirect effect". Third, solar absorbing aerosols such as black carbon can alter heating

rates, the vertical temperature profile, and atmospheric stability, which can lead to cloud adjustments. The radiation flux associated with this adjustment is termed the aerosol "semi-direct effect" [*Hansen et al.,* 1997].

Satellite observations have been used to understand the influence of smoke aerosols on boundary layer clouds in the southeastern Atlantic [*Painemal et al.,* 2014; *Diamond et al*., 2018]. The consensus from such studies is that the location of the smoke layer relative to the cloud deck ultimately determines the resulting effect. When smoke resides above the cloud deck, there tends to be a strengthening of the inversion layer and cloud radiative effect whereas smoke within the boundary layer leads to decreased cloud fraction and increased temperatures within the boundary layer [*Wilcox*, 2010, 2012].

There have been few studies that look into how smoke aerosols may impact the SCT [*Sandu and Stevens*, 2011; *Yamaguchi et al*., 2017; *Terai et al*., 2014*; Painemal et al*., 2015; *Zhou et al*., 2015] and fewer studies that use observations in the Atlantic Ocean. The Atlantic Stratocumulus Transition Experiment-ASTEX [*Albrecht et al*., 1995] conducted in 1992 resulted in data leading to a coherent understanding as well the first measurements of its kind for cloud microphysical properties in the SCT of the northeastern subtropical Atlantic but did not investigate the impact of smoke aerosols.

In the southeastern subtropical Atlantic, there has not been an observational study solely looking at how aerosols may impact the SCT for the month of June. The ORACLES campaign looks into aerosol-cloud interactions over the southeast Atlantic throughout the majority (August

2017, September 2016 and October 2018) of the biomass burning season [*Zuidema et al.*, 2016; *Cochrane et al*., 2019; *Pistone et al*., 2019] Some studies that use large-eddy simulations (LES) to better understand this phenomenon [*Yamaguchi et al*., 2015; *Zhou et al*., 2017] incorporate observed data from the northeastern subtropical Pacific and knowledge of smoke aerosols from active fires interacting with stratocumulus clouds off the coast of Southern Africa. Both studies find evidence of aerosols impacting the SCT but through contrasting mechanisms and end results. *Yamaguchi et al.,* [2015] attribute a delay of the SCT to increased LTS due to aerosol heating above the cloud layer, while *Zhou et al.,* [2017] find a hastened transition due to increased cloud droplet number concentration and cloud water evaporation.

The scientific questions motivating this study are:

1. Can we clearly see a SCT region where biomass burning aerosol emissions impact low-level cloud fraction?
2. What are the important mechanisms of biomass burning aerosols possibly impacting the spatial structure of the SCT?

Knowing that these transitions occur in all four subtropical ocean basins, not many locations can satisfy the added component of solar-absorbing aerosols (black carbon) being present. We have located a region in the equatorial Atlantic with cloud types transitioning from stratocumulus to trade cumulus and even deep convective cumulonimbus that have the potential to be influenced by local smoke aerosol emissions. This study will be extremely important for

designing future field campaigns and testing global climate models (GCMs) abilities to simulate the SCT.

4.2 Data Sources and Methods

Data analysis is conducted for June, representing monsoon onset as well as the establishment of a cold tongue in the eastern equatorial Atlantic Ocean as the intertropical convergence zone (ITCZ) migrates northward, intensifying trade winds and creating large meridional SST gradients. Our study region comprises of the boundary between 15°N-15°S and 10°W-10°E (Figure 1a). Also, it should be noted, SST's decrease 2°C in the Gulf of Guinea (GoG) from the beginning to end of June. In order to prevent potential biases, all data used in this study are detrended by the mean monthly June trend to remove variability arising solely from the seasonal cycle. In order to determine the impact of smoke aerosols on cloud structure and precipitation processes, daily-averaged data are used in this study (with the exception of aerosol extinction). Utilizing daily intervals of data allows for a better sampling resolution as well as capturing mesoscale and synoptic-scale weather processes that would not be resolved with monthly data output.

Daily aerosol optical depth (AOD) for the years 2003-2015 are obtained from Modern-Era Retrospective analysis for Research and Applications, Version 2 (MERRA-2) at 0.5°x0.625° resolution [*GMAO*, 2015]. Having missing AOD data can lead to large errors when undergoing statistical analysis. Using reanalysis data reduces such errors as data not captured by observations are assimilated using a numerical algorithm to create a synthesized estimate of the state of the climate system (*Bengtsson et al*., 2004). Observations, such as the aerosol index and

aerosol absorption optical depth obtained from the Ozone Monitoring Instrument (OMI) measurements and aerosol retrievals from the AErosol RObotic NETwork (AERONET) [*Buchard, et al*., 2015] validated the MERRA data obtained from reanalysis used in our study. This data is based on a version of the NASA Goddard Earth Observing System version 5 (GEOS5) model that is radiatively coupled to the Goddard Chemistry, Aerosol, Radiation, and Transport (GOCART) aerosol module and includes assimilation of observations from satellites. In addition, Level 3 aerosol angstrom exponent's over both ocean and land are obtained from the Visible Infrared Imaging Radiometer Suite (VIIRS) in daily format at 1°x1° horizontal resolution for available years that overlap with this study (2013-2015). This product uses a Deep Blue (DB) algorithm over land and Satellite Ocean Aerosol Retrieval (SOAR) algorithm over ocean to determine atmospheric aerosol properties for daytime cloud-free scenes [*Sayer et al*., 2018]. Although this product is limited to cloud-free scenes, Sinozuka et al. [*2020, in review*] shows that AOD above low-level clouds is similar to adjacent clear skies in the southeast Atlantic.

To analyze the effect of aerosols on cloud cover, we obtained computed surface, shortwave radiation fluxes and cloud coverage data spanning 2003 to 2015 from Clouds and the Earth's Radiant Energy System (CERES) data, which is available, daily-averaged, at 1-degree resolution [*Doelling et al*., 2013; *Doelling et al*., 2016]. This data is broken down into 4 vertical cloud levels (low [surface-700mb], mid-low [700mb-500mb], mid-high [500mb-300mb] and high [300mb-tropopause]). Cloud properties are determined using simultaneous measurements by other EOS and S-NPP instruments such as the Moderate Resolution Imaging Spectroradiometer (MODIS) [Platnick et al., 2015]. We calculate aerosol forcings by subtracting surface fluxes from computed surfaces with aerosols removed in order to gain a better

understanding for local radiation budgets. Their computed fluxes are produced using the Langley Fu-Liou radiative transfer model. Here, observed values are obtained using MODIS and computations are constrained to the observed CERES TOA fluxes.

High resolution (0.25°x0.25°) daily SST data is provided by the National Oceanic and Atmospheric Administration's (NOAA) Earth System Research Laboratory (ESRL) Physical Sciences Division [*Reynolds et al*., 2007]. NOAA's 0.25° daily Optimum Interpolation Sea Surface Temperature (OISST) data is compiled from observational platforms taking into account bias adjustments.

Daily wind, temperature, specific humidity, convective available potential energy (CAPE), and cloud liquid water content data at 0.75°x0.75° resolution were obtained at multiple pressure levels ranging from the surface to 500hPa from the European Centre for Medium-Range Weather Forecasts (ECMWF) reanalysis product [*Berrisford et al*., 2011] at a local time of 6 A.M. UTC. This is consistent with the analysis of *Tosca et al*., [2015], who studied the changes in cloud fraction associated with variability in fire emissions and compared meteorological variables in control and high fire scenes using ECMWF reanalysis at a 6 A.M. local time to better understand the influence of mesoscale dynamics. Furthermore, mid-level clouds have been found to dominate cover over West Africa during the monsoon season early in the morning [*Bourgeios et al*., 2018].

In order to quantify the magnitude and location of anomalous changes in rainfall, daily data at 1-degree resolution is obtained from the Global Precipitation Climatology Project,

Version 1.3 (GPCP 1.3). All the GPCP products are produced by optimally merging precipitation estimates computed from microwave, infrared, sounder data observed on board satellites, and ground-based rain gauge analysis, taking advantage of the strengths of each data type [*Adler et al.*, 2017; *Huffman et al*., 2001]. These satellite datasets have been validated against rain gauges on land in West Africa, particularly on sub-monthly time scales [*Nicholson et al*., 2003].

Monthly smoke aerosol extinction coefficients are acquired from NASA's Cloud-Aerosol Lidar and Infrared Pathfinder Satellite Observation (CALIPSO) platform for the years 2003-2015 using the Cloud-Aerosol Lidar with Orthogonal Polarization (CALIOP) instrument. CALIPSO lidar level 3 aerosol data product reports monthly mean profiles of aerosol optical properties on a 2°x5° spatial grid [Winker, 2015] and 60m resolution in the vertical direction. We use monthly data because the return time between overpasses is too long at daily intervals.

For each of the 13 years, the 30 days in each June were classified into pentiles according to the magnitude of AOD averaged between 5°N-5°S and 10°W-10°E in the GoG for that day. The top and bottom pentiles aggregated from each June resulted in 78 days that are referred to as "clean" (lowest AOD) and "dirty" (highest AOD) days. All dates associated with these dirty and clean days are averaged together to create composites that track how aerosol loading evolves with other meteorological variables of interest. Trends are then removed from composited data to reveal detrended, anomalous changes. By utilizing this method, we attempt to determine which variables are impacted by variations in aerosol transport. Statistical significance of results was determined by the 95% confidence interval according to a 2-tailed Student's t-test accounting for serial correlation by using the effective sample size, $n(1-r_1)(1+r_1)^{-1}$, where n is the number of days and r_1 is the lag-1 autocorrelation coefficient leading to ~3 day decorrelation time.

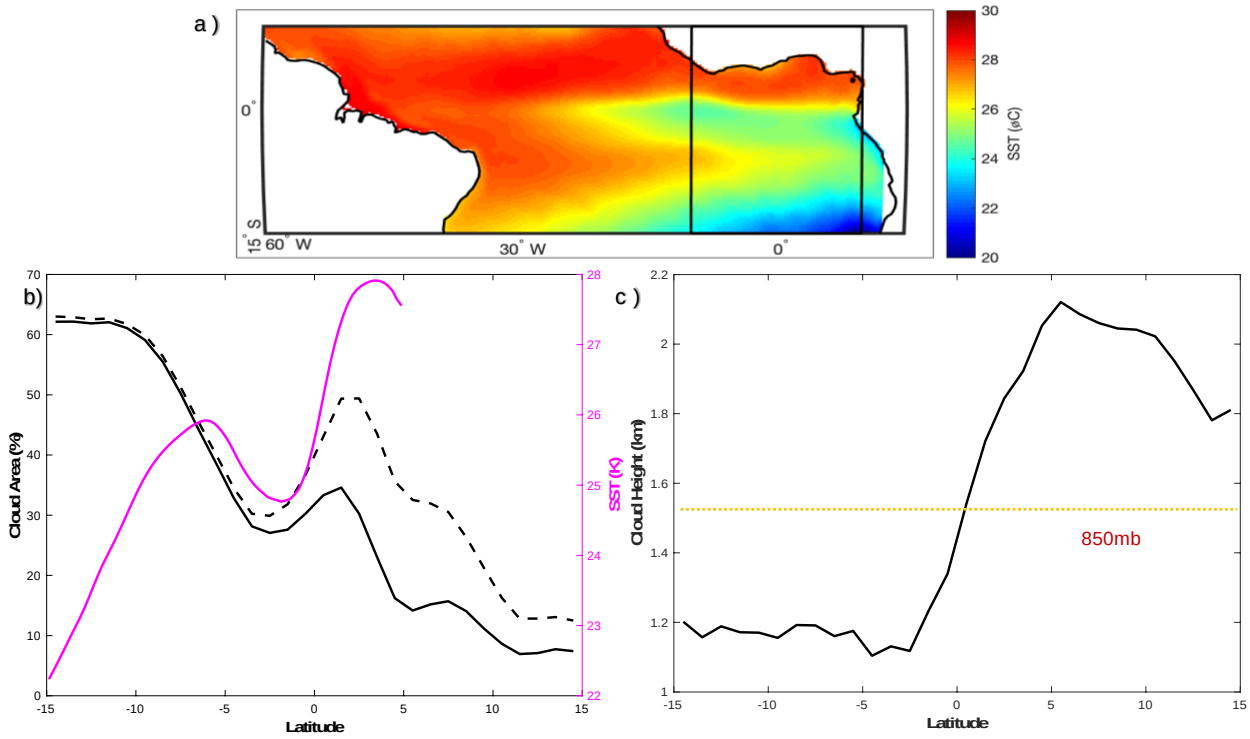

Figure 4.19 (a) Climatological June SST, (**b**) zonally-averaged low cloud area fraction and SST and (**c**) corresponding cloud top height for the years 2003-2015. The black lines in **(a)** represents longitudinal boundaries used to average data in **(b)** and **(c)** as well as subsequent figures. Dashed black lines in **(b)** represent cloud area fraction accounting for obscuration from high level clouds. The 850mb line in **(c)** is shown as a reference for potential aerosol location.

4.3 Results

4.3.1. Study Region Overview

For the month of June, climatological conditions in the Eastern equatorial Atlantic are excellent for studying the SCT. Between the ITCZ migration and trade wind intensification, a large, meridional SST gradient sets up a corresponding cloud structure aloft. Starting in the southern subtropical Atlantic moving equatorward, we see an inverse relationship between increasing SST and decreasing low-level cloud fraction (**Figure 4.1b**). Of particular interest, we notice two locations where cloud fraction decreases to half the value it had farther south (7°S-3°S and 1°N-5°N). We note that this decrease is not as pronounced when accounting for

obscuration from high-level clouds. Within the Gulf of Guinea (GoG), we examine the structure of cloud top height and find a ~700m increase (**Figure 4.1c**) in the same location that the cloud fraction decreases. We believe this is where the boundary layer deepens due to increasing SST in GoG and where the stratocumulus deck transitions into cumulus clouds. Further aloft, increases in higher level clouds (**Fig 4.2a** & **c**) occur within the GoG in addition to precipitation rates rising to a maximum.

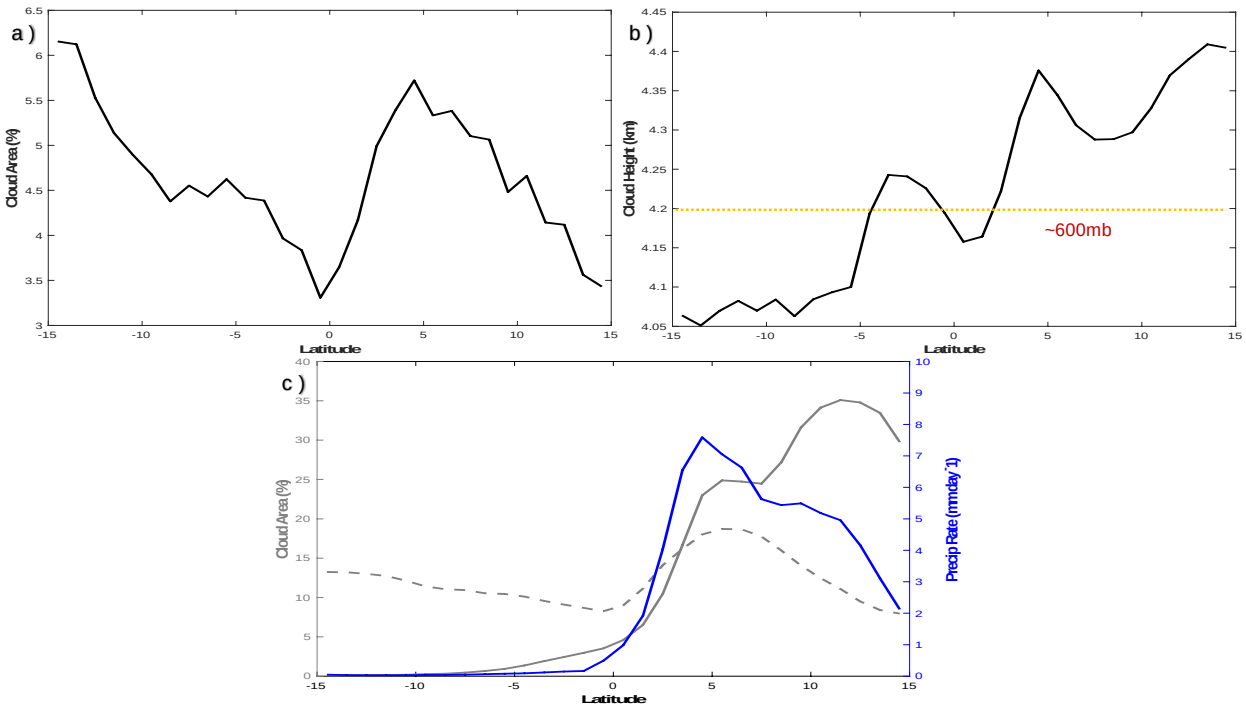

Figure 4.20 (**a**) zonally-averaged mid-low cloud area fraction and (**b**) corresponding cloud top height for the years 2003-2015. The 600mb line in **(b)** is shown as a reference for potential aerosol location. **(c)** Climatological, zonally-averaged mid-high (gray, dashed) and high (gray, solid) cloud fraction overlain with precipitation rates for the years 2003-2015, see Figure 1 for averaging area.

4.3.2. Aerosol-Low Cloud-SST Feedback

In order to understand aerosol-cloud interactions, first we must understand where biomass burning produced aerosols are located. June climatological AOD and 850hPa winds (**Fig 4.3a**) show that, on average, aerosols are loaded over the GoG are due to seasonal trade

winds over the African continent. In addition to total AOD, aerosol angstrom exponents obtained from satellite observations validate that the majority of particulates in our region are in the fine-mode, which carry more absorption properties than coarse mode particulates. Fine-mode aerosols are shown in **figure 4.3b** through solid contour lines (angstrom exponent values greater than 1) Long-term monthly-mean vertical smoke aerosol extinction coefficient profiles representing locations in our study region are shown in **figure 4.4a**. We see the largest values at 4°S and the equator at an altitude just below 1500 meters. This extinction maximum occurs above the low cloud top height (**Fig 4.1c**). Further north, we notice decreases in mean extinction as aerosols enter the boundary layer. Regardless of latitudinal location, values taper toward 0 near 5.5 km. Figure 4b shows that most of the smoke along the 0 longitude is located between 1000m-3000m specifically where AOD anomalies exceed 0.1(~25% of the monthly mean) on dirty and clean days (**Fig 4.3 c**, **d**) and below mid-low level cloud top heights (**Fig 4.2b**). On average, the bulk

of smoke aerosols between 0-4°S are located within the boundary layer and well-mixed throughout the lowest 5km of the troposphere elsewhere.

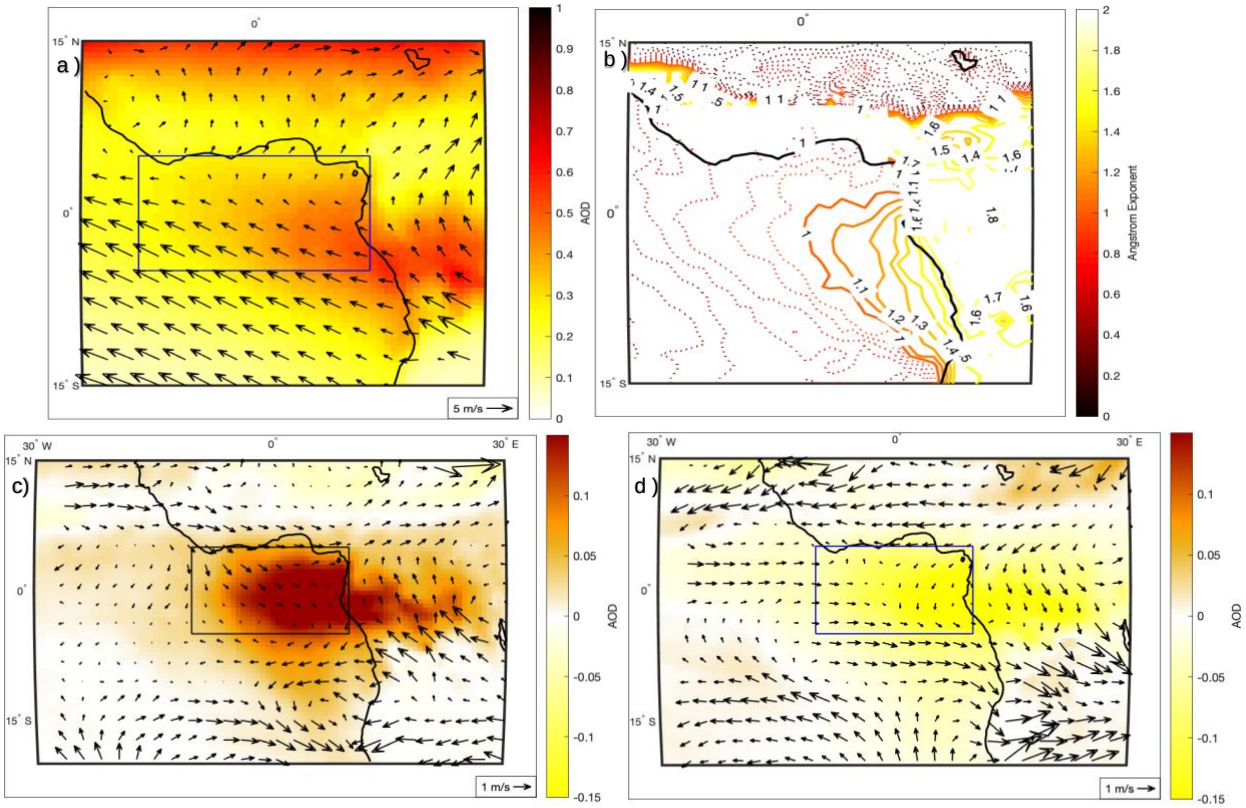

Figure 4.3 (a) Climatological, detrended AOD and 850hPa winds. (b) Aerosol angstrom exponent for years 2013-2015. Contour interval is 0.1 with values larger than 1 represented as solid lines. AOD and 850 hPa wind anomalies for dirty **(c)** and **(d)** clean days during the same time period. Rectangular boxes in (**a**), **(c)** and **(d)** represent averaging areas for composite analysis.

During dirty biomass burning episodes, we find evidence of increased low-cloud fraction specifically within the equatorial Atlantic cold tongue zone and within the area where maximum aerosol loading occurs. Similar results opposite in sign are found for clean episodes (**Fig 4.3c &d**). As low cloud fraction increases, it is possible the amount of shortwave radiation reaching the ocean surface diminishes as is reflected by changes in SST (**Fig 4.5**). In order to check for plausibility, we calculated the changes in downwelling surface shortwave radiation during clean and dirty aerosol events during all sky conditions. Not only can we understand radiative fluxes

due to aerosols and clouds, we can analyze the changes due to the presence of aerosols only. The largest anomalies occur near the equator in the center of our study region. Using the values associated with changes in surface fluxes due to aerosols, we calculate the changes in ocean surface heating rate. However, we find positive low cloud fraction anomalies where cloud top heights reach a minimum near the cold tongue (**Fig 4.1b**). **Figure 4.4b** shows that the bulk of smoke aerosols resides above this height (~1150m). Thus, our results are in agreement with previous studies that find evidence of increased cloud fraction and stronger subsidence beneath smoke layers with enhanced loading [*Wilcox, 2010*; *Wilcox*, 2012; *Li et al*., 2013] and increases in cloudiness when the vertical distance with the above aerosol layer is relatively small [*Adebiyi and Zuidema*, 2018]. As smoke travels north or south within the boundary layer, cloud fraction decreases (**Fig 4.5a**), as found in *Zhang and Zuidema* [2019, in review], although they focus in a region slightly further south. Significant decreases are found south of 5°S as recent evidence shows that the boundary layer is often smoky especially in June [Z*uidema et al.*, 2018].

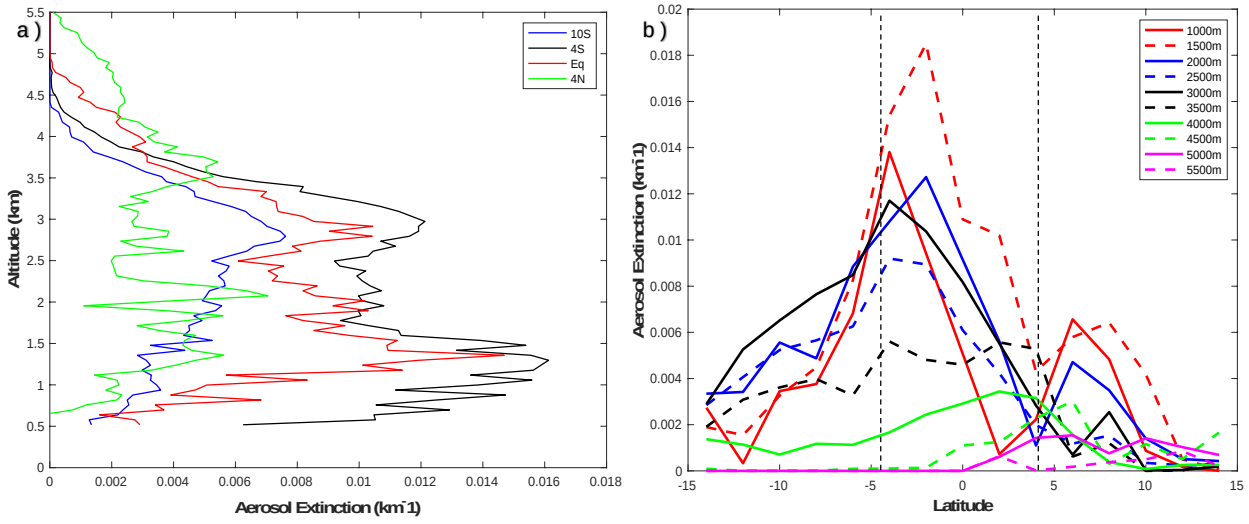

Figure 4.4 (a) Long-term mean vertical and (b) zonally-averaged smoke aerosol extinction profiles derived from CALIOP for the month of June (2003-2015). Data in panel **(a)** represent values along the Prime Meridian. Dotted lines in panel **(b)** between 5°S and 4°N represent the boundary where AOD anomalies exceed 0.1. See Figure 1 for averaging area.

4.3.3. Stability vs. Moisture Aloft

Yamaguchi et al., [2015] find that smoke aerosols delay the SCT by strengthening the inversion layer. In accordance with this study and others that look at LTS as a controlling factor for low cloud amount within SCT regions [*Wood and Bretherton*, 2006; *Sandu and Stevens*, 2011], we examined changes in potential temperature (θ) profiles and cloud top height anomalies (**Fig 4.6a** & **b**). Here, we can clearly see the effects of anomalous smoke loading on atmospheric stability. During dirty smoke episodes, we find significant decreases (25-100 meters) in low-level cloud top height from the cold tongue southwards (**Fig 4.5a**). By analyzing θ anomalies along the 0 longitude transect, we can infer where aerosols impact stability within the lower troposphere (**Fig 4.6b**). As expected, the largest response occurs near 850hPa, which corresponds to ~1500m above sea level (**Fig 4.1c**). In the subtropics (10°S and 4°S), we find the largest changes in cloud height and θ anomalies although smoke aerosol extinction values do not vary much between 750m-4000m. Further north, these changes are less pronounced. We note

significant cooling near the surface during dirty episodes, particularly at the equator where low cloud anomalies peak (**Fig 4.5a** and **4.6b**).

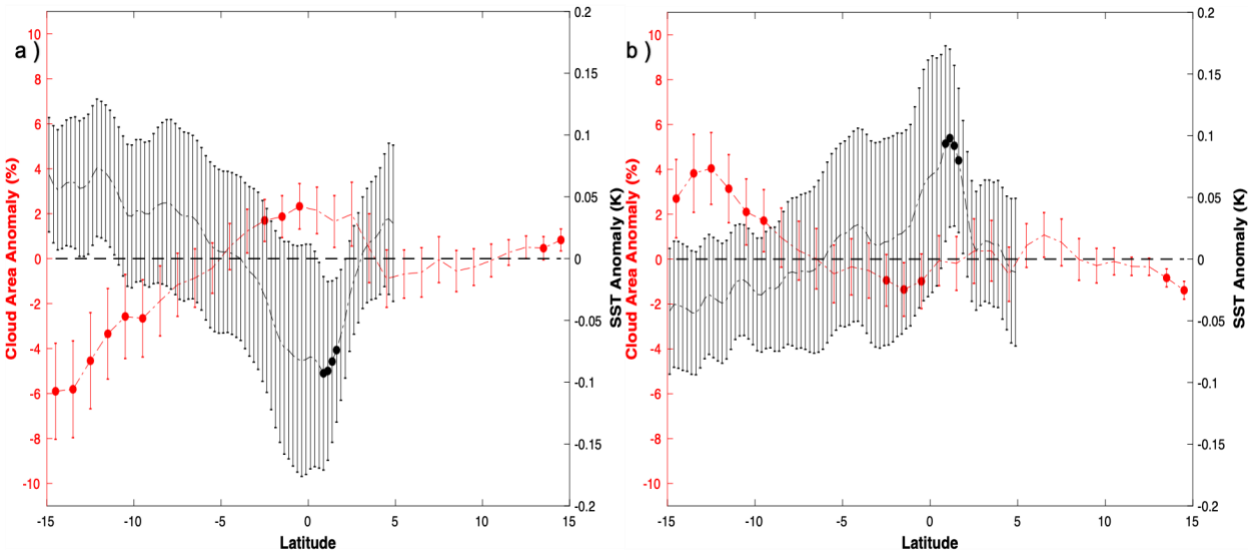

Figure 4.5 Zonally averaged low cloud area fraction and SST anomalies for **(a)** dirty and **(b)** clean smoke episodes. See Figure 1 for averaging area. Error bars range 1 standard error and filled circles represent locations where the difference between sampled means exceed the 95% confidence level.

Using a large eddy simulation (LES), *Zhou et al.*, [2017] find a hastened SCT in time linked to increased cloud droplet number concentration (due to smoke aerosols) that leads to faster evaporation of cloud water which enhances entrainment. Their complementary experiments that included additional moisture aloft, which is believed to accompany biomass burning plumes relative to surrounding air [*Adebiyi et al.*, 2015], revealed similar results. In their study, absorbing aerosols above the cloud layer strengthens the inversion and reduces boundary layer height, in agreement with our findings. However, as aerosols enter into the boundary layer, they find that enhanced entrainment of surrounding warm, dry air reduces cloud cover. North of the equator, we observe low cloud cover and cloud liquid water content at 850hPa slightly change simultaneously (**Fig 4.6c**) where smoke enters into the boundary layer (**Fig 4.1c**) but not significantly. During dirty episodes, we find 10-20% (0.1-0.2 g kg^{-1}) of moisture increases at

850hPa within our region of max AOD loading (**Fig 4.5d**) relative to recent observational studies [*Adebiyi et al*., 2015; *Haywood et al*., 2003]. However, those studies occurred in the southern Atlantic so our estimates may not be directly comparable.

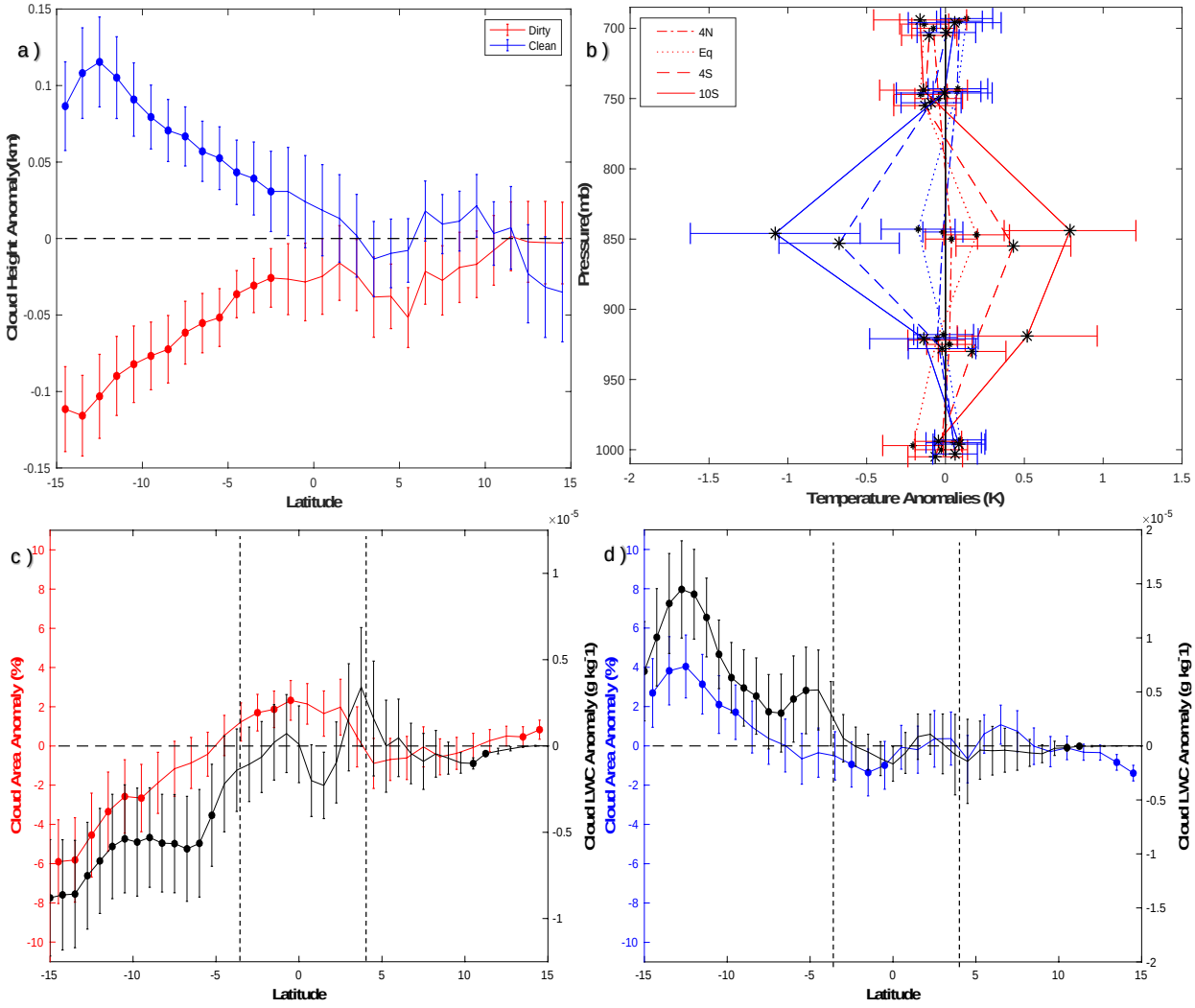

Figure 4.6 Anomalous changes in meteorological variables representing atmospheric stability and moisture: **(a)** cloud top height, **(b)** θ at various latitudes and cloud liquid water content at 850hPa for dirty**(c)** and clean**(d)** conditions. Data plotted in panel **b** are taken along the Prime Meridian. Panels **c** and **d** contain dotted lines representing the boundary where AOD anomalies exceed 0.1. See Figure 1 for averaging area. Error bars range 1 standard error and filled circles represent locations where the difference between sampled means exceed the 95% confidence level.

4.4 Conclusions

The individual impacts of biomass burning produced aerosols on LTS, low cloud cover and moisture availability culminate to extend the SCT in space. Using observation and reanalysis data, we have isolated a mechanism for aerosol modulation on the SCT in the equatorial Atlantic that has not yet been discussed in the literature. This transition is located within the GoG and thus we conducted our AOD composite analysis at this location. As previous research only looks at events with elevated smoke values, our results mainly focus on "dirty" days.

In the subtropical Atlantic (15°S-4°S), we attribute reductions in cloud cover during dirty conditions (**Fig 4.3c** & **Fig 4.6c)** to smoke mixing within the boundary layer (**Fig 4.4a**), possibly reflecting a boundary layer positive semi-direct effect [*Zhang and Zuidema*, 2019, in review]. Within the equatorial Atlantic (4°S-2°N), elevated smoke levels lead to increases (1-2%) in low cloud cover along with decreases in SST (~0.1K) and potential temperature (~0.2K) at the surface. Also, cloud top heights decrease 20-100m, consistent with *Deaconu et al*., 2019. The small, but significant increases in low-level cloud cover occurring within the equatorial Atlantic also coincide with increases in LTS. Thus, our results are in agreement with *Yamaguchi et al.* [2015 who find a delayed transition in time].

We attribute the switch from less low cloud for dirty conditions south of the cold tongue to more low clouds over the cold tongue to special air-sea interactions unique to this region. In the subtropics, trade winds advect the boundary layer over increasing SST's, which favors upward moisture flux from the surface to sustain cloud formations. Here, aerosol heating in the boundary layer can cause the clouds to evaporate. In contrast, when the boundary layer reaches the cold tongue, the atmosphere develops near-surface stratification which cuts off the upward

moisture flux needed to sustain clouds from dry air entrainment of the free troposphere [*Manbach and Norris,* 2007]. Here, it is possible that aerosol heating may increase stratification in the upper part of the boundary layer which would reduce dry air entrainment and lead to longer lasting clouds. Anomalous 850hPa winds (**Fig 4.3c** & **d**) do not reflect a pattern that would control both aerosol and cloud structures, so we rule out the possibility of wind variability causing such changes. Although we find a stronger anticyclonic circulation associated with increased aerosols, we do not find increases in moisture and cloud coverage that would result from increased easterlies over land as documented by *Adebiyi et al*., [2015]

Our study region offers more possibilities for research as we see cumulus clouds transitioning into deep-convective clouds within the GoG. Aerosols do not ascend high enough to have a direct influence on high-level clouds but may do so indirectly via hastening of the SCT and boundary layer moisture adjustments below. Subsequent changes in higher-level clouds and precipitation are small, but still worthy to note.

We acknowledge that this research relies on remotely sensed observations and so may be subjected to uncertainties associated with satellite data, specifically the retrieval of clear-sky AOD and missing VIIRS data due to high cloud presence. Also, with such data, it is difficult to differentiate between mixed aerosol species (e.g., black carbon coated by sulfate). It is our hope that these findings will serve as a foundation for designing future field campaigns and testing modeling studies that investigate the SCT near the equatorial Atlantic.

Acknowledgments, Samples, and Data

All data supporting the conclusions of this research study are available through the references mentioned in the data sources and methods sections.

This research forms a part of the Ph.D. dissertation of OA, who was supported by a National Science Foundation Graduate Research (DGE-1650112), UC Dissertation Year and San Diego Foundation Fellowships. The National Science Foundation Earth System Modeling Program (OCE1419306) provided additional funding that supported this research. We thank Prof. Paquita Zuidema for many constructive comments and suggestions on our research results. Chapter 4, in part is currently being prepared for submission for publication of the material. Ajoku, Osinachi; Miller, Arthur; Norris, Joel. The dissertation author was the primary investigator and author of this material.

4.5 References

Adebiyi, A. A., Zuidema, P., & Abel, S. J. (2015). The convolution of dynamics and moisture with the presence of shortwave absorbing aerosols over the southeast Atlantic. *Journal of Climate*, *28*(5), 1997-2024.

Adebiyi, A. A., & Zuidema, P. (2018). Low cloud cover sensitivity to biomass-burning aerosols and meteorology over the southeast Atlantic. *Journal of Climate*, *31*(11), 4329-4346.

Adler, Robert; Wang, Jian-Jian; Sapiano, Mathew; Huffman, George; Bolvin, David; Nelkin, Eric; and NOAA CDR Program (2017). Global Precipitation Climatology Project (GPCP) Climate Data Record (CDR), Version 1.3 (Daily) [Indicate subset used.]. NOAA National Centers for Environmental Information. doi:10.7289/V5RX998Z [January 10, 2020]

Allen, R. J., and O. Ajoku (2016), Future aerosol reductions and widening of the northern tropical belt, *J. Geophys. Res. Atmos.*, *121*, doi:10.1002/2016JD024803.

Albrecht, B (1989), Aerosols, cloud microphysics, and fractional cloudi-ness, Science, 245, 1227-1230, doi:10.1126/science.245.4923.1227

Albrecht, B. A., Bretherton, C. S., Johnson, D., Scubert, W. H., & Frisch, A. S. (1995). The Atlantic stratocumulus transition experiment—ASTEX. *Bulletin of the American Meteorological Society*, *76*(6), 889-904.

Albrecht, B., Ghate, V., Mohrmann, J., Wood, R., Zuidema, P., Bretherton, C., Schwartz, C., Eloranta, E., Glienke, S., Donaher, S. and Sarkar, M., 2019. Cloud System Evolution in the Trades (CSET): Following the evolution of boundary layer cloud systems with the NSF–NCAR GV. *Bulletin of the American Meteorological Society*, *100*(1), pp.93-121.

Bengtsson, L, Hagemann, S, & Hodges, K I (2004) Can climate trends be calculated from reanalysis data?. *Journal of Geophysical Research: Atmospheres*, *109*(D11)

Berrisford, P., Dee, D., Poli, P., Brugge, R., Fielding, K., Fuentes, M., Kallberg, P., Kobayashi, S., Uppala, S. and Simmons, A., 2011. The ERA-Interim archive, version 2.0.

Bourgeois, E., Bouniol, D., Couvreux, F., Guichard, F., Marsham, J.H., Garcia-Carreras, L., Birch, C.E. and Parker, D.J., 2018. Characteristics of mid-level clouds over West Africa. *Quarterly Journal of the Royal Meteorological Society*, *144*(711), pp.426-442.

Bretherton, C. S. (1992). A conceptual model of the stratocumulus-trade-cumulus transition in the subtropical oceans. In *Proc. 11th Int. Conf. on Clouds and Precipitation*(Vol. 1, pp. 374-377). International Commission on Clouds and Precipitation and International Association of Meteorology and Atmospheric Physics Montreal, Quebec, Canada.

Bretherton, C. S., & Wyant, M. C. (1997). Moisture transport, lower-tropospheric stability, and decoupling of cloud-topped boundary layers. *Journal of the atmospheric sciences*, *54*(1), 148-167.

Bretherton, C. S., Krueger, S. K., Wyant, M. C., Bechtold, P., Van Meijgaard, E., Stevens, B., & Teixeira, J. (1999). A GCSS boundary-layer cloud model intercomparison study of the first ASTEX Lagrangian experiment. *Boundary-Layer Meteorology*, *93*(3), 341-380.

Buchard, V., Da Silva, A.M., Colarco, P.R., Darmenov, A., Randles, C.A., Govindaraju, R., Torres, O., Campbell, J. and Spurr, R., 2015. Using the OMI aerosol index and absorption aerosol optical depth to evaluate the NASA MERRA Aerosol Reanalysis. *Atmospheric Chemistry and Physics*, *15*(10), p.5743.

Chung, D., Matheou, G., & Teixeira, J. (2012). Steady-state large-eddy simulations to study the stratocumulus to shallow cumulus cloud transition. *Journal of the Atmospheric Sciences*, *69*(11), 3264-3276.

Cochrane, S. P., Schmidt, K. S., Chen, H., Pilewskie, P., Kittelman, S., Redemann, J., LeBlanc, S., Pistone, K., Kacenelenbogen, M., Segal Rozenhaimer, M., Shinozuka, Y., Flynn, C., Platnick, S., Meyer, K., Ferrare, R., Burton, S., Hostetler, C., Howell, S., Freitag, S., Dobracki, A., and Doherty, S.: Above-cloud aerosol radiative effects based on ORACLES 2016 and ORACLES 2017 aircraft experiments, Atmos. Meas. Tech., 12, 6505–6528, https://doi.org/10.5194/amt-12-6505-2019, 2019.

Deaconu, L. T., Ferlay, N., Waquet, F., Peers, F., Thieuleux, F., & Goloub, P. (2019). Satellite inference of water vapour and above-cloud aerosol combined effect on radiative budget and cloud-top processes in the southeastern Atlantic Ocean. *Atmospheric Chemistry and Physics*, *19*(17), 11613-11634.

Diamond, M.S., Dobracki, A., Freitag, S., Small Griswold, J.D., Heikkila, A., Howell, S.G., Kacarab, M.E., Podolske, J.R., Saide, P.E. and Wood, R., 2018. Time-dependent entrainment of

smoke presents an observational challenge for assessing aerosol–cloud interactions over the southeast Atlantic Ocean. *Atmospheric Chemistry and Physics*, *18*(19), pp.14623-14636.

Doelling, D.R., Loeb, N.G., Keyes, D.F., Nordeen, M.L., Morstad, D., Nguyen, C., Wielicki, B.A., Young, D.F. and Sun, M., 2013. Geostationary enhanced temporal interpolation for CERES flux products. *Journal of Atmospheric and Oceanic Technology*, *30*(6), pp.1072-1090.

Doelling, D R, Sun, M, Nguyen, L. T, Nordeen, M L, Haney, C O, Keyes, D F, & Mlynczak, P E (2016) Advances in geostationary-derived longwave fluxes for the CERES synoptic (SYN1deg) product. *Journal of Atmospheric and Oceanic Technology*, *33*(3), 503-521

Ferek, R.J., Garrett, T., Hobbs, P.V., Strader, S., Johnson, D., Taylor, J.P., Nielsen, K., Ackerman, A.S., Kogan, Y., Liu, Q. and Albrecht, B.A., 2000. Drizzle suppression in ship tracks. *Journal of the Atmospheric Sciences*, *57*(16), pp.2707-2728.

Ghan, S J, Liu, X, Easter, R C, Zaveri, R, Rasch, P J, Yoon, J H, & Eaton, B (2012) Toward a minimal representation of aerosols in climate models: Comparative decomposition of aerosol direct, semidirect, and indirect radiative forcing. *Journal of Climate*, *25*(19), 6461-6476

Global Modeling and Assimilation Office (GMAO)(2015) MERRA-2 tavgM_2d_int_Nx: 2d, Monthly mean, Time-Averaged, Single-Level, Assimilation, Vertically Integrated Diagnostics V5.12.4, Greenbelt, MD, USA, Goddard Earth Sciences Data and Information Services Center (GES DISC), Accessed [July 7, 2017] 10.5067/FQPTQ4OJ22TL

Hansen, J., Sato, M., & Ruedy, R. (1997). Radiative forcing and climate response. *Journal of Geophysical Research: Atmospheres*, *102*(D6), 6831-6864.

Haywood, J, & Boucher, O (2000) Estimates of the direct and indirect radiative forcing due to tropospheric aerosols: A review. *Reviews of geophysics*, *38*(4), 513-543

Haywood, J. M., Osborne, S. R., Francis, P. N., Keil, A., Formenti, P., Andreae, M. O., & Kaye, P. H. (2003). The mean physical and optical properties of regional haze dominated by biomass burning aerosol measured from the C-130 aircraft during SAFARI 2000. *Journal of Geophysical Research: Atmospheres*, *108*(D13).

Huffman, G.J., R.F. Adler, M. Morrissey, D.T. Bolvin, S. Curtis, R. Joyce, B McGavock, J. Susskind, 2001: Global Precipitation at One-Degree Daily Resolution from Multi-Satellite Observations. J. Hydrometeor., 2(1), 36-50.

Klein, S. A., & Hartmann, D. L. (1993). The seasonal cycle of low stratiform clouds. *Journal of Climate*, *6*(8), 1587-1606.

Li, J., K. von Salzen, Y. Peng, H. Zhang, and x.-Z. Liang (2013), Evolution of black carbon semi-direct radiative effect in a climate model, J. Geophysics. Res. Atmos., 118, 4715-4728, doi:10.1002/jgrd.50327.

Mansbach, D. K., & Norris, J.R. (2007). Low-level cloud variability over the equatorial cold tongue in observations and models. *Journal of climate*, *20*(8), pp. 1555-1570

Nicholson, S.E., Some, B., McCollum, J., Nelkin, E., Klotter, D., Berte, Y., Diallo, B.M., Gaye, I., Kpabeba, G., Ndiaye, O. and Noukpozounkou, J.N., 2003. Validation of TRMM and other rainfall estimates with a high-density gauge dataset for West Africa. Part II: Validation of TRMM rainfall products. *Journal of Applied Meteorology*, *42*(10), pp.1355-1368.

Painemal, D., P. Minnis, and M. Nordeen (2015), Aerosol variability, synoptic-scale processes, and their link to the cloud microphysics over the northeast Pacific during MAGIC,J. Geophys. Res. Atmos., 120,5122–5139, doi:10.1002/2015JD023175.

Painemal, D., S. Kato, and P. Minnis (2014), Boundary layer regulation in the southeast Atlantic cloud microphysics during the biomass burning season as seen by the A-train satellite constellation, J. Geophys. Res. Atmos., 119, 11,288–11,302, doi:10.1002/2014JD022182.

Pistone, K., Redemann, J., Doherty, S., Zuidema, P., Burton, S., Cairns, B., Cochrane, S., Ferrare, R., Flynn, C., Freitag, S. and Howell, S.G., 2019. Intercomparison of biomass burning aerosol optical properties from in situ and remote-sensing instruments in ORACLES-2016. *Atmospheric Chemistry and Physics (Online)*, *19*(PNNL-SA-147352).

Platnick, S., King, M., & Hubanks, P. (2015). MODIS Atmosphere L3 Daily Product, NASA MODIS Adaptive Processing System, Goddard Space Flight Center.

Ramanathan, V C P J, Crutzen, P J, Kiehl, J T, & Rosenfeld, D (2001) Aerosols, climate, and the hydrological cycle. *science*, *294*(5549), 2119-2124

Reynolds, R. W., Smith, T. M., Liu, C., Chelton, D. B., Casey, K. S., & Schlax, M. G. (2007). Daily high-resolution-blended analyses for sea surface temperature. *Journal of Climate*, *20*(22), 5473-5496.

Sandu, I., & Stevens, B. (2011). On the factors modulating the stratocumulus to cumulus transitions. *Journal of the Atmospheric Sciences*, *68*(9), 1865-1881.

Sayer, A. M., N. C. Hsu, C. Bettenhausen, J. Lee, W. V. Kim, and A. Smirnov (2018), Satellite Ocean Aerosol Retrieval (SOAR) Algorithm Extension to S-NPP VIIRS as Part of the "Deep Blue" Aerosol Project, J. Geophys. Res. Atmos., 123, doi:10.1002/2017JD027412

Shinozuka, Y., Kacenelenbogen, M. S., Burton, S. P., Howell, S. G., Zuidema, P., Ferrare, R. A., LeBlanc, S. E., Pistone, K., Broccardo, S., Redemann, J., Schmidt, K. S., Cochrane, S. P., Fenn, M., Freitag, S., Dobracki, A., Segal-Rosenheimer, M., and Flynn, C. J.: Daytime aerosol optical depth above low-level clouds is similar to that in adjacent clear skies at the same heights: airborne observation above the southeast Atlantic, Atmos. Chem. Phys. Discuss., https://doi.org/10.5194/acp-2019-1007, in review, 2020.

Teixeira, J., Cardoso, S., Bonazzola, M., Cole, J., DelGenio, A., DeMott, C., Franklin, C., Hannay, C., Jakob, C., Jiao, Y. and Karlsson, J., 2011. Tropical and subtropical cloud transitions in weather and climate prediction models: The GCSS/WGNE Pacific Cross-Section Intercomparison (GPCI). *Journal of Climate*, *24*(20), pp.5223-5256.

Tosca, M G, Diner, D J, Garay, M J, & Kalashnikova, O V (2015) Human-caused fires limit convection in tropical Africa: First temporal observations and attribution. *Geophysical Research Letters*, *42*(15), 6492-6501

Wilcox, E. M. (2010), Stratocumulus cloud thickening beneath layers of absorbing smoke aerosol, Atmos. Chem. Phys., 10(23), 11,769–11,777, doi:10.5194/acp-10-11769-2010.

Wilcox, E. M. (2012), Direct and semi-direct radiative forcing of smoke aerosols over clouds, Atmos. Chem. Phys., 12(1), 139–149, doi:10.5194/acp-12-139-2012.

Winker, D. (2015). CALIPSO LID_L3_APro_AllSky-StandardHDF File – Version 3.00. NASA Langley Atmospheric Science Data Center DAAC. https://doi.org/10.5067/caliop/calipso/cal_lid_l3_apro_allsky-standard-v3-00

Wood, R., & Bretherton, C. S. (2006). On the relationship between stratiform low cloud cover and lower-tropospheric stability. *Journal of climate*, *19*(24), 6425-6432.

Wood, R., O, K.T., Bretherton, C.S., Mohrmann, J., Albrecht, B.A., Zuidema, P., Ghate, V., Schwartz, C., Eloranta, E., Glienke, S. and Shaw, R.A., 2018. Ultraclean layers and optically thin clouds in the stratocumulus-to-cumulus transition. Part I: Observations. *Journal of the Atmospheric Sciences*, *75*(5), pp.1631-1652.

Yamaguchi, T., G. Feingold, J. Kazil, and A. McComiskey (2015), Stratocumulus to cumulus transition in the presence of elevated smoke layers, Geophys. Res. Lett., 42, 10,478–10,485, doi:10.1002/2015GL066544.

Yamaguchi, T., Feingold, G., & Kazil, J.(2017). Stratocumulus to cumulus transition by drizzle. Journal of Advances in Modeling Earth Systems,9, 2333–2349. https://doi.org/10.1002/2017MS001104

Zhang, J. and Zuidema, P.: Low cloud reduction within the smoky marine boundary layer and the diurnal cycle, Atmos. Chem. Phys. Discuss., https://doi.org/10.5194/acp-2019-448, in review, 2019.

Zhou, X., Ackerman, A. S., Fridlind, A. M., Wood, R., & Kollias, P. (2017). Impacts of solar-absorbing aerosol layers on the transition of stratocumulus to trade cumulus clouds. *Atmospheric Chemistry and Physics*, *17*(20), 12725-12742.

Zhou, X., Kollias, P., & Lewis, E. R. (2015). Clouds, precipitation, and marine boundary layer structure during the MAGIC field campaign. *Journal of Climate*, *28*(6), 2420-2442.

Zuidema, P., Redemann, J., Haywood, J., Wood, R., Piketh, S., Hipondoka, M., & Formenti, P. (2016). Smoke and clouds above the southeast Atlantic: Upcoming field campaigns probe absorbing aerosol's impact on climate. *Bulletin of the American Meteorological Society*, *97*(7), 1131-1135.

Zuidema, P., Sedlacek III, A.J., Flynn, C., Springston, S., Delgadillo, R., Zhang, J., Aiken, A.C., Koontz, A. and Muradyan, P., 2018. The Ascension Island boundary layer in the remote southeast Atlantic is often smoky. *Geophysical Research Letters*, *45*(9), pp.4456-4465.

Chapter 5: Dissertation Summary and Conclusions

5.1 Summary

This dissertation has examined the various impacts that biomass burning-produced aerosols have on the dynamics of the West African monsoon (WAM) as they are transported from central/southern Africa towards the Gulf of Guinea (GoG). These smoke aerosols are primarily absorbing radiation within the shortwave energy spectrum, which alters atmospheric stability. We study how the radiative and microphysical effects of such aerosols alter large-scale cloud formations and precipitation rates in the equatorial Atlantic using both observations and model simulations. The study of the effects that aerosols impose on West Africa's hydrological cycle remains an emerging research topic and is especially significant since this region is home to ~200 million occupants thus carrying a large societal context.

In chapter 2, we use observation and reanalysis data to quantify precipitation suppression over the Guinea coastline when excess aerosols are transported within the GoG. Chapter 3 looks at model simulations that are conducted in order to better understand the vertical representation of fine-mode BC and various cloud properties using observationally constrained meteorology. Changes in radiative fluxes are broken down into three categories; 1) All-sky conditions, 2) Cloud-only and 3) BC-only. In chapter 4, we look at how smoke aerosols influence cloud transitions over the equatorial Atlantic Ocean, which can potentially influence monsoonal rains downstream over land. The main points of the dissertation and its conclusions are summarized as follows:

Chapter 2 focuses on the use of observations and atmospheric reanalysis products in order to understand the impacts of smoke aerosols transported from the Southern Hemisphere on the dynamics of the West African monsoon. Variations in wind strength over biomass burning source regions of smoke aerosols in tropical Africa leads to anomalous aerosol advection towards the GoG. During the peak in the local monsoon season, we found evidence linking increased aerosol presence (33%) with a reduction in precipitation (2.5 mm day^{-1}) over West Africa. To further understand the possible mechanisms by which this occurs, we analyzed other meteorological variables associated with precipitation. Dividing aerosol data into dirty and clean conditions, we examined how various cloud properties, radiation fluxes and CAPE change along with such conditions.

We find increases in low-level cloud fraction over the GoG that we attribute to the aerosol semi-direct effect. At this location, low-level stratocumulus clouds can reside at a lower altitude than smoke aerosols coming from the continent possibly leading to additional cloud coverage. Over land, where deep convection prevails, we find evidence of the aerosol indirect effect. Increases in mid-level clouds, coupled with decreases in droplet effective radius during dirty conditions reflect this in Figure 2.8. The signal for elevated aerosol transport and increased low to mid-level cloud fraction shows itself in the surface SW flux, in which aerosols account for ~ 33% of the reduction in energy reaching the surface during dirty conditions. With the reduction in SW radiation reaching the surface, we see a corresponding decrease in CAPE which probably promotes a decrease in high-level cloud fraction. We suggest that aerosol radiative effects alter local radiation budgets, ultimately weakening the energy available for convection and reducing precipitation rates for the month of August in the WAM region.

In chapter 3, we use CESM2 coupled to specified dynamics to evaluate how well a global climate model can help us to interpret the results achieved in chapter 2. Overall, our runs suggest that this model can reproduce the transport of BC aerosols over the GoG and corresponding precipitation suppression but more work is needed. Model simulations reveal the presence of fine-mode BC vertically up to about 700mb, higher than our previous assumption of 850mb in chapter 2. We associate increases in BC aerosols with drier atmospheric conditions and less cloud liquid water availability throughout the equatorial Atlantic. Mixtures of aerosols and drier air within the boundary leads to decreased low-cloud fraction and limits deep convection over land associated with the West African monsoon. Reductions in cloud development yields a positive SW surface CRE up to 20 W m^{-2} (twice as much as LW CRE) and SWCF ~40 W m^{-2} along the Guinea coastline (heavily outweighing changes in LWCF), with the contribution of BC to this forcing being minimal. Values are higher for SWCF because values are calculated at the top of atmosphere and include changes to cloud albedo and radiation reflected back into space. Because the isolated direct effect of BC is so minimal, we attribute cloud reductions to a positive aerosol semidirect effect. Variables describing cloud microphysical effects in cloud droplet number concentration and droplet effective radius are mainly restricted to below 700mb.

Together, increased aerosol loading, and cloud fraction reductions warm the lower troposphere and cool the surface reinforcing reductions in turbulence and convection. We recognize the dissimilarity of low cloud fractions between observations and our model runs. Further model runs are needed to separate potential pseudo-radiative effects caused by temperature nudging since model physics are driven by temperature lapse rates.

Using observation and reanalysis data, chapter 4 discusses a mechanism for aerosol modulation on the SCT in the equatorial Atlantic that has not yet been discussed in breadth in the research literature. Our results show two opposing effects that the presence of biomass burning aerosols have on clouds over the Atlantic Ocean. In the subtropical Atlantic (15°S-4°S), we attribute reductions in cloud cover during dirty conditions (Fig 3c & 6c) to smoke mixing within the boundary layer (Fig 4a), possibly reflecting a boundary layer positive semi-direct effect [*Zhang and Zuidema*, 2019, in review]. Within the equatorial Atlantic (4°S-2°N), elevated smoke levels lead to increases (1-2%) in low cloud cover along with decreases in SST (~0.1K) and potential temperature (~0.2K) at the surface. Also, cloud top heights decrease 20-100m during dirty conditions, consistent with results in chapters 2 & 3. We attribute the switch from less low cloud for dirty conditions south of the cold tongue to more low clouds over the cold tongue to the unique air-sea interactions in this region.

In the subtropics, trade winds advect the boundary layer over increasing SST, which favors upward moisture flux from the surface to sustain cloud formations. Here, aerosol heating in the boundary layer can cause the clouds to evaporate. In contrast, when the boundary layer reaches the cold tongue, the atmosphere develops near-surface stratification which cuts off the upward moisture flux needed to sustain clouds from dry air entrainment of the free troposphere. Our results carry potential importance over land, where deep-convective clouds overlay lower level clouds. Aerosols do not ascend high enough to influence these high-level clouds but may do so indirectly via a hastening of the SCT and boundary layer moisture adjustments below.

This thesis has demonstrated an existing relationship between biomass burning produced aerosols and precipitation rates over West Africa during the monsoon season. Interhemispheric aerosol transport leads to complex atmospheric interactions and we attempted to differentiate between aerosol effects and background meteorology. The progression of this thesis lays a foundation for studying how future changes to aerosol emissions can impact West African climate. It is necessary to highlight how human interactions influence the research presented. A large portion of biomass burning is anthropogenic in nature and occurs as farmers lay fire to agricultural waste. A portion of my future research direction will include looking at model simulations of future scenarios of aerosol emissions. As agricultural demands and the planet's climate continues to change, it is imperative to keep an eye on short-term and long-term changes in BC radiative forcing locally and globally.